AD_____

Award Number:
W81XWH-09-1-0728

TITLE:

Nanoplatinates for Breast Cancer

PRINCIPAL INVESTIGATOR:

 Abhimanyu Paraskar, Ph.D.

CONTRACTING ORGANIZATION:

The Brigham and Women's Hospital, Inc.
Boston, MA 02115

REPORT DATE:
October 2010

TYPE OF REPORT:

Annual Summary

PREPARED FOR: U.S. Army Medical Research and Materiel Command
               Fort Detrick, Maryland 21702-5012

DISTRIBUTION STATEMENT:

        Approved for public release; distribution unlimited

REPORT DOCUMENTATION PAGE

Form Approved
OMB No. 0704-0188

Public reporting burden for this collection of information is estimated to average 1 hour per response, including the time for reviewing instructions, searching existing data sources, gathering and maintaining the data needed, and completing and reviewing this collection of information. Send comments regarding this burden estimate or any other aspect of this collection of information, including suggestions for reducing this burden to Department of Defense, Washington Headquarters Services, Directorate for Information Operations and Reports (0704-0188), 1215 Jefferson Davis Highway, Suite 1204, Arlington, VA 22202-4302. Respondents should be aware that notwithstanding any other provision of law, no person shall be subject to any penalty for failing to comply with a collection of information if it does not display a currently valid OMB control number. **PLEASE DO NOT RETURN YOUR FORM TO THE ABOVE ADDRESS.**

1. REPORT DATE *(DD-MM-YYYY)*	2. REPORT TYPE	3. DATES COVERED *(From - To)*
01-10-2010	Annual Summary	**21 SEP 2009 - 20 SEP 2010**

4. TITLE AND SUBTITLE
Nanoplatinates for Breast Cancer

5a. CONTRACT NUMBER

5b. GRANT NUMBER
W81XWH-09-1-0728

5c. PROGRAM ELEMENT NUMBER

6. AUTHOR(S)
Abhimanyu Paraskar

aparaskar@rics.bwh.harvard.edu

5d. PROJECT NUMBER

5e. TASK NUMBER

5f. WORK UNIT NUMBER

7. PERFORMING ORGANIZATION NAME(S) AND ADDRESS(ES)

The Brigham and Women's Hospital, Inc.

Boston MA 02115

8. PERFORMING ORGANIZATION REPORT NUMBER

9. SPONSORING / MONITORING AGENCY NAME(S) AND ADDRESS(ES)

U.S. Army Medical Research and Materiel
Command, Fort Detrick, Maryland 21702-5012

10. SPONSOR/MONITOR'S ACRONYM(S)

11. SPONSOR/MONITOR'S REPORT NUMBER(S)

12. DISTRIBUTION / AVAILABILITY STATEMENT

Approved for public release; distribution unlimited

13. SUPPLEMENTARY NOTES

14. ABSTRACT

We demonstrate that the rational engineering of a polymer inspired by the bioactivation of cisplatin and oxaliplatin enables the engineering of a unique nanoplatinates, which improves antitumor efficacy of cisplatin by capitalizing on the inherent properties of nanoscale. This opens up the possibility to increase the maximal tolerated dose of cisplatin, which is an effective chemotherapeutic agent but dose limited due to nephrotoxicity. The clinical familiarity of using an established and globally used chemotherapeutic, together with the low cost of the basic building blocks used in fabricating the nanoparticle, can facilitate the rapid translation of this technology, thereby validating the potential of nanotechnology to impact global health. Additionally, we developed fullerenol as novel anti-angiogenic drug delivery vehicle, with its cisplatin conjugate showed improved antitumor efficacy by synergistic anti-angiogenic and anti-cancer activity.

15. SUBJECT TERMS
Cisplatin, Chemotherapy, Polymer, selfassembly, Nanovehicles

16. SECURITY CLASSIFICATION OF:			17. LIMITATION OF ABSTRACT	18. NUMBER OF PAGES	19a. NAME OF RESPONSIBLE PERSON USAMRMC
a. REPORT U	**b. ABSTRACT** U	**c. THIS PAGE** U	UU	121	**19b. TELEPHONE NUMBER** *(include area code)*

Standard Form 298 (Rev. 8-98)
Prescribed by ANSI Std. Z39.18

Table of Contents

Introduction

The platinum drugs represented by the parent compound, cis-dichloro diamine platinum (II) (CDDP) commonly known as cisplatin is one of the oldest known broad spectrum antineoplastic agents available to the clinical oncologist and it is a first line therapy for most malignancies including testicular, ovarion, cervical and lung cancer (1). It was also shown recently to be effective in triple negative breast cancer (2). However its clinical application is limited due to nephrotoxicity. Much attention is currently focused on the design of new generations of platinum anticancer complexes that circumvent nephrotoxicity caused by cisplatin. To overcome this problem we envisioned that nanotechnology based strategy could be harnessed. It is now well documented that nanoparticles >5 nm will avoid renal clearance (3), and thereby could potentially reduce cisplatin nephrotoxicity.

Body

In the continuing search for effective treatments for cancer, an emerging paradigm is the use of nanotechnology to uncap the full potential of existing chemotherapy agents (4). Integral physicochemical properties of nanovectors can be modulated to improve the antitumor efficacy of chemotherapeutic agents (5). For example, the shape and size of nanostructures can play a deterministic role in the biological outcome (6–8). Similarly, surface modifications to increase hydrophilicity can mask the nanovectors from the reticuloendothelial system, thereby increasing circulation time and altering the pharmacokinetics of the active agents (5). Such nanovectors accumulate preferentially in the tumors due to the unique leaky tumor vasculature coupled with impaired intratumoral lymphatic drainage, which contributes to an enhanced permeation and retention (EPR) effect (9, 10). The development of a cisplatin nanoparticle has been a challenge resulting from its physicochemical properties, which make it difficult to entrap it in polymeric sustained-release nanoparticles (11, 12). Strategies based on the conjugation of platinum to polymers (for example, a polyamidoamine dendrimer-platinum complex), resulted in 200–550-fold reduction in cytotoxicity than free cisplatin as a result of strong bonds that are formed between the polymer and Pt (13). Similarly, AP5280, a N-(2-hydroxypropyl) methacrylamide copolymer-bound platinum was found to exert minimal nephrotoxicity in clinical studies (14), but was less potent than carboplatin as the platinum is held to an aminomalonic acid chelating agent coupled to the COOH-terminal glycine of a tetrapeptide spacer (15). These studies also shed light on the impact of the complexation environment of the platinum on the efficacy. We used this structure-activity relationship underlying the activation of platinum to engineer a unique nanoplatinate that exhibited significantly improved antitumor efficacy in terms of tumor growth delay in lung and breast cancer and tumor regression in ovarian cancer models, along with reduced systemic and nephrotoxicity (16).

Similarly oxaliplatin based nanoparticles are designed, synthesized and evaluated for breast cancer studies. We rationalized that the design of a nanoparticle modeled on the leaving group would offer the greatest possibility of retaining the e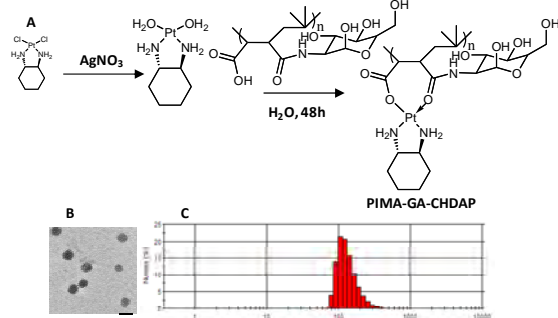fficacy of oxaliplatin while the size of nanoparticle could bypass renal clearance and thereby reduce nephrotoxicity. As the first step, we identified a polymer, where each monomeric unit could serve as the leaving group of oxaliplatin. As shown in **Fig. 1**, we rationalized that derivatizing one arm of each monomer unit of the polymer with biocompatible glucosamine to generate a PIMA-glucosamine conjugate (PIMA-GA) would convert the dicarboxylato bonds with Pt to a monocarboxylato bond and a coordinate bond, which should release Pt more easily (**Fig. 1A**). The complexation of cisplatin to PIMA-glucosamine (PIMA-GA) polymer at a ratio of 15:1 resulted in selfassembly into nanoparticles in the desired narrow size bandwidth of 90–170 nm as confirmed by DLS (**Fig. 1C**) and high-resolution

Fig. 1. (A) Schematic shows the PIMA-Oxaliplatin synthesis and size of particles shown in the (B) HRTEM images of Fullerol-cisplatin nanoparticles Bar= 100 nm. And DLS measurement (C).
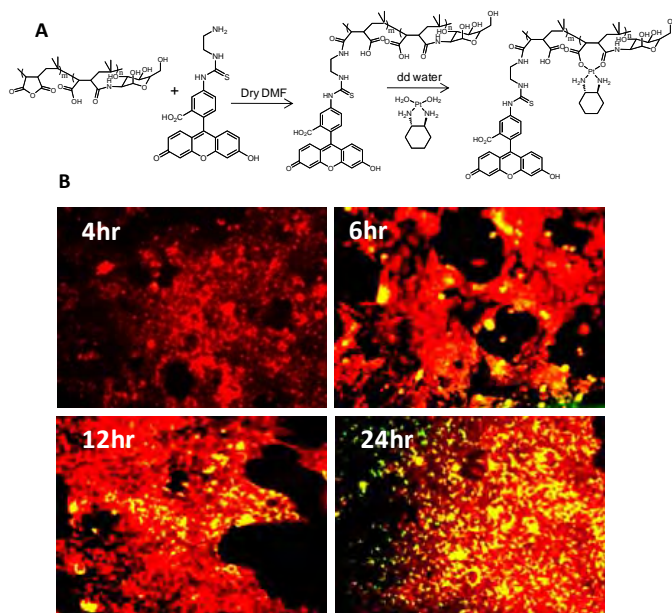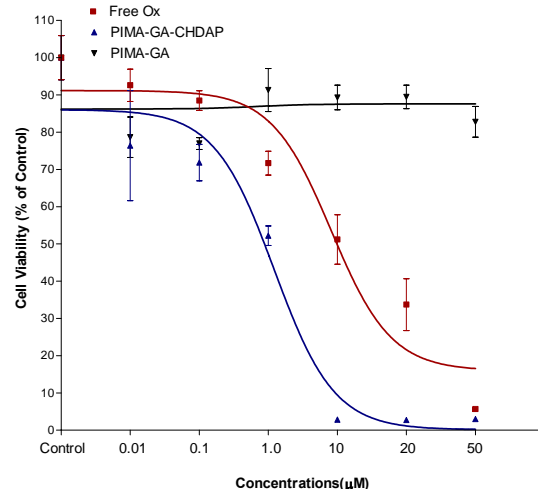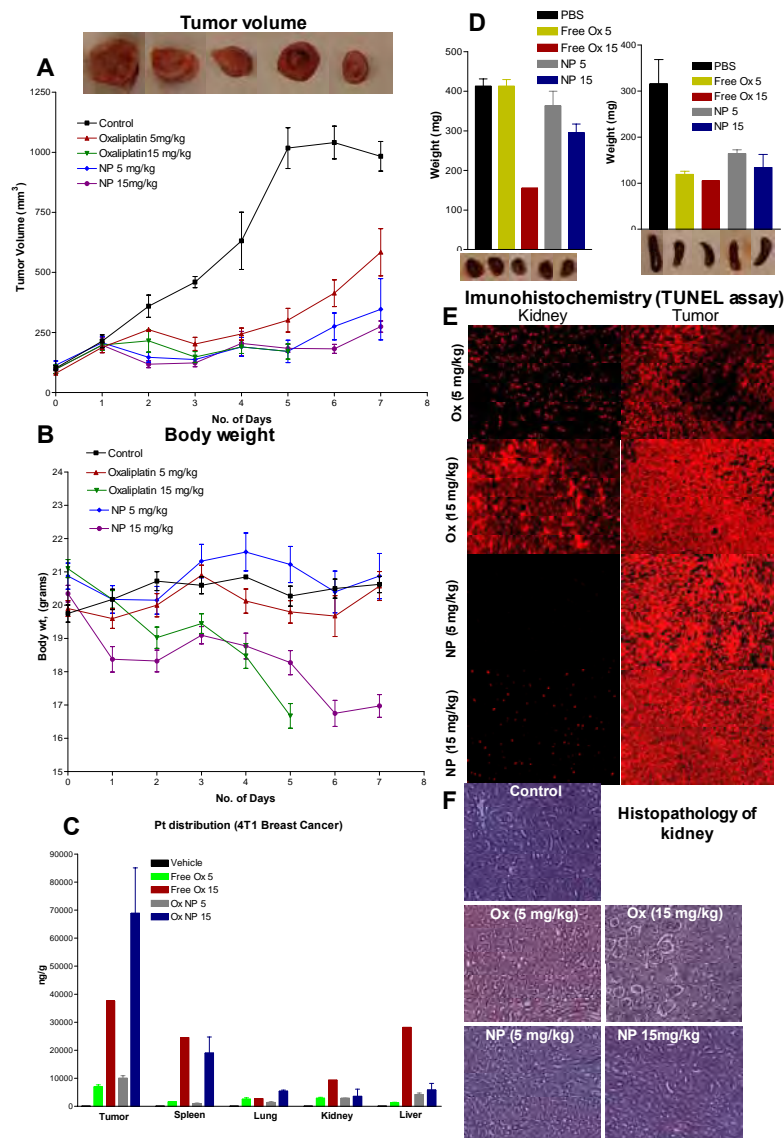

Fig. 3. (A) Scheme shows the synthesis of the labeled PIMA-Oxaliplatin conjugates with FITC to enable the tracking of cellular uptake of the nanoparticles. (B) Epifluorescence images shows the temporal uptake of FITC-labeled PIMA-Oxaliplatin conjugates into 4T1 breast cancer cells. The cells were counter-labeled with lysotracker-Red to highlight the endolysosomal compartments. Colocalization of the signals in the merge images reveals internalization of the nanoparticles into the endolysosomal compartments.

Fig. 2. Graphs show effect of Fullerol-cisplatin nanoparticles on 4T1 cells viability measured using MTS assay.

2

transmission electron microscopy (TEM) (**Fig. 1B**). To test the efficacy of the PIMA-GA-oxaliplatin nanoparticles in vitro, we performed cell viability assays using 4T1 breast cancer cell line. Cell viability was quantified using a 3-(4,5-dimethylthiazol-2-yl)-5-(3-carboxymethoxyphenyl)-2-(4-sulfophenyl)-2H-tetrazolium, inner salt (MTS) assay at 48 h post-incubation. PIMA-GA-oxaliplatin nanoparticles demonstrated significant 4T1 cell kill comparable to oxaliplatin supporting the hypothesis that the rate of aquation is critical for efficacy (**Fig. 2**). Tagging the polymer with fluorescein (**Fig. 3**) enabled the temporal tracking of uptake of the nanoparticles into the cells, which were colabeled with a lysotracker-red dye to label the endolysosomal compartments. As shown in **Fig. 3**, a rapid uptake of the nanoparticles and internalization into the endolysosomal compartment was observed in the case of 4T1 cells. As the nanoparticles localized to the lysosomal compartment, we tested the release of Pt from the nanoparticles at pH 5.5, mimicking the acidic pH of the endolysosomal compartment of the tumor (17). As PIMA-GA- oxaliplatin nanoparticles exhibited the desired release rates for platinum and also exhibited in vitro efficacy comparable to free oxaliplatin, we validated the therapeutic efficacy of these nanoparticles in vivo. Mice bearing established 4T1 breast cancer were randomized into five groups and treated thrice with (i) vehicle (PBS) control; (ii) oxaliplatin (5 mg/kg), (iii) oxaliplatin (15 mg/kg), (iv) PIMA-GA oxaliplatin nanoparticles (5 mg/kg) and (v) PIMA-GA oxaliplatin nanoparticles (15 mg/kg). The mice injected with vehicle formed large tumors and were euthanized. The animals in the other groups were also sacrificed at the same time point to evaluate the effect of the treatments on tumor pathology. As shown in **Fig. 4**, whereas both free oxaliplatin and the oxaliplatin-nanoparticles exhibited similar tumor inhibition, the free drug resulted in a significant reduction in body weight indicating systemic toxicity. Furthermore, necropsy revealed that treatment with free oxaliplatin results in a significant reduction in the weights of kidney and spleen, indicating nephrotoxicity and hematotoxicity consistent with previous reports. In contrast, oxaliplatin nanoparticles had no effect on the weights of the kidneys or the spleen (**Fig. 4 D**). To elucidate the mechanism underlying cytotoxicity, we TUNEL-stained tumor sections, which revealed a significant induction of apoptosis following treatment with
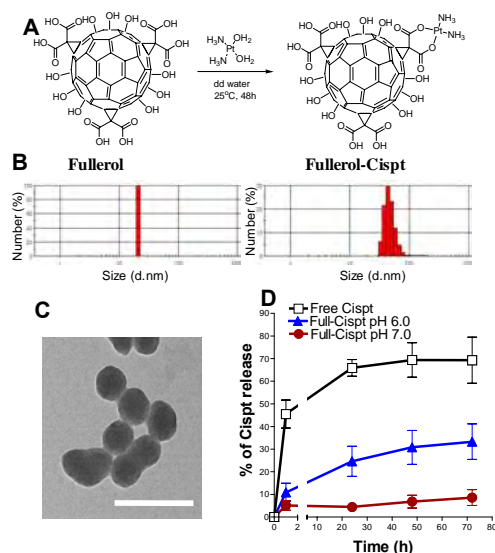

Fig. 4. Top panel shows tumors excised from animals treated with free or nanoparticles or vehicle. Graphs show the effect of treatments on tumor volume (A) and body weight (B) over the treatment period. Biodistribution (C) of Pt in tumor, kidney, spleen and liver as measured using ICP-MS spectroscopy 24 h hours following administration of drugs. (D) Graphs show the effect of treatment on the organ weight of kidneys and spleen as a marker for nephrotoxicity and hematological toxicity [n=4]. (E) Epifluorescence images of representative drug-treated tumor cross-sections that were TUNEL-labeled for apoptosis using Texas red-labeled nucleotide. (F) Images show H&E stained cross-sections of kidney of animals demonstrating severe nephrotoxicity induced by the free drug.

Fig. 5. (A) Schematic shows the Fullerol-cisplatin conjugation and its effect on size of particles shown in the DLS measurement (B). (C) HRTEM images of Fullerol-cisplatin nanoparticles Bar= 100 nm. (D) Graph shows the pH-dependent release of cisplatin from the nanoparticles.

both free oxaliplatin and oxaliplatin nanoparticles (**Fig. 4E**). Labeling the kidney sections for TUNEL validated significant apoptosis in the animals treated with free oxaliplatin as opposed to minimal nephrotoxicity in the nanoparticle-treated group (**Fig. 4E**). Indeed, biodistribution studies using inductively coupled plasma-spectrometry revealed that the concentration of Pt in the kidney following administration of the cisplatin-nanoparticle is negligible as compared to that attained following administration of free drug (**Fig. 4C**), which can explain the reduction in nephrotoxicity. Similarly, the concentration of platinum in the reticuloendothelial system (RES) was lower when administered as a nanoparticle as compared with free drug, indicating that the nanoparticles can

3

escape the RES. Furthermore, we explored the novel application of fullerenol in drug delivery. We demonstrate that the fullerenols enable the conjugation of high levels of the chemotherapeutic agent, cisplatin, which is released in a sustained manner under conditions mimicking tumor pathophysiology. Treatment with fullerol-cisplatin exerted an improved antitumor outcome as compared to free cisplatin, without the systemic toxicity associated with the latter. Our findings demonstrate that the fullerols could emerge as a anti-angiogenic agent for delivery of anticancer drugs.

At first we identified a malonic acid functionalized fullerol, where each malonic acid could serve as the conjugation site for cisplatin. We found that these fullerol–cisplatin conjugates selfassembles in to nanometer size **Fig. 5 B&C**. We next tested the Fullerol-cisplatin nanoparticle on a 4T1 *in vitro.* As shown in **Fig. 6 A**. fullerol-cisplatin nanoparticles demonstrated significant cell kill comparable to cisplatin. To further explore the uptake mechanism we labeled the fullerol-Cis with FITC, and tracked its internalization into the cells and into the lysosomes through colocalization of the FITC-signal (green fluorescence) with Lysotracker Red (red fluorescence). As shown in **Fig. 7**, a rapid uptake of the nanoparticles and internalization into the endolysosomal compartment was observed in the 6 h of treatment.

To study the release kinetics of the active drug from the nanoparticle-drug conjugates, we incubated the nanostructures at pH 6.0, mimicking the acidic pH of the endolysosomal compartment of the tumor. We also selected pH7.0 as a reference pH in the neutral range. We observed that acidic condition fullerol-cisplatin nanoparticles exhibited significantly higher rates of Pt release as compared with neutral condition. To further evaluate the endothelial tubulogenesis, we used a well characterized *in vitro* matrigel assay. As shown in **Fig. 6B** free cisplatin and fullerol alone induced inhibition of tube formation, but fullerol-cisplat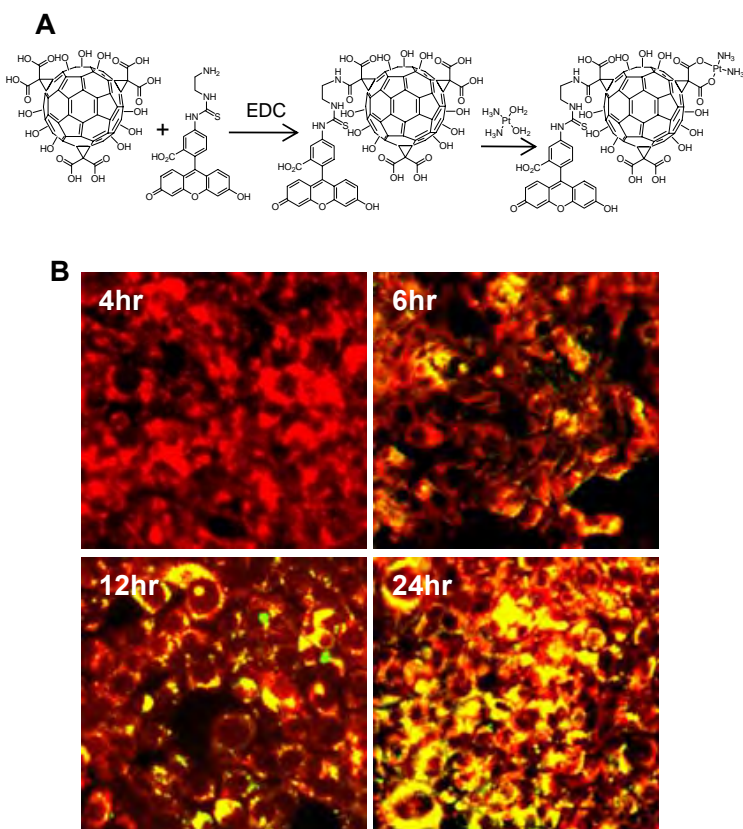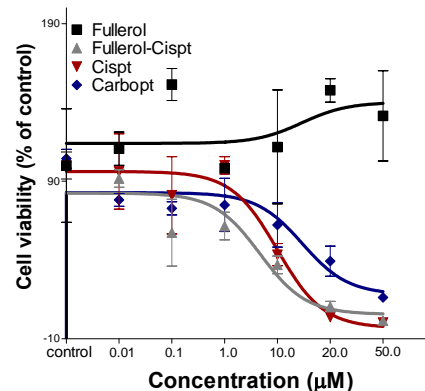in showed increased anti-angiogenic effect. To study the mechanisms underlying cisplatin and its nanostructure treatment, we monitored the effect of
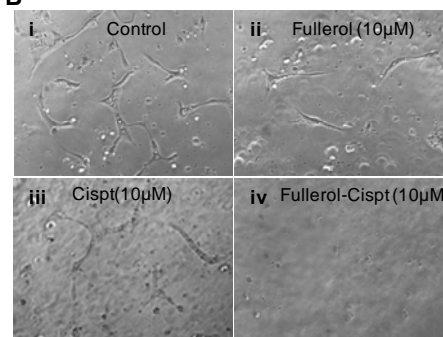

A

B

Fig. 6. (A) Graphs show effect of Fullerol-cisplatin nanoparticles on 4T1 cells viability measured using MTS assay. (B) Effect of Fullerol-cisplatin conjugates free cisplatin and fullerols on tubulogenesis.
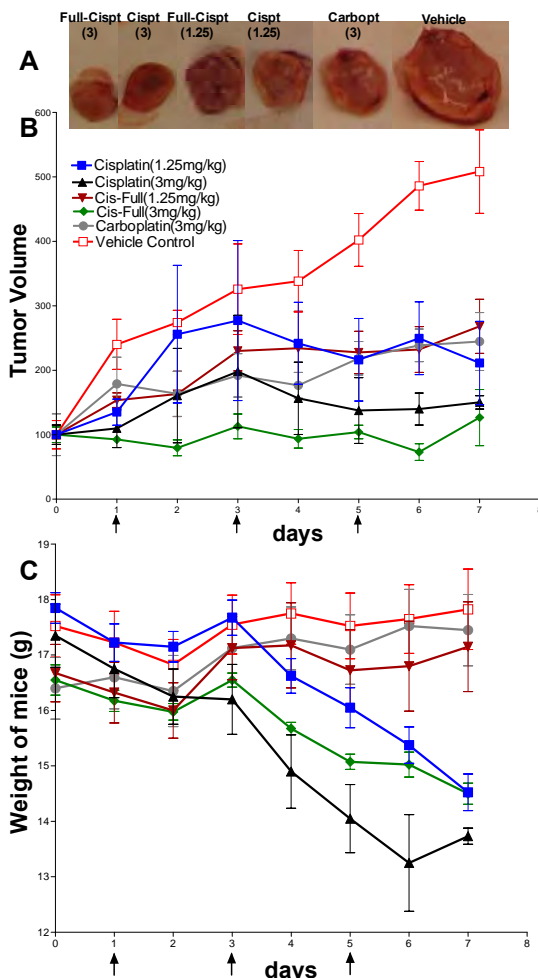
Fig. 8. (A) Top panel shows tumors excised from animals treated with free or fullerol-cisplatin conjugates or vehicle. Graphs show the effect of treatments on tumor volume (B) and body weight (C) over the treatment period. The animals were dosed thrice (shown by arrows on x-axis). Data shown are mean±SE, n=4.

A

B

Fig. 7. (A) Scheme shows the synthesis of the labeled Fullerol-cisplatin conjugates with FITC to enable the tracking of cell ular uptake of the nanoparticles. (B) Ep ifluorescence images shows the temporal uptake of FITC-labeled Fullerol-cisplatin conjugates into 4T1 breast cancer cells. The cells were counter-labeled with lysotracker-Red to highlight the endolysosomal compartments. Colocalization of the signals in the merge images reveals internalization of the nanoparticles into the endolysosomal compartments.

treatment on cell cycle. To test whether the inhibition of cell cycle by cisplatin nanoparticles induce apoptosis, we probed the drug-treated cancer cells with annexin-V, which binds to the externalized phosphatidylserine on the surface of apoptotic cells. Counterstaining the cells with propidium iodide enables the distinction between necrotic and apoptotic cells and it revealed that the cisplatin nanoparticle treatment could induce apoptotic cell death. As fullerol-cisplatin nanoparticles exhibited the inhibition of tubulogenesis in endothelial cells and also exhibited *in vitro* efficacy comparable to cisplatin, we validated the therapeutic efficacy of
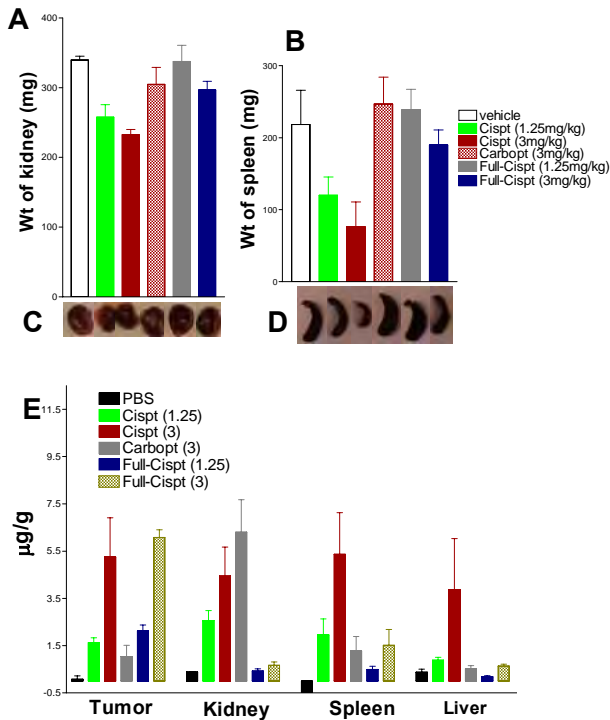

Fig. 9. Graphs show the effect of treatment on the organ weight of kidneys (A) and spleen (B) as a marker for nephrotoxicity and hematological toxicity [n=4]. The images on bottom of each graph (C & D) show representative organs from each treatment group. Biodistribution (E) of Pt in tumor, kidney, spleen and liver as measured using ICP-MS spectroscopy 24 h hours following administration of free or cisplatin fullerol conjugates.

these nanoparticles *in vivo*. Mice bearing 4T1 breast cancer were randomized into three groups and treated three times with (i) vehicle control; (ii) Cisplatin (1.25 and 3 mg/kg); (iii) Carboplatin (3 mg/kg); (iv) fullerol-Cisplatin nanoparticles (1.25 and 3 mg/kg). The mice injected with vehicle formed large tumors by day 16 and were euthanized. The animals in the other groups were also sacrificed at the same time point to evaluate the effect of the treatments on tumor pathology. As shown in **Fig. 8A**, cisplatin induced dose dependent tumor inhibition, and at a dose equivalent to 3 mg/kg of platinum, administration of the nanoparticle formulation resulted in greater inhibition of breast cancer progression as compared with the free drug. The necropsy revealed that treatment with free cisplatin resulted in a significant reduction in the weights of kidney and spleen [**Fig. 9A&B**], indicating nephrotoxicity and hematotoxicity consistent with previous reports. Cisplatin nanoparticles had no

Fig. 10. Representative images of cross-sections of tumor and kidney from animals exposed to different treatments. (A) Images show H&E stained cross-sections of kidney of animals treated with free cisplatin or Fullerol-cisplatin conjugates demonstrating severe nephrotoxicity induced by the free drug. (B) Epifluorescence images of representative drug-treated tumor cross-sections that were TUNEL-labeled for apoptosis using Texas red-labeled nucleotide. (C) To evaluate effect of fullerol-cisplatin conjugates on tumor angiogenesis the tumor crossections were immunolabeled with von Willebrand Factor (vWF) antibody and then probed with Alexa 488 conjugated secondary antibody. The sections were counterstained with propidium iodide. Images were captured with a Nikon Ti epifluorescence microscope at low magnification to capture a large view field.

effect on the weights of the kidneys, and reduced spleen size only at the highest dose. This was further validated by pathological analysis of kidney H&E stained crosssections, which revealed significant tubular necrosis in the animals treated with free cisplatin as compared with cisplatin nanoparticle [**Fig. 10A**]. Biodistrubution studies clearly indicates that free cisplatin and carboplatin accumulated evenly in tissues while fullerol cisplatin conjugates are preferentially observeed in tumor tissue (**Fig. 9E**). To elucidate the mechanism underlying tumor inhibition, we labeled the tumor cross sections for TUNEL, which revealed a significant induction of apoptosis following treatment with both free cisplatin and fullerol-cisplatin nanoparticles [**Fig. 6B**]. Labeling the kidney sections for TUNEL demonstrated significant apoptosis in the animals treated with free cisplatin as opposed to minimal nephrotoxicity in the nanoparticle-treated group [**Fig. 10B**]. To test the effect on tumor angiogenesis, tumor sections were immune-labeled for Von Willebrand factor (vWF), an endothelial cell marker. From **fig. 10 C** it is clearly seen that fullerol-cisplatin conjugate inhibited angiogenesis compared with vehicle treated
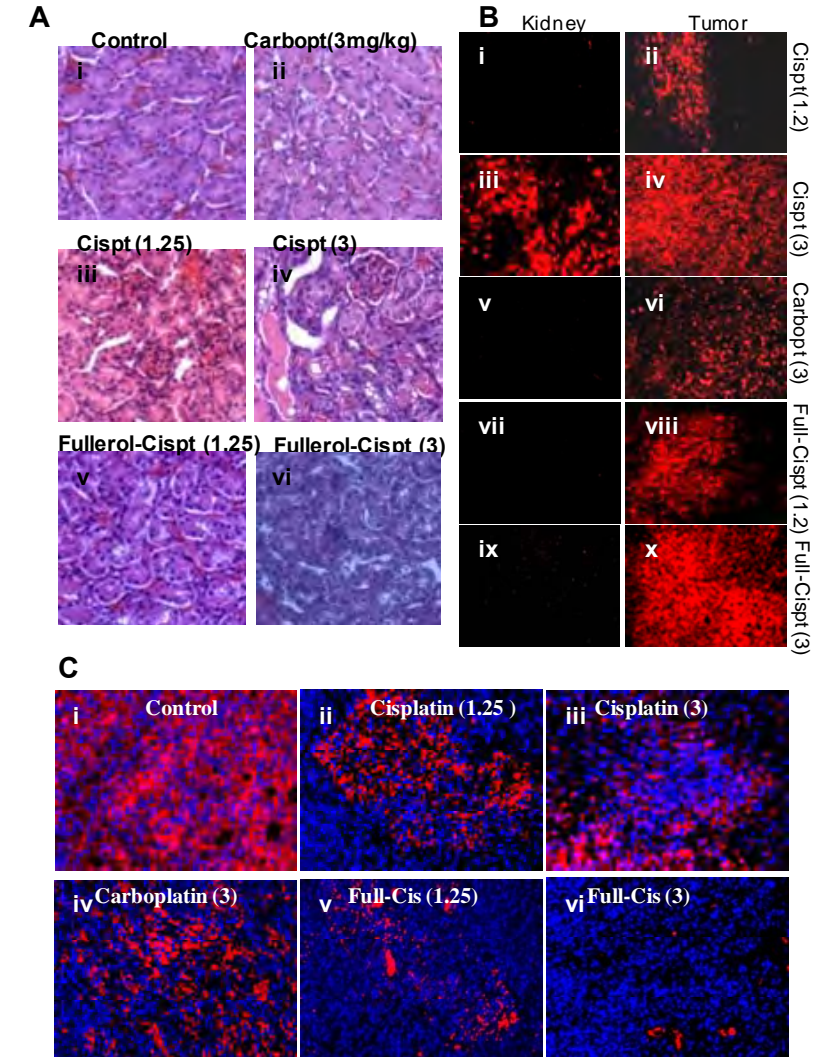
controls or cisplatin alone. These results indicate that the fullerol-cisplatin conjugate increases the therapeutic index of the cytotoxic agent. This could arise from the synergistic effect of anti-angiogenic activity and cytotoxicity.

Key Research Accomplishments

- Rationally engineered polymer inspired by the bioactivation of cisplatin and oxaliplatin improving antitumor efficacy of cisplatin by capitalizing on the inherent properties of nanoscale.
- Opening up the possibility to increase the maximal tolerated dose of cisplatin and oxaliplatin.
- Additionally developed fullerol as drug delivery vehicle which has its inherent anti-angiogenic activity which synergistic with anticancer drug cisplatin.
- These fulleroplatinates showed improved efficacy of cisplatin by passively home in to tumors while anti-angiogenic vehicle (fullerenol) disrupts blood flow to the tumors.
- Our findings demonstrate that the fullerenols could emerge as anti-angiogenic agent for delivery of anticancer drugs.

Reportable Outcomes

Original research publications: Paraskar A, Soni S, Chin K, Chaudhuri, P, Muto K, Berkowitz J, Handlogten M, Alves N J, Bilgicer B, Dinulescu D, Mashelkar R A, Sengupta S. (2010) Harnessing structure-activity relationship to engineer a cisplatin nanoparticle for enhanced antitumor efficacy. Proc Natl Acad Sci USA. 107: 12435-12440.

Patents: Paraskar, A. S.; Soni, S., Sengupta, S. (2010) Nanoscale platinum compounds and methods of use thereof. US Patent # WO 2010091192.

Conclusion

In conclusion, we demonstrate that the rational engineering of a polymer inspired by the bioactivation of cisplatin and oxaliplatin enables the engineering of a unique nanoplatinates, which improves antitumor efficacy of cisplatin by capitalizing on the inherent properties of nanoscale. This opens up the possibility to increase the maximal tolerated dose of cisplatin, which is an effective chemotherapeutic agent but dose limited due to nephrotoxicity. The clinical familiarity of using an established and globally used chemotherapeutic, together with the low cost of the basic building blocks used in fabricating the nanoparticle, can facilitate the rapid translation of this technology, thereby validating the potential of nanotechnology to impact global health (32). Additionally, we developed fullerenol as novel anti-angiogenic drug delivery vehicle, with its cisplatin conjugate showed improved antitumor efficacy by synergistic anti-angiogenic and anti-cancer activity.

References

1. Kelland L (2007) The resurgence of platinum-based cancer chemotherapy. *Nat Rev Cancer* 7:573–584.
2. Leong CO, et al. (2007) The p63⁄p73 network mediates chemosensitivity to cisplatin in a biologically defined subset of primary breast cancers. *J Clin Invest* 117:1370–1380.
3. Choi HS, et al. (2007) Renal clearance of quantum dots. *Nat Biotechnol* 25:1165–1170.
4. Ferrari M (2005) Cancer nanotechnology: Opportunities and challenges. *Nat Rev Cancer* 5:161–171.
5. Moghimi SM, et al. (2001) Long-circulating and target-specific nanoparticles: Theory to practice. *Pharmacol Rev* 53:283–318.
6. Decuzzi P, et al. (2009) Intravascular delivery of particulate systems: Does geometry really matter? *Pharm Res* 26:235–243.
7. Chaudhuri P, et al. (2010) Shape effect of carbon nanovectors on angiogenesis. *ACS Nano* 4:574–582.
8. Gratton SE, et al. (2008) The effect of particle design on cellular internalization pathways. *Proc Natl Acad Sci USA* 105:11613–11618.
9. Yuan F, et al. (1995) Vascular permeability in a human tumor xenograft: Molecular size dependence and cutoff size. *Cancer Res* 55:3752–3756.
10. Yuan F, et al. (1994) Microvascular permeability and interstitial penetration of sterically stabilized (stealth) liposomes in a human tumor xenograft. *Cancer Res* 54:3352–3356.
11. Avgoustakis K, et al. (2002) PLGA-mPEG nanoparticles of cisplatin: In vitro nanoparticle degradation, in vitro drug release, and in vivo drug residence in blood properties. *J Controlled Release* 79:123–135.
12. Fujiyama J, et al. (2003) Cisplatin incorporated in microspheres: Development and fundamental studies for its clinical application. *J Controlled Release* 89:397–408.
13. Haxton KJ, Burt MH (2009) Polymeric drug delivery of platinum-based anticancer agents. *J Pharm Sci* 98:2299–2316.
14. Rademaker-Lakhai JM, et al. (2004) A Phase I and pharmacological study of the platinum polymer AP5280 given as an intravenous infusion once every 3 weeks in patients with solid tumors. *Clin Cancer Res* 10:3386–3395.
15. Lin X, et al. (2004) Improved targeting of platinum chemotherapeutics. The antitumour activity of the HPMA copolymer platinum agent AP5280 in murine tumour models. *Eur J Cancer* 40:291–297.
16. Paraskar A, et al. (2010) Harnessing structure-activity relationship to engineer a cisplatin nanoparticle for enhanced antitumor efficacy. *Proc Natl Acad Sci USA.* 107: 12435-12440.
17. Song CW, et al. (2006) Influence of tumor pH on therapeutic response. Cancer Drug Discovery and Development: Cancer Drug Resistance, ed B Teicher (Humana Press, Totowa, NJ), pp 21–42.
18. Salamanca-Buentello F, et al. (2005) Nanotechnology and the developing world. *PLoS Med* 2:e97.

Appendices

Harnessing structure-activity relationship to engineer a cisplatin nanoparticle for enhanced antitumor efficacy

Abhimanyu S. Paraskar[a,b,1], Shivani Soni[a,b,1], Kenneth T. Chin[c], Padmaparna Chaudhuri[a,b], Katherine W. Muto[c], Julia Berkowitz[c], Michael W. Handlogten[d], Nathan J. Alves[d], Basar Bilgicer[d], Daniela M. Dinulescu[b,c], Raghunath A. Mashelkar[e,2], and Shiladitya Sengupta[a,b,c,f,g,h,i,2]

[a]Department of Medicine, Brigham and Women's Hospital, Cambridge, MA 02139; [b]Harvard Medical School, Boston, MA 02115; [c]Department of Pathology, Brigham and Women's Hospital, Boston, MA 02115; [d]University of Notre Dame, Notre Dame, IN 46556; [e]National Chemical Laboratories, Pune 411008, India; [f]Harvard–MIT Division of Health Sciences and Technology, Cambridge, MA 02139; [g]Indo–US Joint Center for Nanobiotechnology, Cambridge, MA 02139; [h]Dana Farber Cancer Institute, Brookline, MA 02445; and [i]Translational Health Science and Technology Institute, New Delhi 110067, India

Cisplatin is a first line chemotherapy for most types of cancer. However, its use is dose-limited due to severe nephrotoxicity. Here we report the rational engineering of a novel nanoplatinate inspired by the mechanisms underlying cisplatin bioactivation. We engineered a novel polymer, glucosamine-functionalized polyisobutylene-maleic acid, where platinum (Pt) can be complexed to the monomeric units using a monocarboxylato and an O → Pt coordinate bond. We show that at a unique platinum to polymer ratio, this complex self-assembles into a nanoparticle, which releases cisplatin in a pH-dependent manner. The nanoparticles are rapidly internalized into the endolysosomal compartment of cancer cells, and exhibit an IC50 (4.25 ± 0.16 μM) comparable to that of free cisplatin (3.87 ± 0.37 μM), and superior to carboplatin (14.75 ± 0.38 μM). The nanoparticles exhibited significantly improved antitumor efficacy in terms of tumor growth delay in breast and lung cancers and tumor regression in a K-ras$^{LSL/+}$/Pten$^{fl/fl}$ ovarian cancer model. Furthermore, the nanoparticle treatment resulted in reduced systemic and nephrotoxicity, validated by decreased biodistribution of platinum to the kidney as quantified using inductively coupled plasma spectroscopy. Given the universal need for a better platinate, we anticipate this coupling of nanotechnology and structure-activity relationship to rationally reengineer cisplatin could have a major impact globally in the clinical treatment of cancer.

chemotherapy | nanomedicine | cancer

In the continuing search for effective treatments for cancer, an emerging paradigm is the use of nanotechnology to uncap the full potential of existing chemotherapy agents (1). Integral physicochemical properties of nanovectors can be modulated to improve the antitumor efficacy of chemotherapeutic agents (2). For example, the shape and size of nanostructures can play a deterministic role in the biological outcome (3–5). Similarly, surface modifications to increase hydrophilicity can mask the nanovectors from the reticuloendothelial system, thereby increasing circulation time and altering the pharmacokinetics of the active agents (2). Such nanovectors accumulate preferentially in the tumors due to the unique leaky tumor vasculature coupled with impaired intratumoral lymphatic drainage, which contributes to an enhanced permeation and retention (EPR) effect (6, 7). Indeed, nanovectors were shown to deliver between 5–11× more doxorubicin to Kaposi sarcoma lesions than to normal skin (8). Similarly, the tumor paclitaxel concentration-time area under the curve was found to be 33% higher when administered as an albumin-paclitaxel nanoparticle, and is currently approved for use in metastatic breast cancer (9).

Cisplatin [cis-dichlorodiammineplatinum(II)] is one of the most commonly used chemotherapeutic agents besides doxorubicin and paclitaxel, and is a first line therapy for most malignancies, including testicular, ovarian, cervical, and lung cancer (10). It

was also shown recently to be effective in triple negative breast cancer (11). Its clinical use, however, is dose-limited due to systemic toxicity, primarily to the kidney (12). Consequently, developing an improved cisplatin has been a holy grail in cancer drug discovery. We rationalized that this challenge could be addressed by harnessing a nanotechnology-based strategy. It is now well-documented that nanoparticles >5 nm will avoid renal clearance (13), and thereby could potentially reduce cisplatin nephrotoxicity.

The development of a cisplatin nanoparticle has been a challenge resulting from its physicochemical properties, which make it difficult to entrap it in polymeric sustained-release nanoparticles (14, 15). In a recent study, Dhar et al. generated a platinum (IV) complex (c,t,c-[Pt(NH$_3$)$_2$(O$_2$CCH$_2$CH$_2$CH$_2$CH$_3$)$_2$Cl$_2$]), which had sufficient hydrophobicity for encapsulation in PLGA-b-PEG nanoparticles, but the prodrug had to be intracellularly processed into cisplatin (16). Alternative strategies based on the conjugation of platinum to polymers (for example, a polyamidoamine dendrimer-platinum complex), resulted in 200–550-fold reduction in cytotoxicity than free cisplatin as a result of strong bonds that are formed between the polymer and Pt (17). Similarly, AP5280, a N-(2-hydroxypropyl) methacrylamide copolymer-bound platinum was found to exert minimal nephrotoxicity in clinical studies (18), but was less potent than carboplatin as the platinum is held to an aminomalonic acid chelating agent coupled to the COOH-terminal glycine of a tetrapeptide spacer (19). These studies also shed light on the impact of the complexation environment of the platinum on the efficacy. We used this structure-activity relationship underlying the activation of platinum to engineer a unique nanoplatinate that exhibited significantly improved antitumor efficacy in terms of tumor growth delay in lung and breast cancer and tumor regression in K-ras$^{LSL/+}$/Pten$^{fl/fl}$ ovarian cancer models, along with reduced systemic and nephrotoxicity.

Results

Cisplatin Bioactivation-Inspired Polymer Design for Nanoparticle Engineering. Cisplatin gets rapidly activated through intracellular

ENGINEERING

MEDICAL SCIENCES

aquation of the chloride leaving groups to form *cis*-[Pt(NH$_3$)$_2$ Cl(OH$_2$)]$^+$ and *cis*-[Pt(NH$_3$)$_2$(OH$_2$)]$^{2+}$, following which Pt forms covalent bonds to the N7 position of purine bases to form prevalent GpG and ApG intrastrand and interstrand crosslinks (20). In comparison, carboplatin and oxaliplatin have a cyclobutane-1, 1-dicarboxylato and an oxalate respectively as the leaving groups, which chelate the platinum more strongly conferring greater stability to the leaving group-Pt complex (Fig. 1) (21). As a result both carboplatin and oxaliplatin exhibit improved nephrotoxicity profile but also lesser efficacy than cisplatin (22, 23). We rationalized that the design of a nanoparticle

modeled on the leaving group would offer the greatest possibility of retaining the efficacy of cisplatin while the size of nanoparticle could bypass renal clearance and thereby reduce nephrotoxicity. As the first step, we identified a polymer, where each monomeric unit could serve as the leaving group of cisplatin. As shown in Fig. 1, hydrolysis of poly-isobutylene-maleic anhydride, comprised of 40 units of maleic acid linked linearly through an isobutylene linker, resulted in the generation of poly-isobutylene-maleic acid (PIMA), where each monomer can be complexed to *cis*-[Pt(NH$_3$)$_2$(OH$_2$)]$^{2+}$ through dicarboxylato linkages. Complexing all 40 monomeric units of the polymer with Pt resulted in gelation. However, lower Pt to polymer ratio resulted in self-assembly into nanoparticles as revealed by dynamic laser light scatter (DLS), with the size being governed by the Pt:polymer unit ratio [Fig. 2A]. At a Pt:polymer ratio of 15:1, we obtained nanoparticles that were narrowly distributed in 80–140 nm size range. It is now well-established that nanoparticles in the optimal size range of 80–160 nm home preferentially into tumors resulting from the EPR effect (7), suggesting that the polymeric-cisplatin nanoparticle (PIMA-cisplatin) could potentially reduce systemic side effects and exhibit increased intratumoral delivery. We next tested the PIMA-cisplatin nanoparticle on a Lewis lung carcinoma cell line in vitro. As shown in Fig. 3A whereas PIMA-cisplatin nanoparticle induced cell kill, the efficacy was significantly lower than free cisplatin and similar to carboplatin, consistent with the stable dicarboxylato complexation between the platinum and the maleic acid monomers (22, 23).
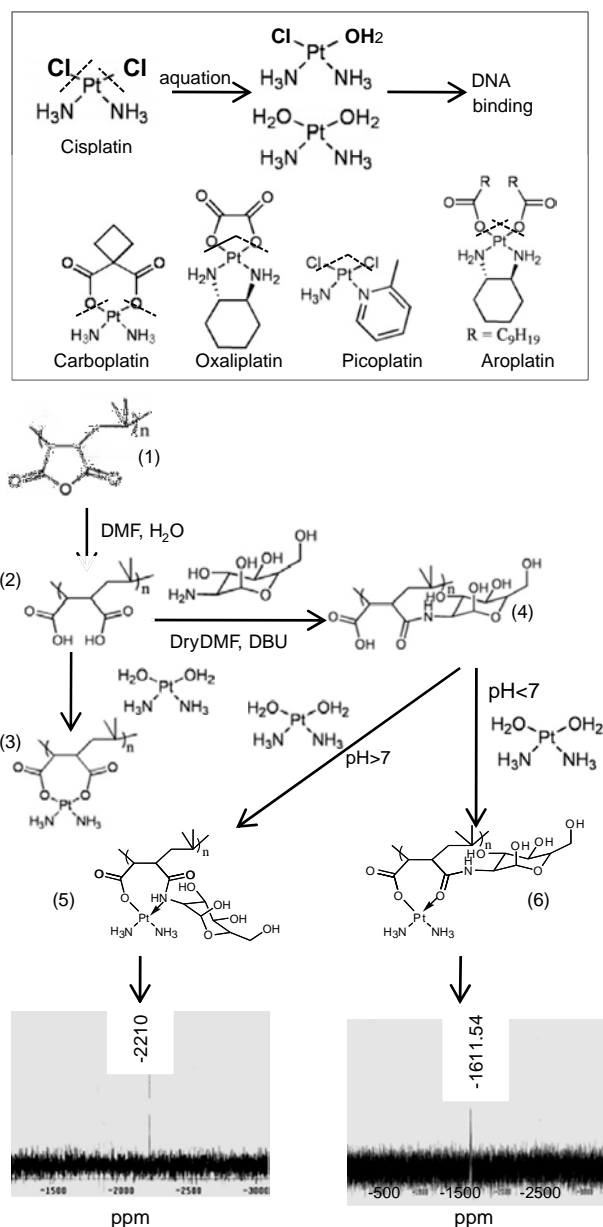

Fig. 1. Structure-activity relationship inspired engineering of a cisplatin nanoparticle. (*A*) Schematic shows the mechanism underlying the intracellular activation of cisplatin and analogues through aquation (dash lines). (*B*) Scheme shows the synthesis of PIMA-cisplatin and PIMA-glucosamine (PIMA-GA)-cisplatin complex. Transformation of polymaleic anhydride (*n* = 40) (*1*) to polymaleic acid [PIMA] (*2*) enables complexation of [NH$_2$]$_2$Pt[OH]$_2$ through dicarboxylato bonds (*3*). Derivatization of one arm of PIMA with glucosamine to generate PIMA-GA (*4*), and complexation with [NH$_2$]$_2$Pt[OH]$_2$ can lead to two isomers (*5*, *6*) depending on pH, characterized by unique NMR signatures.
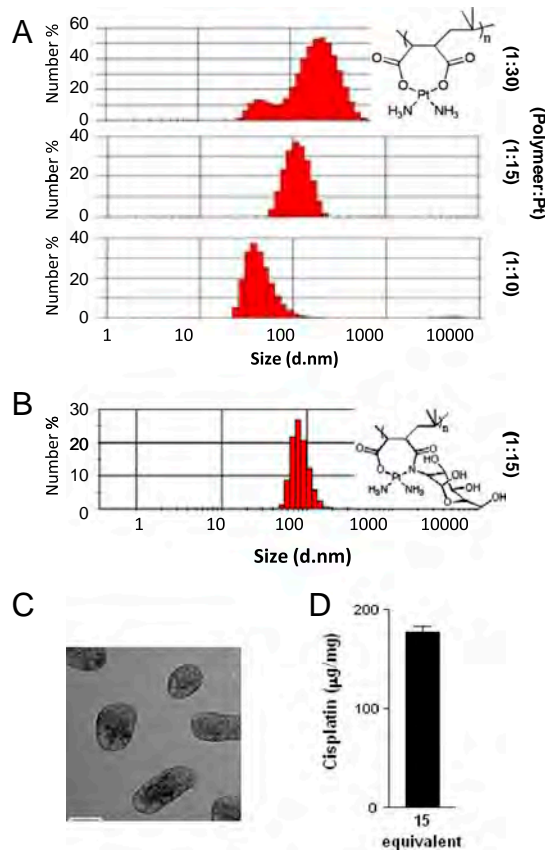
Fig. 2. Physicochemical characterization of nanoparticles. (*A*). Graphs show the relationship between the size distribution of PIMA-cisplatin nanoparticles as a function of polymer to platinum ratio as measured by DLS. (*B*) Size distribution of PIMA-GA-CisPt (O → Pt) nanoparticle at a 15:1 Pt:polymer ratio measured using DLS. (*C*) Representative high-resolution TEM images of PIMA-GA-cisplatin nanoparticles Bar = 125 nm (*D*) Graph shows the total platinum loaded per mg of polymer at this ratio. The data shown are mean ± SE from *n* = at least 3 independent experiments.

Fig. 3. In vitro characterization of cisplatin nanoparticle. Graphs show the concentration-effect of different treatments on cellular viability of (A) LLC and (B) 4T1 breast cancer cells as measured using MTS assay. The x-axis shows the equivalent concentrations of platinum. Where blank polymeric controls were us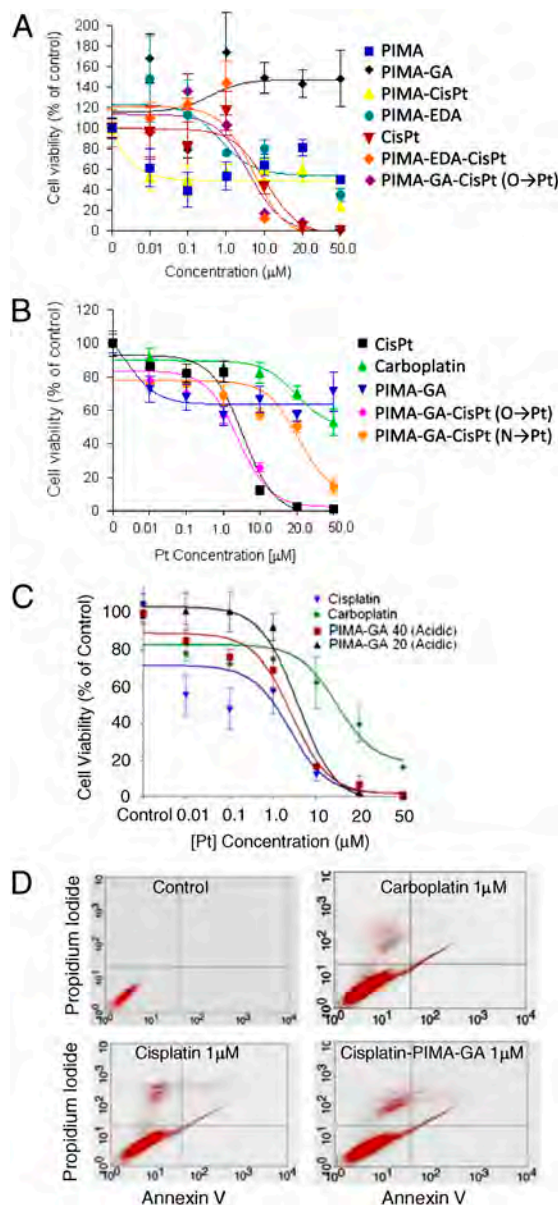ed, dose of polymer used was equivalent to that used to deliver that specific dose of cisplatin in the complexed form. (C) Graph shows effect of PIMA-GA-cisplatin (O → Pt) nanoparticles on LLC cells viability, where the either 20 or all 40 monomers of the PIMA backbone is derivatized with glucosamine, thereby altering the Pt environment. (D) Representative FACS images of LLC cells labeled with Annexin V-FITC and PI to monitor apoptosis and necrosis. Cells were incubated with the drugs for 24 h. The data shown are mean ± SE, n = 3.

Rational Optimization of the Polymer Based on Structure-Activity Relationship. As the next step, to improve efficacy of the nanoparticles, we rationalized that derivatizing one arm of each monomer unit of the polymer with biocompatible glucosamine to generate a PIMA-glucosamine conjugate (PIMA-GA) would convert the dicarboxylato bonds with Pt to a monocarboxylato bond and a coordinate bond, which should release Pt more easily (Fig. 1). NMR characterization of the Pt environment revealed that complexation of PIMA-GA and cisplatin in an acidic pH generated an isomeric molecule, [PIMA-GA-cisplatin (O → Pt)], characterized by the monocarboxylato and a O → Pt coordination complex as

indicated by a single Pt NMR peak at −1611.54 ppm. Complexing the cisplatin with PIMA-GA at an alkaline pH (pH 8.5) favored the formation of an isomeric PIMA-GA-cisplatin (N → Pt) complex, where the Pt is complexed through a monocarboxylato and a more stable N → Pt coordinate bond characterized by a unique peak at −2210 ppm. The possibility of generating these two pH-dependent states allowed us to further dissect the impact of Pt environment, specifically the leaving groups, on the biological efficacy. The complexation of cisplatin to PIMA-glucosamine (PIMA-GA) polymer at a ratio of 15:1 resulted in self-assembly into nanoparticles in the desired narrow size bandwidth of 80–150 nm as confirmed by DLS (Fig. 2B) and high-resolution transmission electron microscopy (TEM) (Fig. 2C). Furthermore, we achieved a loading of 175 ± 5 μg/mg of polymer (Fig. 2D), which is significantly higher than can be achieved using traditional nanoparticle formulations (14, 15).

Characterizing the Uptake and Efficacy of Nanoparticles In Vitro. To test the efficacy of the PIMA-GA-cisplatin nanoparticles in vitro, we performed cell viability assays using Lewis lung carcinoma (LLC) and 4T1 breast cancer cell lines. Cell viability was quantified using a 3-(4,5-dimethylthiazol-2-yl)-5-(3-carboxymethoxy-phenyl)-2-(4-sulfophenyl)-2H-tetrazolium, inner salt (MTS) assay at 48 h postincubation. The LLC cells (Fig. 3A) were more susceptible to the cisplatin-nanoparticles than the 4T1 breast cancer cells (Fig. 3B). PIMA-GA-cisplatin (O → Pt) nanoparticles demonstrated significant LLC cell kill (IC50 = 4.25 ± 0.16 μM) comparable to cisplatin (IC50 = 3.87 ± 0.37 μM) and superior to carboplatin (IC50 = 14.75 ± 0.38 μM), supporting the hypothesis that the rate of aquation is critical for efficacy (Fig. 3). A similar efficacy was observed when we replaced glucosamine with ethylene diamine, which creates a similar Pt complexation environment as glucosamine (Fig. 3A). This was additionally supported by the observation that PIMA-GA-cisplatin (N → Pt) nanoparticles (IC50 = 6.36 ± 0.19 μM) were significantly less active than cisplatin, suggesting that the platinum environment is critical in defining the rate of aquation. To further validate the role of complexation environment, we generated PIMA-GA (20), where only 20 of the 40 monomers comprising a PIMA polymer were derivatized with glucosamine, thereby introducing a mixture of dicarboxylato bonds and monocarboxylato plus coordinate bonds that complex Pt to PIMA-GA. As shown in Fig. 3C, the concentration-efficacy curve shifts to the right with PIMA-GA(20)-cisplatin (IC50 = 5.85 ± 0.13 μM) as compared with PIMA-GA-cisplatin (O → Pt) nanoparticles, where all the 40 monomers are derivatized with glucosamine. Empty PIMA-GA polymer had no effect on the cell viability.

Labeling the cells for expression of phosphatidylserine on the cell surface revealed that the cisplatin nanoparticle treatment could induce apoptotic cell death, with LLCs being more susceptible than 4T1 cells (Fig. 3D and Fig. S1). Tagging the polymer with fluorescein (Fig. S2) enabled the temporal tracking of uptake of the nanoparticles into the cells, which were colabeled with a lysotracker-red dye to label the endolysosomal compartments. As shown in Fig. S2, a rapid uptake of the nanoparticles and internalization into the endolysosomal compartment was observed in the LLC cells within 15 min of treatment with in contrast to 2 h in the case of 4T1 cells.

Release of Active Cisplatin from Nanoparticle Is pH-Dependent. As the nanoparticles localized to the lysosomal compartment, we tested the release of Pt from the nanoparticles at pH 5.5, mimicking the acidic pH of the endolysosomal compartment of the tumor (24). We also selected pH 8.5 as a reference pH in the alkaline range. As shown in Fig. 4, at pH 5.5 PIMA-GA-cisplatin (O → Pt) nanoparticles resulted in a sustained release of cisplatin monitored over a 70 h period. In contrast the release at pH 8.5 was significantly lower, indicating a pH-dependent release of Pt. PIMA-
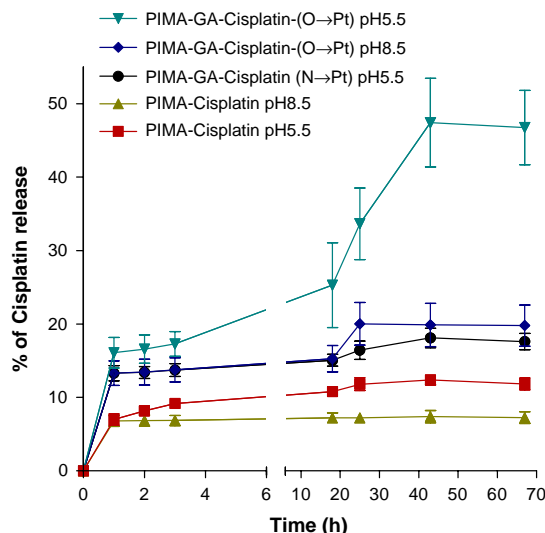
Fig. 4. Graph shows the pH-dependent release of cisplatin from the nanoparticles. The nanoparticles were incubated at pH 5.5 or pH 8.5 in a dialysis bag, and release over time was quantified. The data shown are mean ± SE from $n = 3$.

GA-cisplatin (N → Pt) released Pt at a slower rate even at pH 5.5, consistent with the fact that the N → Pt coordinate bond is stronger than the O → Pt linkage. As expected, we observed that PIMA-cisplatin nanoparticles exhibited significantly lower rates of Pt release as compared with both PIMA-GA-cisplatin (N → Pt) and PIMA-GA-cisplatin (O → Pt) as the Pt is held by more stable dicarboxylato bonds instead of a monocarboxylato and a coordinate bond.

Nanoparticle Induces Tumor Growth Delay and Regression with Reduced Nephrotoxicity. As PIMA-GA-cisplatin (O → Pt) nanoparticles exhibited the desired release rates for platinum and also exhibited in vitro efficacy comparable to cisplatin, we validated the therapeutic efficacy of these nanoparticles in vivo. Mice bearing established 4T1 breast cancer were randomized into five groups and treated thrice with (*i*) vehicle (PBS) control; (*ii*) Cisplatin (1.25 mg/kg); (*iii*) Cisplatin (3 mg/kg); (*iv*) PIMA-GA-Cisplatin (O → Pt) nanoparticles (1.25 mg/kg); and (*v*) PIMA-

GA-Cisplatin (O → Pt) nanoparticles (3 mg/kg). The mice injected with vehicle formed large tumors by day 16 and were euthanized. The animals in the other groups were also sacrificed at the same time point to evaluate the effect of the treatments on tumor pathology. As shown in Fig. 5, whereas both free cisplatin and the cisplatin-nanoparticles exhibited similar tumor inhibition, the free drug resulted in a significant reduction in body weight indicating systemic toxicity. Furthermore, necropsy revealed that treatment with free cisplatin results in a significant reduction in the weights of kidney and spleen, indicating nephrotoxicity and hematotoxicity consistent with previous reports. In contrast, cisplatin nanoparticles had no effect on the weights of the kidneys or the spleen (Fig. 5 *D* and *E*). To elucidate the mechanism underlying cytotoxicity, we TUNEL-stained tumor sections, which revealed a significant induction of apoptosis following treatment with both free cisplatin and PIMA-GA-cisplatin (O → Pt) nanoparticles (Fig. 5*F*). Labeling the kidney sections for TUNEL validated significant apoptosis in the animals treated with free cisplatin as opposed to minimal nephrotoxicity in the nanoparticle-treated group (Fig. 5*F*). Indeed, biodistribution studies using inductively coupled plasma-spectrometry revealed that the concentration of Pt in the kidney following administration of the cisplatin-nanoparticle is negligible as compared to that attained following administration of free drug (Fig. 5*G*), which can explain the reduction in nephrotoxicity. Similarly, the concentration of platinum in the reticuloendothelial system (RES) was lower when administered as a nanoparticle as compared with free cisplatin or carboplatin, indicating that the nanoparticles can escape the RES. In a separate experiment, animals bearing Lewis lung carcinoma were similarly treated and exhibited similar superior outcome with the nanoparticles (Fig. S3).

We next evaluated the PIMA-GA-cisplatin (O → Pt) nanoparticles in a K-ras$^{LSL/+}$/Pten$^{fl/fl}$ ovarian cancer model, in which cisplatin is a first line drug of choice. The discovery of frequent somatic *PTEN* mutations and loss of heterozygosity at the 10q23 *PTEN* locus in endometrioid ovarian cancer implicates a key role for *PTEN* in the etiology of this epithelial ovarian cancer subtype (25, 26). Similarly, *K-RAS* oncogene is also mutated in endometrioid ovarian cancer, albeit at a lesser frequency (27). In a recent study, the combination of these two mutations in the ovarian surface epithelium was found to induce invasive and widely metastatic endometrioid ovarian adenocarcinomas with complete penetrance, making it a good model for mimicking
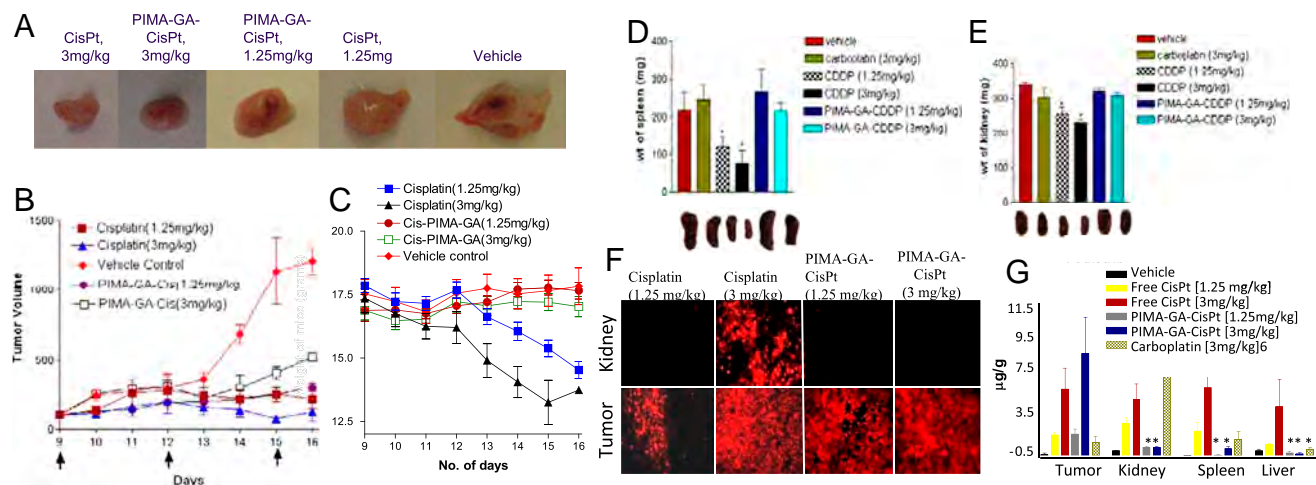

Fig. 5. In vivo characterization of PIMA-GA-cisPt nanoparticle in a 4T1 breast cancer model. (*A*) Representative 4T1 breast tumors excised from animals treated with cisplatin or PIMA-GA-cisPt (O → Pt) nanoparticle. Graphs show the effect of treatments on (*B*) tumor volume, (*C*) body weight, (*D*) spleen weight, and (*E*) kidney weight. The animals were dosed thrice (shown by arrows on x-axis). Data shown are mean ± SE, $n = 4$–8. The images on below of each graph show representative organs from each treatment group. (*F*) Representative images of cross-sections of tumor and kidney stained for TUNEL. Images were captured using a Nikon Ti epifluorescence microscope at low magnification to capture a large view field. (*G*) Tissue distribution of platinum following treatment in free (as cisplatin or carboplatin) or nanoparticle form. ($n = 3$–5 per treatment group.) *$P < 0.05$ vs. vehicle-treated group (ANOVA followed by Newman Keuls Post Hoc test).

human tumor progression (28). Vehicle-treated animals exhibited rapid tumor progression as quantified by luciferase expression. Treatment with the cisplatin-nanoparticles resulted in a dose-dependent inhibition of tumor progression, with the lower dose equivalent to 1.25 mg/kg exerting a similar inhibition as a 3 mg/kg dose of free cisplatin (Fig. 6). Treatment with the higher dose of cisplatin-nanoparticle (equivalent to 3 mg/kg of cisplatin) resulted in greater tumor inhibition without any significant loss of body weight or nephrotoxicity (Fig. 6D) compared with equi-dose of free cisplatin. Interestingly, we observed different levels of systemic toxicity in the different mouse strains, indicating distinct levels of susceptibility to the cytotoxic. This can potentially be explained by an enhanced distribution to the tumor with reduced clearance by the RES (Fig. 6E).

Discussion

Despite the development of targeted therapeutics (29), cytotoxic chemotherapeutics are still the first line therapy for all tumors. This necessitates novel strategies that can increase the therapeutic index of cytotoxics. In this study, we merged the mechanism of cisplatin bioactivation with the inherent advantages of nanotechnology to rationally engineer a unique polymeric nanoparticle that increases the therapeutic index of cisplatin. Furthermore, we used this platform to validate that the complexation environment of platinum plays a critical role in the efficacy of platinum-based cytotoxics.

Cisplatin is one of the most commonly used cytotoxic agents in cancer chemotherapy, and exerts its activity by interfering with transcription and other DNA-mediated cellular functions (30). In an elegant study, Davies et al. used a 1H-13N heteronuclear sequential quantum correlation NMR spectroscopy to demonstrate that aquation of cisplatin results in the rapid formation of cis-$[Pt(NH_3)_2Cl(OH_2)]^+$ and cis-$[Pt(NH_3)_2(OH_2)]^{2+}$ (31) with a rate constant of 8×10^{-5} s^{-1}. In contrast the rate constant for aquation of carboplatin was found to be 7.2×10^{-7} s^{-1}. This difference in their rate of activation was matched by their rates of binding to DNA (21, 22), which can explain the increased IC50 value of carboplatin compared with cisplatin (22). This was further validated in our studies as the PIMA-cisplatin nanoparticles, where both the dicarboxylato and the monocarboxylato plus N → Pt linkages confer greater stability to the Pt-polymer complex as seen in the release kinetics experiments. In contrast, we demonstrate that the rational introduction of an O → Pt coordinate linkage facilitates rapid activation of platinum, which can explain the increased efficacy of the PIMA-GA-Cisplatin (O → Pt) nanoparticles. The EPR effect combined with the approximately 100 nm nanoparticle size that exceed the 5 nm cutoff for clearance by the kidney could potentially explain the preferential accumulation of the PIMA-GA-Cisplatin (O → Pt) nanoparticles in the tumor with decreased renal platinum concentration as observed in this study. Together with the rapid release of platinum, this can explain the increased antitumor efficacy of PIMA-GA-Cisplatin (O → Pt) nanoparticle compared with free cisplatin at lower concentrations and increased therapeutic index at the highest concentrations as seen in vivo.

In conclusion, we demonstrate that the rational engineering of a polymer inspired by the bioactivation of cisplatin enables the engineering of a unique nanoplatinate, which improves antitumor efficacy of cisplatin by capitalizing on the inherent properties of nanoscale. This opens up the possibility to increase the maximal tolerated dose of cisplatin, which is an effective chemotherapeutic agent but dose limited due to nephrotoxicity. The clinical familiarity of using an established and globally used chemotherapeutic, together with the low cost of the basic building blocks used in fabricating the nanoparticle, can facilitate the rapid translation of this technology, thereby validating the potential of nanotechnology to impact global health (32).
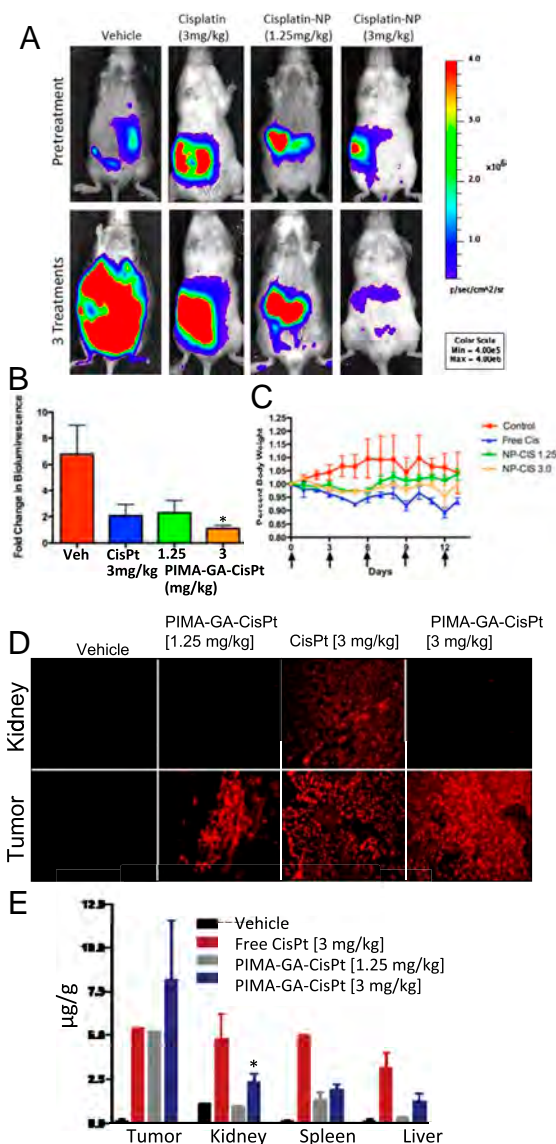

Fig. 6. PIMA-GA-cisplatin nanoparticle inhibits tumor growth in a K-ras[LSL/+]/Pten^{fl/fl} ovarian cancer model. (A). Representative pictures from 4 treatment groups before and after treatment. Tumor images was obtained with the IVIS Lumina II Imaging System. Quantification of bioluminescence was achieved by using the Living Image Software 3.1. Mice received 150 mg/kg of D-luciferin firefly potassium salt via intraperitoneal injection prior to imaging. (B). Bioluminescence quantification indicates a significantly decreased tumor luciferase signal in mice treated with cisplatin-NP compared to vehicle ($p < 0.05$, one-way ANOVA analysis). (C). Graph shows drug toxicity assessed by measurements in overall body weight. Daily recording of body weights indicated a significant loss of body weight in the free cisplatin group as compared to both cisplatin-NP (1.25 mg/kg and 3 mg/kg) treated groups ($p < 0.05$, two-way ANOVA analysis). (D) Epifluorescence images of cross sections of tumor treated with free of nanoparticle cisplatin that were stained for TUNEL as a marker for apoptosis. (E) Tissue distribution of platinum following treatment in free (as cisplatin or carboplatin) or nanoparticle form. ($n = 3$ per treatment group.) *$P < 0.05$ vs. vehicle-treated group (ANOVA followed by Newman Keuls Post Hoc test).

Materials and Methods

Synthesis of Cisplatin Nanoparticles. Poly(isobutylene-*alt*-maleic anhydride) was dissolved in dry dimethylformamide (DMF) in round bottom flask to which double distilled water was added. Solvent was removed under vacuum and low molecular weight impurities were removed using dialysis (MWCO: 1000 KD, Spectrapor). The solution was then lyophilized to get poly(isobutylene-*alt*-maleic acid) (PIMA). To generate PIMA-glucosamine polymer, poly(isobutylene-*alt*-maleic anhydride) was dissolved in DMF to which

Diaza(1, 3)bicyclo[5.4.0]undecane (DBU) and glucosamine was added. The resulting reaction mixture was allowed to stir at room temperature for 48 h and then quenched by adding double distilled water. The organic solvent was evaporated under vacuum. The resulting pale yellow solid was purified by dialysis. Nanoparticles were engineered by dissolving the polymers in double distilled water containing cisplatin for 48 h. The polymer-cisplatin conjugates were purified by dialysis. The dialyzed solutions were lyophilized, and resuspended to obtain the nanoparticles. The products were characterized at each step using ^{1}H, ^{13}C, and Pt NMR.

Particle Size Measurement. See *SI Text*.

Physicochemical Release Kinetics Studies. See *SI Text*.

In Vitro Cell Viability Assay. See *SI Text*.

FACS Analysis for Apoptosis. See *SI Text*.

Cellular Uptake Studies. See *SI Text*.

In Vivo Murine Lewis Lung Carcinoma and 4T1 Breast Cancer Models. The LLC cells and 4T1 Breast cancer cells (3×10^5) were implanted subcutaneously in the flanks of 4-week-old C57/BL6 and BALB/c mice (weighing 20 g, Charles River Laboratories) respectively. The drug therapy was started on day 6 for LLC and day 9 for the 4T1 tumors. Free or nanoparticle cisplatin was administered through tail vein at doses equivalent to 1.25 and 3 mg/kg of platinum in PBS (100 μL). The tumor volumes, calculated using formula $L \times B^2$, and body weights were monitored on a daily basis. The animals were sacrificed when the average tumor size of the control exceeded 2000 mm^3 in the control group. The tumors were harvested immediately following sacrifice and stored in 10% formalin for further analysis. All animal procedures were approved by the Harvard Institutional Use and Care of Animals Committee.

In Vivo Murine Ovarian Cancer Tumor Model. Ovarian adenocarcinomas were induced in genetically engineered K-ras$^{LSL/+}$/Pten$^{fl/fl}$ mice via intrabursal delivery of adenovirus carrying Cre recombinase, as described previously (28). Tumor cells were engineered to express luciferase once activated by Adeno-Cre, to make tumor imaging feasible before and after drug treatment. Once mice developed medium to large tumors they were placed into one of four treatment groups (tumor imaging in vivo was performed with the IVIS Lumina II Imaging System). Quantification of bioluminescence was achieved by using the Living Image Software 3.1 (Caliper Life Sciences). Mice received 150 mg/kg of D-luciferin firefly potassium salt via i.p. injection prior to imaging. Five min postluciferin injection, animals were anesthetized in a 2.5% isoflurane induction chamber. Once anesthesized, mice were placed into the imaging chamber where they were kept under anesthesia by a manifold supplying isoflurane and their body temperature was maintained by a 37 °C temperature stage. Bioluminescent signal was collected 15 min after luciferin administration for an exposure time of 30 s. Images were taken a day prior to treatment (day 0, baseline) and 1 d following the final treatment. Treatment efficacy was quantified by examining the fold increase in bioluminescence of the posttreatment signal as compared to baseline.

Biodistribution of Cisplatin. See *SI Text*.

Histopathology and TUNEL Assay (Apoptotic Assay). See *SI Text*.

Toxicity Assessment of Drug Treatment. Body weights were recorded daily to assess toxicity. In addition, livers and spleens were removed at the end of treatment to record weights and perform extensive pathological examination to assess toxicity of vital organs. Cell apoptosis in vital organs was measured using TUNEL assay.

Statistical Analysis. Data were expressed as means $\pm$ S.D from at least $n = 3$. Statistical analysis was conducted using the Prism software (GraphPad). The statistical differences were determined by ANOVA followed by Newman Keuls Post Hoc test or Student's t test. $p < 0.05$ was considered to indicate significant differences.

1. Ferrari M (2005) Cancer nanotechnology: Opportunities and challenges. *Nat Rev Cancer* 5:161–171.
2. Moghimi SM, et al. (2001) Long-circulating and target-specific nanoparticles: Theory to practice. *Pharmacol Rev* 53:283–318.
3. Decuzzi P, et al. (2009) Intravascular delivery of particulate systems: Does geometry really matter? *Pharm Res* 26:235–243.
4. Chaudhuri P, et al. (2010) Shape effect of carbon nanovectors on angiogenesis. *ACS Nano* 4:574–582.
5. Gratton SE, et al. (2008) The effect of particle design on cellular internalization pathways. *Proc Natl Acad Sci USA* 105:11613–11618.
6. Yuan F, et al. (1995) Vascular permeability in a human tumor xenograft: Molecular size dependence and cutoff size. *Cancer Res* 55:3752–3756.
7. Yuan F, et al. (1994) Microvascular permeability and interstitial penetration of sterically stabilized (stealth) liposomes in a human tumor xenograft. *Cancer Res* 54:3352–3356.
8. Northfelt DW, et al. (1996) Doxorubicin encapsulated in liposomes containing surface-bound polyethylene glycol: Pharmacokinetics, tumor localization, and safety in patients with AIDS-related Kaposi's sarcoma. *J Clin Pharmacol* 36:55–63.
9. Desai N, et al. (2006) Increased antitumor activity, intratumor paclitaxel concentrations, and endothelial cell transport of cremophor-free, albumin-bound paclitaxel, ABI-007, compared with cremophor-based paclitaxel. *Clin Cancer Res* 12:1317–1324.
10. Kelland L (2007) The resurgence of platinum-based cancer chemotherapy. *Nat Rev Cancer* 7:573–584.
11. Leong CO, et al. (2007) The p63/p73 network mediates chemosensitivity to cisplatin in a biologically defined subset of primary breast cancers. *J Clin Invest* 117:1370–1380.
12. Madias NE, Harrington JT (1978) Platinum nephrotoxicity. *Am J Med* 65:307–314.
13. Choi HS, et al. (2007) Renal clearance of quantum dots. *Nat Biotechnol* 25:1165–1170.
14. Avgoustakis K, et al. (2002) *PLGA*-mPEG nanoparticles of cisplatin: In vitro nanoparticle degradation, in vitro drug release, and in vivo drug residence in blood properties. *J Controlled Release* 79:123–135.
15. Fujiyama J, et al. (2003) Cisplatin incorporated in microspheres: Development and fundamental studies for its clinical application. *J Controlled Release* 89:397–408.
16. Dhar S, et al. (2008) Targeted delivery of cisplatin to prostate cancer cells by aptamer functionalized Pt(IV) prodrug-PLGA-PEG nanoparticles. *Proc Natl Acad Sci USA* 105:17356–17361.
17. Haxton KJ, Burt MH (2009) Polymeric drug delivery of platinum-based anticancer agents. *J Pharm Sci* 98:2299–2316.
18. Rademaker-Lakhai JM, et al. (2004) A Phase I and pharmacological study of the platinum polymer AP5280 given as an intravenous infusion once every 3 weeks in patients with solid tumors. *Clin Cancer Res* 10:3386–3395.
19. Lin X, et al. (2004) Improved targeting of platinum chemotherapeutics. The antitumour activity of the HPMA copolymer platinum agent AP5280 in murine tumour models. *Eur J Cancer* 40:291–297.
20. Huang H, et al. (1995) Solution structure of a cisplatin-induced DNA interstrand cross-link. *Science* 270:1842–1845.
21. Hongo A, et al. (1994) A comparison of in vitro platinum-DNA adduct formation between carboplatin and cisplatin. *Int J Biochem* 26:1009–1016.
22. Knox RJ, et al. (1986) Mechanism of cytotoxicity of anticancer platinum drugs: Evidence that *cis*-diamminedichloroplatinum(II) and *cis*-diammine-(1,1-cyclobutanedicarboxylato)platinum(II) differ only in the kinetics of their interaction with DNA. *Cancer Res* 46:1972–1979.
23. Go RS, et al. (1999) Review of the comparative pharmacology and clinical activity of cisplatin and carboplatin. *J Clin Oncol* 17:409–422.
24. Song CW, et al. (2006) Influence of tumor pH on therapeutic response. *Cancer Drug Discovery and Development: Cancer Drug Resistance*, ed B Teicher (Humana Press, Totowa, NJ), pp 21–42.
25. Obata K, et al. (1998) Frequent PTEN/MMAC1 mutations in endometrioid but not serous or mucinous epithelial ovarian tumors. *Cancer Res* 58:2095–2097.
26. Sato N, et al. (2000) Loss of heterozygosity on 10q23.3 and mutation of the tumor suppressor gene *PTEN* in benign endometrial cyst of the ovary: Possible sequence progression from benign endometrial cyst to endometrioid carcinoma and clear cell carcinoma of the ovary. *Cancer Res* 60:7052–7056.
27. Cuatrecasas M (1998) K-ras mutations in nonmucinous ovarian epithelial tumors. *Cancer* 82:1088–1095.
28. Dinulescu DM (2005) Role of K-ras and Pten in the development of mouse models of endometriosis and endometrioid ovarian cancer. *Nat Med* 11:63–70.
29. Shawver LK, et al. (2002) Smart drugs: Tyrosine kinase inhibitors in cancer therapy. *Cancer Cell* 1:117–123.
30. Jamieson ER, Lippard SJ (1999) Structure, recognition, and processing of cisplatin-DNA adducts. *Chem Rev* 99:2467–2498.
31. Davies MS, et al. (2000) Slowing of cisplatin aquation in the presence of DNA nut not in the presence of phosphate. Improved understanding of the sequence selectivity and the roles of monoaquated and diaquated species in the binding of cisplatin to DNA. *Inorg Chem* 39:5603–5613.
32. Salamanca-Buentello F, et al. (2005) Nanotechnology and the developing world. *PLoS Med* 2:e97.

(12) INTERNATIONAL APPLICATION PUBLISHED UNDER THE PATENT COOPERATION TREATY (PCT)

(51) International Patent Classification:
C08F 222/06 (2006.01)   A61K 47/48 (2006.01)
C08F 22/06 (2006.01)   A61P 35/00 (2006.01)
C08F 8/42 (2006.01)

(21) International Application Number:
PCT/US2010/023217

(22) International Filing Date:
4 February 2010 (04.02.2010)

(25) Filing Language: English

(26) Publication Language: English

(30) Priority Data:
61/149,725   4 February 2009 (04.02.2009)   US
61/240,007   4 September 2009 (04.09.2009)   US

(71) Applicant (for all designated States except US): THE BRIGHAM AND WOMEN'S HOSPITAL, INC. [US/US]; 75 Francis Street, Boston, MA 02115 (US).

(72) Inventors; and
(75) Inventors/Applicants (for US only): SENGUPTA, Shiladitya [IN/US]; 4613 Stearns Hill Road, Waltham, MA 02451 (US). SONI, Shivani [IN/US]; 127 Washington Street, Apartment 47, Brighton, MA 02135 (US).

PARASKAR, Abhimanyu [IN/US]; 43 White Street, Belmont, MA 02478 (US).

(74) Agents: RESNICK, David, S. et al.; Nixon Peabody LLP, 100 Summer Street, Boston, MA 02110-2131 (US).

(81) Designated States (unless otherwise indicated, for every kind of national protection available): AE, AG, AL, AM, AO, AT, AU, AZ, BA, BB, BG, BH, BR, BW, BY, BZ, CA, CH, CL, CN, CO, CR, CU, CZ, DE, DK, DM, DO, DZ, EC, EE, EG, ES, FI, GB, GD, GE, GH, GM, GT, HN, HR, HU, ID, IL, IN, IS, JP, KE, KG, KM, KN, KP, KR, KZ, LA, LC, LK, LR, LS, LT, LU, LY, MA, MD, ME, MG, MK, MN, MW, MX, MY, MZ, NA, NG, NI, NO, NZ, OM, PE, PG, PH, PL, PT, RO, RS, RU, SC, SD, SE, SG, SK, SL, SM, ST, SV, SY, TH, TJ, TM, TN, TR, TT, TZ, UA, UG, US, UZ, VC, VN, ZA, ZM, ZW.

(84) Designated States (unless otherwise indicated, for every kind of regional protection available): ARIPO (BW, GH, GM, KE, LS, MW, MZ, NA, SD, SL, SZ, TZ, UG, ZM, ZW), Eurasian (AM, AZ, BY, KG, KZ, MD, RU, TJ, TM), European (AT, BE, BG, CH, CY, CZ, DE, DK, EE, ES, FI, FR, GB, GR, HR, HU, IE, IS, IT, LT, LU, LV, MC, MK, MT, NL, NO, PL, PT, RO, SE, SI, SK, SM, TR), OAPI (BF, BJ, CF, CG, CI, CM, GA, GN, GQ, GW, ML, MR, NE, SN, TD, TG).

(54) Title: NANOSCALE PLATINUM COMPOUNDS AND METHODS OF USE THEREOF
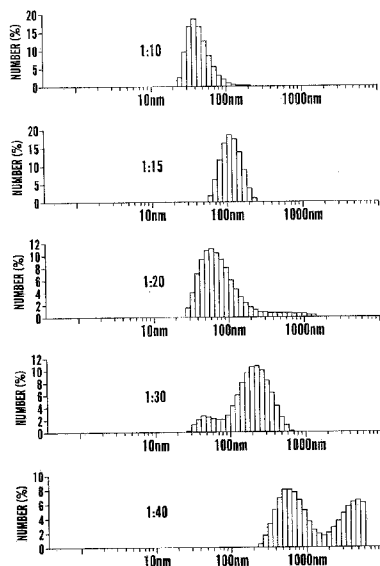
FIG. 1B

(57) Abstract: The invention is directed to biocompatible conjugated polymer nanoparticles including a copolymer backbone, a plurality of sidechains covalently linked to said backbone, and a plurality of platinum compounds dissociably linked to said backbone. The invention is also directed to dicarbonyl-lipid compounds wherein a platinum compound is dissociably linked to the dicarbonyl compound. The invention is also directed to methods of treating cancer or metastasis. The methods includes selecting a subject in need of treatment for cancer or metastasis and administering to the subject an effective amount of any of the nanoparticles, compounds, or compositions of the invention.

WO 2010/091192 A2 ||||||||||||||||||||||||||||||||||||||||||||||||||||||||||||||||||||||||||||||||||||

NANOSCALE PLATINUM COMPOUNDS AND METHODS OF USE THEREOF

RELATED APPLICATIONS

[0001] This application claims priority to and benefit under 35 U.S.C. § 119(e) of the U.S. Provisional Application Nos. 61/149,725, filed February 4, 2009 and 61/240,007, filed September 4, 2009, the content of both of which are incorporated herein by reference in their entirety.

GOVERNMENT SUPPORT

FIELD OF THE INVENTION

[0003] This invention relates to biocompatible conjugated polymer nanoparticles including a copolymer backbone, a plurality of sidechains covalently linked to the backbone, and, a plurality of platinum compounds dissociably linked to the backbone.

BACKGROUND OF THE INVENTION

[0004] Cancer is the second leading cause of mortality in the United States, with an estimated 1,444,180 new cases and 565,650 deaths in 2008. Cytotoxic agents, which are used in standard chemotherapy, non-specifically target all dividing cells resulting in dose-limiting toxicities. There is an urgent need to develop novel strategies that are more specifically targeted against the tumor.

[0005] The use of nanovectors holds the potential to revolutionize cancer chemotherapy by specifically targeting the tumor. A number of polymeric nanovectors are currently in development or in clinics, and are dramatically altering the pharmacodynamic and pharmacokinetic profile of the active agent. However, most of these polymeric constructs decrease the potency of the conjugated active agent, relying on increased uptake into the tumor for the improved therapeutic index.

[0006]   Cisplatin is one of the mainstays in chemotherapy regimes for most types of

Cancer (Kelland L. The resurgence of platinum-based cancer chemotherapy. Nat Rev

Cancer. 2007 Aug;7(8):573-84). However, its use is does-limited due to severe

nephrotoxicity . Furthermore, the nanovector formulation of cisplatin, which is a first-line

therapy for multiple cancers, has been a challenge.

SUMMARY OF THE INVENTION

[0007]   Reported herein is a rational engineering of a polymeric construct of

platinum-based chemotherapeutics such as cisplatin and oxaliplatin, which results in self-

assembly into a nanoparticle. The nanoparticle sustains the potency of the active agent, and

compared with cisplatin or oxaliplatin or carboplatin, exhibits increased anti-tumor effects

with reduced systemic- and nephro-toxicity when administered intravenously to tumor-

bearing mice. This nanotechnology-enabled improvement in the therapeutic index of cisplatin

or oxaliplatin can be utilized for using nanoplatinates in the clinical management of multiple

types of cancer.

[0008]   The invention is directed to a biocompatible conjugated polymer nanoparticle

including a copolymer backbone, a plurality of sidechains covalently linked to said backbone,

and, a plurality of platinum compounds dissociably linked to said backbone. Generally, the

platinum compound is dissociably linked to backbone via linkage through the sidechain. In

some embodiments, the platinum compound is linked to the sidechain through at least one

coordination bond.

[0009]   Another aspect of the invention is directed to biocompatible conjugated

polymer nanoparticles including a polymaleic acid (PMA) such as a poly(isobutylene-*alt*-

maleic acid) (PIMA) backbone. The backbone consists of from 25 to 50 monomers. Also

included are a plurality of PEG sidechains covalently linked to said backbone. The PEG

sidechains have a molecular weight of from 200 to 3000 Dalton. The PEG sidechains number

between 50% and 100%, inclusive, of the number of monomeric units of the polymer

backbone. Also included are a plurality of cisplatin or oxaliplatin side groups dissociably

linked to the backbone. The cisplatin side groups number between 25% and 75%, inclusive,

of the number of monomeric units of the polymer backbone.

[0010]   Yet another aspect of the invention is directed to biocompatible conjugated

polymer nanoparticles including a poly(isobutylene-*alt*-maleic acid) backbone. The

backbone consist of about 40 monomers. Also included are a plurality of PEG sidechains

covalently linked to the backbone. The PEG sidechains have a molecular weight of about

2000 Dalton. The PEG sidechains number greater than 90% of monomeric units of said polymer backbone. Also included are a plurality of cisplatin or oxaliplatin side groups dissociably linked to the backbone. The cisplatin or oxaliplatin side groups number between 25% and 75%, inclusive, of the number of monomeric units of the polymer backbone.

[0011]   Still another aspect of the invention is directed to biocompatible conjugated polymer nanoparticles including a poly(isobutylene-*alt*-maleic acid) backbone. The backbone consists of from 25 to 50 monomers. Also included are a plurality of glucosamine sidechains covalently linked to said backbone. The glucosamine sidechains number between 50% and 100%, inclusive, of monomeric units of said polymer backbone. Also included are a plurality of cisplatin or oxaliplatin side groups dissociably linked to the backbone. The cisplatin or oxaliplatin side groups number between 25% and 75%, inclusive, of the number of monomeric units of the polymer backbone.

[0012]   Another aspect of the invention is directed to biocompatible conjugated polymer nanoparticles including a poly(isobutylene-*alt*-maleic acid) backbone. The backbone consists of from 25 to 50 monomers. Also included are a plurality of glucosamine sidechains covalently linked to said backbone. The glucosamine sidechains number greater than 75% of monomeric units of said polymer backbone. Also included are a plurality of cisplatin or oxaliplatin side groups dissociably linked to the backbone. The cisplatin or oxaliplatin side groups number between 25% and 75%, inclusive, of the number of monomeric units of the polymer backbone.

[0013]   Yet another aspect of the invention is directed to carboxylic acid-platinum II (Pt(II)) complex conjugated nanoparticles including a carboxylic acid-(Pt(II)) complex and a plurality of lipid-polymer chains. The carboxylic acid portion of said carboxylic acid-cisplatin/oxaliplatin complex is covalently bound to said lipid-polymer chains.

[0014]   Another aspect of the invention is directed to a vesicle, micelle, or liposome compound comprising a plurality of nanoparticles of claim as described herein.

[0015]   Still another aspect of the invention is directed to pharmaceutical compositions including any of the nanoparticles or compounds described herein and a pharmaceutically acceptable carrier.

[0016]   Yet another aspect of the invention is directed to a method of treating cancer or metastasis. The method includes selecting a subject in need of treatment for cancer or metastasis and administering to the subject an effective amount of any of the nanoparticles, compounds, or compositions described herein.

BRIEF DESCRIPTION OF THE DRAWINGS

[0017]   Figure 1 shows a schematic of synthesis of PMA-Cisplatin. Loading of different numbers of cisplatin per polymer affects the size of the nanoparticles as measured using DLS or TEM. And a graph of Cytotoxicity study of Polyisobutylene maleic acid carrier (PIMA) **2** and conjugate (PIMA-CISPLATIN) **(6)**.

[0018]   Figure 2 shows a scheme showing derivatization of PMA with EDA. The derivatized polymer was used to synthesize the cisplatin-complex. The graph shows the effect of different treatments on LLC viability following 48 hours of incubation.

[0019]   Figure 3 shows a scheme of the synthesis of PMA-GA-Cisplatin. Complexation with cisplatin was carried out over a 48 hour period. This resulted in the formation of nanoparticles in the size range of around 100 nm as seen from the DLS measurements.

[0020]   Figure 4 The graph on the left shows the amount of active cisplatin that is released from the PMA-GA-Cisplatin nanoparticle when incubated with LLC lysate. The concentration-effect graph of the right shows the effect of different treatments on the viability of Lewis Lung Carcinoma cells when incubated with the active agents for 48 hours. Cell viability was measured using an MTS assay.

[0021]   Figures 5A-5E are line graphs (Figs.5A and 5B) and bar graphs (Figs. 5C-5E) showing efficacy and toxicity profile of free and nanoparticle cisplatin in Lewis Lung carcinoma model. Tumors were induced by injecting LLC cells in c57/BL6 mouse. The effect of treatments on tumor volume (Fig, 15A) and body weight (Fig. 5B) over the treatment period is shown. The animals were dosed thrice (shown by arrows on x-axis). Data shown are mean±SE, n=4-8. The effect of treatment on the organ weight of kidneys (Fig. 5C) and spleen (Fig. 5D) as a marker for nephrotoxicity and hematological toxicity is also shown (n=4-6). The images on top of each graph show representative organs from each treatment group. Fig. 5E shows the biodistribution of Pt in kidney and tumor as measured using ICP-spectroscopy 24 h hours following administration of free or cisplatin nanoparticles (8mg/kg cisplatin dose)

[0022]   Figure 6 is a scheme showing synthesis of PMA-GA-Cisplatin **(8)**.

[0023]   Figure 7 Effect of PMA-PEG-Cisplatin on Lewis Lung Carcinoma. Cell were incubated for 48 hours with the drugs or vehicles and then tested for viability using an MTS assay.

[0024]   Figure 8 Effect of different treatments on tumor growth and body weight in vivo. Tumors were induced by injecting LLC cells in c57/BL6 mouse.

[0025]   Figure 9 is a graph of the amount of platination of the polymer was quantified using a uv-vis spectroscopy method.

[0026]   Figure 10 Scheme showing synthesis of lipid maleic acid-cipslatin complex, which can form micelles in water.

[0027]   Figures 11A and 11B aree schematics showing SAR-inspired engineering of a cisplatin nanoparticle. Fig. 11A shows the mechanism underlying the intracellular activation of cisplatin through aquation. The leaving groups of cisplatin and analogues (shown with blue lines) are replaced with OH prior to DNA-binding. Fig. 11B shows the chemical synthesis of PIMA-cisplatin and PIMA-glucosamine (PIMA-GA)-cisplatin complex. Transformation of polymaleic anhydride (n=40) (1) to polymaleic acid [PIMA] (2) enables complexation of $[NH_2]_2Pt[OH]_2$ through dicarboxylato bond (6). Derivatization of one arm of PIMA with glucosamine (4), and complexation with $[NH_2]_2Pt[OH]_2$ can lead to two isomers (8) and (10) depending on pH, characterized by unique Pt NMR signatures (Fig. 11B).

[0028]   Figures 12A and 12B show characterization of cisPt-NP. Increasing the number of Pt on a PIMA (n=40) backbone increased the size of nanoparticle formed. At an optimal Pt to polymer ratio, the inventors obtained nanoparticles smaller than 150 nm, the size cut-off below which enables preferential homing to tumors. Fig. 12A shows that derivatization of all the monomeric units of PIMA with glucosamine and subsequent complexation with Pt forms nanoparticles smaller than 150 nm. Fig. 12B shows the total platinum loaded per mg of polymer at this ratio.

[0029]   Figures 13A-13E are line graphs showing in vitro characterization of cisplatin nanoparticles. Figs. 13A and 13B show the concentration-effect of different treatments on cellular viability as measured using MTS assay. X-axis shows the equivalent concentrations of cisplatin. Where blank polymeric controls were used, dose of polymer used was equivalent to that used to deliver that specific dose of cisplatin in the complexed form. PIMA was also derivatized with ethylene diamine to generate PIMA-EDA, which offers a similar complexation environment to platinum as PIMA-GA. Unlike PIMA-GA, PIMA-EDA exerted inherent toxicity. PIMA-GA-Cisplatin[acidic] refers to the isomer formed under acidic complexation environment while PIMA-GA-Cisplatin[basic] refers to the isomer formed under alkaline environment. Figs. 13C-13E show effect of PIMA-GA-cisplatin nanoparticles on LLC cells viability, when the PIMA backbone (40 monomeric units) is derivatized to different degrees. PIMA-30GA-Cisplatin has 30 of the 40 monomeric units derivatized with

glucosamine while PIMA-GA-40 and PIMA-GA-200 have all the monomeric units derivatized. [a] and [b] refers to isomers formed in acidic and basic environments when the polymers are complexed with cisplatin. Table 1 shows the corresponding IC50 values.

[0030] Figures 14A-14J show FACS images (Figs. 14A-14H) and bar graphs (Figs. 14I and 14J) showing that treatment with PIMA-GA-Cisplatin induces cell death. Representative FACS images of 4T1 (Figs. 14A-14D) and LLC (Figs. 14E-14H) cells showing the percentage in each quadrant following treatments with free or nanoparticle-cisplatin. Carboplatin was used as a control for comparison (Figs. 14D and 14H). The cells were incubated with the drugs for 24h, following which they were labeled with Annexin-V FITC and counterstained with propidium iodide.

[0031] Figure15 is a schematic showing the labeling of the PIMA-GA polymer with FITC to enable the tracking of cellular uptake of the nanoparticles.

[0032] Figure16 is a line graph showing the effect of pH and Pt complexation environment on release kinetics. The nanoparticles were incubated at pH 5.5 or pH8.5 in a dialysis bag, and release over time was quantified. The nanoparticles [PIMAGA-Cisplatin (O->Pt)] used were generated by complexing the polymer and cisplatin in an acidic pH [6.4] unless in the case of PIMA-GA-Cisplatin (Pt->N), where the complexation was carried out in a basic pH to generate the stable isomer [PIMA-GA-Cisplatin (N->Pt)]. The data shown are mean$\pm$SE from n=3.

[0033] Figures 17A-17D are line graphs (Figs. 17A and 17B) and bar graphs (Figs. 17C and 17D) showing PIMA-GA-cisplatin nanoparticle exerts similar anti-tumor effect with reduced systemic toxicity compared to free cisplatin in a 4T1 breast cancer model. Line graphs show the effect of treatments on tumor volume (Fig. 17A) and body weight (Fig. 17B) over the treatment period. The animals were dosed thrice (shown by arrows on x-axis). Data shown are mean$\pm$SE, n=4-8. Bar graphs show the effect of treatment on the organ weight of spleen (Fig. 18C) and kidneys (Fig. 17D) as a marker for nephrotoxicity and hematological toxicity (n=4-6)*$P<0.05$ vs vehicle-treated group [ANOVA followed by Newman Keuls Post Hoc test]. Carboplatin [3mg/kg] was used as a control.

[0034] Figures 18A and 18B are a bar graph (Fig. 18A) and a line graph (Fig. 18B) showing PIMA-GA-cisplatin nanoparticle inhibits tumor growth in a K-ras[LSL/+]/Pten^{fl/fl} ovarian cancer model. As shown in Fig. 18A, bioluminescence quantification indicated a significantly decreased tumor luciferase signal in mice treated with cisplatin-NP compared to vehicle (p< 0.05, one-way ANOVA analysis). Fig. 18B shows drug toxicity assessed by measurements in overall body weight. Daily recording of body weights indicated a

significant loss of body weight in the free cisplatin group as compared to both cisplatin-NP (1.25 mg/kg and 3 mg/kg) treated groups (P < 0.05, two-way ANOVA analysis).

[0035]   Figures 19A and 19B are bar graphs showing the distribution of Pt following administration of cisplatin, cisplatin-nanoparticle ([PIMA-GA-Cisplatin (O->Pt)] or carboplatin in breast cancer or ovarian cancer. Treatment was administered as described in Figs. 17 and 18. The level of Pt in different tissues harvested following necropsy was quantified using inductively coupled plasma-spectrometry (ICP).

[0036]   Figures 20A and 20B are schematic showing SAR-inspired engineering of a oxaliplatin nanoparticle. Figure 20A shows the mechanism underlying the intracellular activation of oxaliplatin through aquation. Figure 20B shows the chemical synthesis of PIMA-oxaliplatin and PIMA-glucosamine (PIMA-GA)-oxaliplatin complex. Oxaliplatin-OH can be complexed with PIMA through dicarboxylato bonds. Derivatization of one arm of PIMA with glucosamine, and complexation with oxaliplatin can lead to two isomers depending on pH.

[0037]   Figures 21A and 21B are line graphs showing the concentration-effect of different treatments on cellular viability as measured using MTS assay. Breast cancer cell line, Lewis lung cancer (Fig. 21A) and 4T1 (Fig. 21B) cell lines were used for this study. X-axis shows the equivalent concentrations of platinum. Where blank polymeric controls were used, dose of polymer used was equivalent to that used to deliver that specific dose of oxaliplatin in the complexed form. PIMA-GA-Ox refers to the isomer [PIMA-GA-Oxaliplatin (O->Pt)] formed under acidic complexation environment. The PIMA-GA-oxaliplatin curve shifted to the left, indicating that the nanoparticles are more effective than free oxaliplatin in anti-tumor efficacy.

[0038]   Figures 22A-22E are line graphs (Figs. 26A and 26B) and bargraphs (Figs. 22C-22E), showing PIMA-GA-oxaliplatin nanoparticle exerts similar anti-tumor effect with reduced systemic toxicity compared to free oxaliplatin in a 4T1 breast cancer model. Line graphs show the effect of treatments on tumor volume (Fig. 22A) and body weight (Fig. 22B) over the treatment period. The animals were dosed thrice. Data shown are mean ± SE, n=4-8. Bar graphs show the effect of treatment on the weight of tumor (Fig. 22C), kidney (Fig. 22D), and spleen (Fig. 22E) as a marker for nephrotoxicity and hematological toxicity (n=4-6).

[0039]   Figure 23 is a line graph showing concentration-effect of different oxaliplatin complexes on cellular viability as measured using MTS assay.

[0040] Figure 24 is a line graph showing the effect of cisplatin, carboplatin and PIMA-GA-200(A) on cell viability.

[0041] Figure 25A is a scheme showing the synthesis of cholesterol-succinic acid conjugate and the complexation of Pt to the conjugate.

[0042] Figure 25B shows a dynamic laser light scatter of liponanoparticles. The size of the liponanoparticles is less than 150 nm.

[0043] Figure 26 is a line graph showing the release kinetics of Pt from the liponanoparticle with time and the influence of pH. The rate of release is faster in an acidic pH, which facilitates selective release of active platinate in the tumor, consistent with the acidic intratumoral pH.

[0044] Figures 27A-27C are line graphs showing the effect of cisplatin-liponanoparticle on viability of 4T1 breast cancer cells. Cell viability was measured using MTS assay. The treatment with liponanoparticles results in rapid cell kill within 12 hours as compared with either cisplatin or carboplatin (Fig. 27A). At all three time points cisplatin-liponanoparticle was found to be more effective than cisplatin. Carboplatin is the least effective of all platinates tested (Fis. 27A-27C).

[0045] Figures 28A and 28B are line graphs showing the effect of cisplatin-liponanoparticle on viability of a cisplatin-resistant hepatocellular cancer cell line (CP20) and on a Lewis lung cancer cell line (LLC). Cisplatin acts on CP20 only at the highest concentration, while the cells are susceptible to the cisplatin-liponanoparticle (Fig. 28A). Carboplatin has no effect at this concentration range (Figs. 28A and 28B). Cisplatinliponanoparticle exerted superior anticancer effect than free cisplatin on LLCs (Fig. 28B).

[0046] Figures 29A-29E are line graphs (Figs. 29A and 29B) and bar graphs (Figs. 29C-29E) showing the efficacy of cisplatin-liponanoparticle in a 4T1 syngeneic tumor model in vivo. Line graphs show the effect of different treatments on tumor growth (Figs. 29A and 29C) and body weight (as a marker for systemic toxicity, Fig. 29B). Bar graphs show kidney (Fig. 29D) and spleen (Fig. 29E) weights as markers for nephrotoxicity and hematological toxicity. As seen in the figure, cisplatin-liponanoparticle induced greater antitumor activity with reduced systemic, nephrotoxicity.

DETAILED DESCRIPTION OF THE INVENTION

[0047] The invention is directed to biocompatible conjugated polymer nanoparticles including a copolymer backbone, a plurality of sidechains covalently linked to said backbone, and, a plurality of platinum compounds dissociably linked to said backbone. Generally, the platinum compounds are linked to the backbone via a linkage to the sidechains.

[0048] In some embodiments, the copolymer comprises maleic acid monomers.

[0049] In a preferred embodiment, the copolymer is poly(isobutylene-*alt*-maleic acid) (PIMA or PMA).

[0050] In some embodiments, the copolymer comprises from 2 to 100 monomeric units. In some embodiments, the copolymer comprises from 25 to 50 monomeric uints.

[0051] In some embodiments, the sidechains are selected from the group consisting of polymers, monosaccharides, carboxylic acids, dicarboxylic acids, amides, and combinations thereof.

[0052] In preferred embodiments, the sidechains are polyethylene glycol (PEG). PEG sidechains can be represented by –C(O)-NH-PEG.

[0053] In some embodiments, the PEG sidechains have a molecular weight of from 100 to 5000 Dalton. In some embodiments, the PEG sidechains have a molecular weight of from 1000 to 3000 Dalton. In a preferred embodiment, the PEG sidechains have a molecular weight of about 2000 Dalton.

[0054] In some embodiments, the sidechains are monosaccharides. In a preferred embodiment, the monosaccharides are glucosamine. The monosaccharide sidechains can be represented by –C(O)-saccharide.
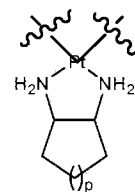
[0055] Any platinum compound can be used in the invention. Preferably, the platinum compound is a platinum(II) or platinum (IV) compound. In some embodiments, the platinum (II) compound is selected from the group consisting of cisplatin, oxaliplatin, carboplatin, paraplatin, sartraplatin, and combinations thereof. In a preferred embodiment, the platinum (II) compound side group is cisplatin or oxalipaltin.

[0056] In some embodiments, the platinum(II) compound is selected from the group
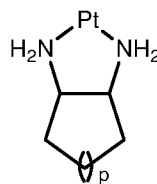
consisting of $Pt(NH_3)_2$, $Pt(NH_3)$(2-methylpyridine), and , wherein p is 0 - 3. In a preferred embodiment, the platinum (II) compound is $Pt(NH_3)_2$.
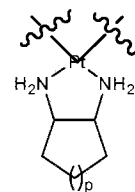
[0057]   In some embodiments, the platinum (II) compound is ![structure], wherein p is 0 - 3.

[0058]   In some embodiments, the platinum (II) compound comprises at least two nitrogen atoms, where said nitrogen atoms are directly linked to platinum. In a further embodiment, the two nitrogen atoms are linked to each other via an optionally substituted linker, e.g. acyclic or cyclic linker. A cyclic linker means a linking moiety that comprises at least one ring structure. Cyclic linkers can be aryl, heteroaryl, cyclyl or heterocyclyl.

[0059]   In some embodiments, at least one nitrogen that is linked to platinum is a ring atom of a heteroaryl or a heterocyclyl. In a preferred embodiment, heteroaryl is optionally substituted pyridine, e.g., 2-methylpyridine.

[0060]   In some embodiments, the plurality of sidechains corresponds to a number between 50% and 100%, inclusive, of the number of monomeric units of said polymer backbone. This means that between 50% to 100% of the monomeric units have at least one sidechain linked to the monomeric unit.   The total number of sidechains can be greater than the total number of the monomeric units. For example, two sidechains can be attached to a maleic acid monomer.

[0061]   In some embodiments, the plurality of sidechains corresponds to a number greater than 90% of the number of monomeric units of said polymer backbone.

[0062]   In some embodiments, the plurality of platinum compounds corresponds to number between 10% and 100%, inclusive, of the number of monomeric units of said polymer backbone. Generally there is a one-to-one relationship between platinum compounds and monomeric subunits. Thus, the percent refers to the number of monomeric units that are linked to a platinum compound to the total number of monomeric units present in the polymer backbone.

[0063]   In some embodiments, the plurality of platinum compounds corresponds to number between 25% and 75%, inclusive, of the number of monomeric units of said polymer backbone.

[0064]   Generally from 10 to 500 ug of the platinum compound can be loaded on 1 mg of the polymer. Preferably, 50 to 250 ug, more preferably 150 to 200 ug of the platinum compound is loaded on 1 mg of the polymer. In some experiments, the inventors obtained a loading of 175 ± 5 ug/mg of polymer.

[0065]   In some embodiments, the sidechains comprise dicarboxylic acids. In some embodiments, the dicarboxylic acids are of the formula HOOC-R-COOH, wherein R is a C1-C6 alkyl, C2-C6 alkenyl, or C2-C6 alkynyl. In a preferred embodiment, the dicarboxylic acid is maleic acid.

[0066]   In some embodiments, the copolymer comprises at least one monomer having the formula $-CH(CO_2H)-R-CH(C(O)R')-$, wherein R is a bond, C_1-C_6 alkylene, where the alkylene can comprise one or more double or triple bonds; and R' is a substituted nitrogen atom. Preferably, R is a bond.
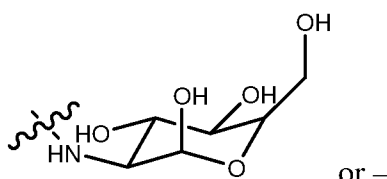
[0067]   In some embodiments, between 50% to 100%, inclusive, of the monomeric subunits in the polymeric backbone are $-CH(CO_2H)-R-CH(C(O)R')-$, wherein R is a bond, C_1-C_6 alkylene, where the alkylene can comprise one or more double or triple bonds; and R' is a substituted nitrogen atom.

[0068]   In some embodiments, at least 90% or more of the monomeric subunits in the polymeric backbone are $-CH(CO_2H)-R-CH(C(O)R')-$, wherein R is a bond, C_1-C_6 alkylene, where the alkylene can comprise one or more double or triple bonds; and R' is a substituted nitrogen atom.

[0069]   In some embodiments, the copolymer comprises at least one monomer having the formula $-CH(CO_2H)-R-CH(C(O)R')CH_2C(Me_2)-$ or $-CH(C(O)R')-R-CH(CO_2H)-CH_2C(Me_2)-$, wherein R is a bond, C_1-C_6 alkylene, where the alkylene can comprise one or more double or triple bonds; and R' is a substituted nitrogen atom. Preferably, R is a bond.

[0070]   In some embodiments, the copolymer comprises between 50% to 100%, inclusive of monomers having the formula $-CH(CO_2H)-R-CH(C(O)R')CH_2C(Me_2)-$ or $-CH(C(O)R')-R-CH(CO_2H)-CH_2C(Me_2)-$, wherein R is a bond, C_1-C_6 alkylene, where the alkylene can comprise one or more double or triple bonds; and R' is a substituted nitrogen atom.

[0071]   In some embodiments, the copolymer comprises at least 90% of monomers having the formula $-CH(CO_2H)-R-CH(C(O)R')CH_2C(Me_2)-$ or $-CH(C(O)R')-R-CH(CO_2H)-CH_2C(Me_2)-$, wherein R is a bond, C_1-C_6 alkylene, where the alkylene can comprise one or more double or triple bonds; and R' is a substituted nitrogen atom.

[0072]   In some embodiments, R' is or $-$NH$(CH_2CH_2O)_mCH_3$, wherein m is 1-150.

[0073]   In some embodiments, at least one monomer of the polymer comprises two sidechains selected from the group consisting of carboxylic acid, amide, and ester. Said sidechains being separated from each other by 1, 2, 3, 4, 5, 6, 7, 8, 9 or ten carbon, oxygen, nitrogen, sulfur atoms, or combination thereof. Preferably, said amide and ester sidechains are separated from each other by two carbon atoms. Preferably, at least one of the sidechains is not a carboxylic acid.

[0074]   In some embodiments, at least one monomer of the polymer comprises two carboxylic acid sidechains. Said carboxylic acid sidechains being separated from each other by 1, 2, 3, 4, 5, 6, 7, 8, 9 or ten carbon, oxygen, nitrogen, sulfur atoms, or combination thereof. Preferably, said carboxylic acid sidechains are separated from each other by two carbon atoms. The said carbon atoms can be linked to each other through a single bond or a double bond.

[0075]   In some embodiments, at least one monomer of the polymer comprises a carboxylic acid and an amide sidechains. Said carboxylic acid sidechains and amide sidechains being separated from each other by 1, 2, 3, 4, 5, 6, 7, 8, 9 or ten carbon, oxygen, nitrogen, sulfur atoms, or combination thereof. Preferably, said carboxylic acid and amide sidechains are separated from each other by two carbon atoms. The said carbon atoms can be linked to each other through a single bond or a double bond.

[0076]   In some embodiments, at least one monomer of the polymer comprises a carboxylic acid and an ester sidechains. Said carboxylic acid sidechains and ester sidechains being separated from each other by 1, 2, 3, 4, 5, 6, 7, 8, 9 or ten carbon, oxygen, nitrogen, sulfur atoms, or combination thereof. Preferably, said carboxylic acid and ester sidechains are separated from each other by two carbon atoms. The said carbon atoms can be linked to each other through a single bond or a double bond.

[0077]   In some embodiments, at least one monomer of the polymer comprises an amide and an ester sidechains. Said amide sidechains and ester sidechains being separated from each other by 1, 2, 3, 4, 5, 6, 7, 8, 9 or ten carbon, oxygen, nitrogen, sulfur atoms, or combination thereof. Preferably, said amide and ester sidechains are separated from each other by two carbon atoms. The said carbon atoms can be linked to each other through a single bond or a double bond.

[0078]   In some embodiments, at least one monomer of the polymer comprises two amide sidechains. Said amide sidechains being separated from each other by 1, 2, 3, 4, 5, 6, 7, 8, 9 or ten carbon, oxygen, nitrogen, sulfur atoms, or combination thereof. Preferably, said amide and ester sidechains are separated from each other by two carbon atoms.

[0079]   In some embodiments, at least one monomer of the polymer comprises two ester sidechains. Said ester sidechains being separated from each other by 1, 2, 3, 4, 5, 6, 7, 8, 9 or ten carbon, oxygen, nitrogen, sulfur atoms, or combination thereof. Preferably, said amide and ester sidechains are separated from each other by two carbon atoms.

[0080]   In some embodiments, the polymer comprises two sidechains selected from the group consisting of carboxylic acid, amide, and ester. Said sidechains being separated from each other by 1, 2, 3, 4, 5, 6, 7, 8, 9 or ten carbon, oxygen, nitrogen, sulfur atoms, or combination thereof. Preferably, said amide and ester sidechains are separated from each other by two carbon atoms. Preferably, at least least one of the sidechains is not a carboxylic acid.

[0081]   In some embodiments, the polymer comprises at least two carboxylic acid sidechains. Said carboxylic acid sidechains being separated from each other by 1, 2, 3, 4, 5, 6, 7, 8, 9 or ten carbon, oxygen, nitrogen, sulfur atoms, or combination thereof. Preferably, said carboxylic acid sidechains are separated from each other by two carbon atoms.

[0082]   In some embodiments, the polymer comprises a carboxylic acid and an amide sidechains. Said carboxylic acid sidechains and amide sidechains being separated from each other by 1, 2, 3, 4, 5, 6, 7, 8, 9 or ten carbon, oxygen, nitrogen, sulfur atoms, or combination thereof. Preferably, said carboxylic acid and amide sidechains are separated from each other by two carbon atoms.

[0083]   In some embodiments, the polymer comprises a carboxylic acid and an ester sidechains. Said carboxylic acid sidechains and ester sidechains being separated from each other by 1, 2, 3, 4, 5, 6, 7, 8, 9 or ten carbon, oxygen, nitrogen, sulfur atoms, or combination thereof. Preferably, said carboxylic acid and ester sidechains are separated from each other by two carbon atoms.

[0084]   In some embodiments, the polymer comprises an amide and an ester sidechains. Said amide sidechains and ester sidechains being separated from each other by 1, 2, 3, 4, 5, 6, 7, 8, 9 or ten carbon, oxygen, nitrogen, sulfur atoms, or combination thereof. Preferably, said amide and ester sidechains are separated from each other by two carbon atoms. The said carbon atoms can be linked to each other through a single bond or a double bond.

[0085]   In some embodiments, the polymer comprises two amide sidechains. Said amide sidechains being separated from each other by 1, 2, 3, 4, 5, 6, 7, 8, 9 or ten carbon, oxygen, nitrogen, sulfur atoms, or combination thereof. Preferably, said amide and ester sidechains are separated from each other by two carbon atoms.

[0086]   In some embodiments, the polymer comprises two ester sidechains. Said ester sidechains being separated from each other by 1, 2, 3, 4, 5, 6, 7, 8, 9 or ten carbon, oxygen, nitrogen, sulfur atoms, or combination thereof. Preferably, said amide and ester sidechains are separated from each other by two carbon atoms.

[0087]   The nanoparticles of the invention can range in size from 25-250nm, preferably 50-200nm, more preferably 80-160nm, and most preferably 90-110nm. Without wishing to be bound by theory, nanoparticles in the size range of 80-160 home preferentially into tumors resulting from the enhanced permeability and retention. See for example, Moghimi, et al., Pharmacol Rev. 2001 Jun; 53(2):283-318.

[0088]   In some embodiments, the platinum compound is dissociably linked to said backbone through at least one coordination bond. Without wishing to be bound by theory, the coordination bond is more liable and thus releases the platinum compound more easily.

[0089]   In some embodiments, linking of the platinum compound to the biopolymer backbone further comprises a carboxylato bond. In some embodiments, the platinum compound is linked to the backbone through a coordination bond and a carboxylato bond.

[0090]   It is to be understood that although linkage to backbone is recited, one of skill in the art understands that the platinum compound is generally linked to one or more sidechains which themselves are linked to the backbone. So any recitation of linking of a platinum compound to backbone encompasses the situations where the platinum compound is linked to a sidechain which is then linked to the backbone.

[0091]   In some embodiments, the coordination bond is between platinum atom of the platinum compound and an oxygen of the sidechain. Preferably the coordination bond is between platinum and a carbonyl oxygen.

[0092]   In some embodiments, the coordination bond is between platinum atom of the platinum compound and an amide oxygen of the sidechain. In some embodiments, the coordination bond is between platinum atom of the platinum compound and an ester carbonyl oxygen of the sidechain.

[0093]   In some embodiments, the copolymer comprises at least one maleic acid monomer, wherein at least one carboxylic acid of said at least maleic acid is derivatized to an amide.

[0094]   In some embodiments, between 50% to 100%, inclusive, of the monomeric units in the polymer backbone are maleic acid monomer and wherein at least one carboxylic acid of said maleic acid monomer is derivatized to an amide.

[0095]   In some embodiments, at least 90% of the monomeric units in the polymer backbone are maleic acid monomer and wherein at least one carboxylic acid of said maleic acid monomer is derivatized to an amide.

[0096]   The loading of platinum compound onto the polymer can be represented by as percent mg of platinum compound per mg of polymer. For example, a maximum of 0.375 mg of cisplatin can be loaded onto the PIMA-GA polymer therefore a loading of 37.5% represents the maximum loading for that particular polymer. The loading can range from about 1% to the theoretical total loading for a polymer.

[0097]   In some embodiments, the platinum compound loading is from 1%-37.5%. The percent loading represent mg of platinum compound linked with per mg of polymer.

[0098]   In some embodiments, the platinum compound loading is from 1%-6%. In some embodiments, the Pt(II) compound loading is from 0.01% to 1%.

[0099]   Another aspect of the invention is directed to biocompatible conjugated polymer nanoparticles including a poly(isobutylene-*alt*-maleic acid) backbone. The backbone consists of from 25 to 50 monomers. Also included are a plurality of PEG sidechains covalently linked to said backbone. The PEG sidechains have a molecular weight of from 1000 to 3000 Dalton. The PEG sidechains number between 50% and 100%, inclusive, of the number of monomeric units of the polymer backbone. Also included are a plurality of cisplatin side groups dissociably linked to the backbone. The cisplatin side groups number between 25% and 75%, inclusive, of the number of monomeric units of the polymer backbone.

[00100]   Yet another aspect of the invention is directed to biocompatible conjugated polymer nanoparticles including a poly(isobutylene-*alt*-maleic acid) backbone. The backbone consist of 40 monomers. Also included are a plurality of PEG sidechains covalently linked to the backbone. The PEG sidechains have a molecular weight of 2000 Dalton. The PEG sidechains number greater than 90% of monomeric units of said polymer backbone. Also included are a plurality of cisplatin side groups dissociably linked to the backbone. The cisplatin side groups number between 25% and 75%, inclusive, of the number of monomeric units of the polymer backbone.

[00101]   Still another aspect of the invention is directed to biocompatible conjugated polymer nanoparticles including a poly(isobutylene-*alt*-maleic acid) backbone. The backbone consists of from 25 to 50 monomers. Also included are a plurality of glucosamine sidechains covalently linked to said backbone. The glucosamine sidechains number between 50% and 100%, inclusive, of monomeric units of said polymer backbone. Also included are

a plurality of cisplatin side groups dissociably linked to the backbone. The cisplatin side groups number between 25% and 75%, inclusive, of the number of monomeric units of the polymer backbone.

[00102]   Another aspect of the invention is directed to biocompatible conjugated polymer nanoparticles including a poly(isobutylene-*alt*-maleic acid) backbone. The backbone consists of from 25 to 50 monomers. Also included are a plurality of glucosamine sidechains covalently linked to said backbone. The glucosamine sidechains number greater than 90% of monomeric units of said polymer backbone. Also included are a plurality of cisplatin side groups dissociably linked to the backbone. The cisplatin side groups number between 25% and 75%, inclusive, of the number of monomeric units of the polymer backbone.

[00103]   Yet another aspect of the invention is directed to carboxylic acid-platinum compound complex conjugated nanoparticles including a carboxylic acid-platinum compound complex and a plurality of lipid-polymer chains. The carboxylic acid portion of said carboxylic acid-platinum complex is covalently bound to said lipid-polymer chains.

[00104]   In a preferred embodiment, the carboxylic acid is maleic acid. In some embodiments, the polymer is PEG.

[00105]   In certain embodiments, the platinum compound loading is from 1%-37.5%. In certain embodiments, the platinum compound loading is from 1%-6%.

[00106]   The platinum compound can be Pt(II) compound or a Pt(IV) compound. In some embodiments, the Pt(II) compound is selected from the group consisting of cisplatin, oxaliplatin, carboplatin, paraplatin, sartraplatin, and combinations thereof. In a preferred embodiment, the Pt(II) compound is cisplatin.

[00107]   Another aspect of the invention is directed to a vesicle, micelle, or liposome compound comprising a plurality of nanoparticles of claim as described herein.

[00108]   Still another aspect of the invention is directed to a pharmaceutical composition including any of the nanoparticles or compounds described herein and a pharmaceutically acceptable carrier.

[00109]   Yet another aspect of the invention is directed to a method of treating cancer or metastasis. The method includes selecting a subject in need of treatment for cancer or metastasis and administering to the subject an effective amount of any of the nanoparticles, compounds, or compositions described herein.

[00110]   In some embodiments, the cancer or metastasis is selected from the group consisting of platinum susceptible or resistant tumors including breast, head and neck,

ovarian, testicular, pancreatic, oral-esophageal, gastrointestinal, liver, gall bladder, lung, melanoma, skin cancer, sarcomas, blood cancers, brain tumors including glioblastomas, and tumors of neuroectodermal origin.

[00111]   In yet another aspect, the invention provide for methods of formulating platinum compound polymer nanoparticles, method comprising conjugation of platinum compound with a biocompatible polymer or biocompatible copolymer. Without wishing to be bound by theory, conjugation of platinum compound with the biocompatible polymer at acidic pH results in nanoparticles that are more active *in vivo* than when conjugation is done at basic pH.

[00112]   Accordingly, in some embodiments, conjugation is done at pH below 7, preferably a pH between 1 and 6.9. In some more preferred embodiments, conjugation is carried out at a pH of 6.5.

[00113]   The inventors have observed that conjugation under basic conditions favor the formation of an isomeric PIMA-GA_Cisplantin complex with a monocarboxylato and a more stable Pt<->N coordinate bond. In contrast, complexxation PIMA-GA and cisplatin in an acidic pH generates the isomeric state characterized by the monocarboxylato bond and Pt<->O coordinate bond. Thus, conjugations conditions that lead to the formation of a Pt<->O coordinate bond over a Pt<->N coordinate bond are preferred for conjugation.

[00114]   Generally an excess of the Pt(II) compound to the polymer is used. In some embodiments, 5-25 mole access of Pt(II) compound to polymer is used. Preferably 10-20 mole access of platinum(II) compound to polymer is used . In one preferred 15 mole access of Pt(II) compound to polymer is used.

[00115]   In yet another aspect, the invention provides a dicarbonyl molecule linked to a lipid molecule.   Such a compound can be represented by the structure lipid-linker-dicarbnoyl. These molecules can be used to complex platinum compounds such as cisplatin, oxaliplatin or other platinates and platinum compounds described herein through carboxylato-linkage and/or coordination bonds. These can then be mixed with appropriate lipids/phospholipids to nanoparticles of less than 150 nm, which release Pt in a pH-dependent manner. Once formulated these nanoparticles exhibit improved efficacy and toxicity profile as compared with carboplatin and cisplatin, and are active in a cisplatin-resistant cancer.

[00116]   These nanoparticles can be formulated to comprise pharmaceutically active agents for delivery.

[00117]   The term "Lipid" is used in the conventional sense to refer to molecules that are soluble to a greater or lesser degree in organic solvents, like alcohols, and relatively

insoluble in aqueous media. Thus, the term "lipid" includes compounds of varying chain length, from as short as about 2 carbon atoms to as long as about 28 carbon atoms. Additionally, the compounds may be saturated or unsaturated. and in the form of straight- or branched-chains or in the form of unfused or fused ring structures. Exemplary lipids include, but are not limited to, fats, waxes, sterols, steroids, bile acids, fat-soluble vitamins (such as A, D, E, and K), monoglycerides, diglycerides, phospholipids, glycolipids, sulpholipids, aminolipids, chromolipids (lipochromes), glycerophospholipids, sphingolipids, prenol lipids, saccharolipids, polyketides, and fatty acids. In some embodiments, the lipid is cholesterol or distearoylphosphatidylethanolamine.

[00118]   Generally any molecule that has two carbonyl groups can be used. In some embodiments, the dicarbonyl molecule is a dicarboxylic acid, or a keto-carboxylic acid. In some preferred embodiments, the dicarbonyl molecule is succinic acid.

[00119]   In some embodiments, the dicarbonyl molecule is R'OC(O)-R-C(O)-, wherein R is C_1-C_6 alkylene, where the alkylene can comprise one or more double or triple bonds and/or the backbone of the alkylene can be interrupted with one or more of O, S, S(O), SO_2, NH, C(O); and R' is H, alkyl, alkenyl, alkynyl, aryl, heteroaryl, acylcy, heterocyclyl, each of which can be optionally substituted.. Preferably R is CH_2, $-CH_2CH_2-$, $-CH_2CH_2-CH_2-$ or $-CH=CH-$. Preferably R' is H.

[00120]   The dicarbonyl molecule can be linked with the lipid molecule directly or through a linker molecule. The term "linker" means an organic moiety that connects two parts of a compound. Linkers typically comprise a direct bond or an atom such as oxygen or sulfur, a unit such as NH, C(O), C(O)NH, SO, SO_2, SO_2NH or a chain of atoms, such as substituted or unsubstituted alkyl, substituted or unsubstituted alkenyl, substituted or unsubstituted alkynyl, arylalkyl, arylalkenyl, arylalkynyl, heteroarylalkyl, heteroarylalkenyl, heteroarylalkynyl, heterocyclylalkyl, heterocyclylalkenyl, heterocyclylalkynyl, aryl, heteroaryl, heterocyclyl, cycloalkyl, cycloalkenyl, alkylarylalkyl, alkylarylalkenyl, alkylarylalkynyl, alkenylarylalkyl, alkenylarylalkenyl, alkenylarylalkynyl, alkynylarylalkyl, alkynylarylalkenyl, alkynylarylalkynyl, alkylheteroarylalkyl, alkylheteroarylalkenyl, alkylheteroarylalkynyl, alkenylheteroarylalkyl, alkenylheteroarylalkenyl, alkenylheteroarylalkynyl, alkynylheteroarylalkyl, alkynylheteroarylalkenyl, alkynylheteroarylalkynyl, alkylheterocyclylalkyl, alkylheterocyclylalkenyl, alkylhererocyclylalkynyl, alkenylheterocyclylalkyl, alkenylheterocyclylalkenyl, alkenylheterocyclylalkynyl, alkynylheterocyclylalkyl, alkynylheterocyclylalkenyl, alkynylheterocyclylalkynyl, alkylaryl, alkenylaryl, alkynylaryl, alkylheteroaryl,

alkenylheteroaryl, alkynylhereroaryl, where one or more methylenes can be interrupted or terminated by O, S, S(O), SO$_2$, NH, C(O). It is to be understood that the diacarbonyl molecule and/or the lipid can be modified to comprise functional groups for linking to each other or to the linker.

[00121]   In some embodiments, linker is a diamine such as ethylene diamine. In some embodiments, linker is PEG-NH$_2$.

[00122]   In one preferred embodiment, linker is –NHCH$_2$CH$_2$C(O)-. In another preferred embodiment, linker is –CH$_2$CH$_2$NHC(O)-[OCH$_2$CH$_2$]$_z$-NH-, where z is 1-50. Preferably z is 45.

[00123]   In some embodiments, the lipid-dicarbonyl compound is as shown in Figs. 10 (compound 2) and 25 (compound 5).

[00124]   In another aspect, the invention provide a biocompatible polymer comprising at least one monomer having the formula –CH(CO$_2$H)-R-CH(C(O)R')- , wherein R is a bond, C$_1$-C$_6$ alkylene, where the alkylene can comprise one or more double or triple bonds; and R' is a substituted nitrogen atom. Preferably, R is a bond.
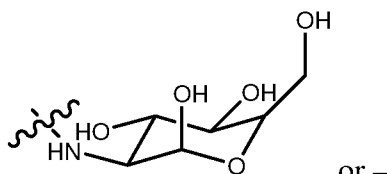
[00125]   In some embodiments, the polymer comprises from 2 to 100 monomeric units having the formula –CH(CO$_2$H)-R-CH(C(O)R')-, wherein R is a bond, C$_1$-C$_6$ alkylene, where the alkylene can comprise one or more double or triple bonds; and R' is a substituted nitrogen atom.

[00126]   In some embodiments, the polymer comprises from 25 to 50 monomeric units having the formula –CH(CO$_2$H)-R-CH(C(O)R')-, wherein R is a bond, C$_1$-C$_6$ alkylene, where the alkylene can comprise one or more double or triple bonds; and R' is a substituted nitrogen atom.

[00127]   In some embodiments, between 50% to 100%, inclusive, of the monomeric subunits in the polymeric backbone are –CH(CO$_2$H)-R-CH(C(O)R')-, wherein R is a bond, C$_1$-C$_6$ alkylene, where the alkylene can comprise one or more double or triple bonds; and R' is a substituted nitrogen atom.

[00128]   In some embodiments, at least 90% or more of the monomeric subunits in the polymeric backbone are –CH(CO$_2$H)-R-CH(C(O)R')-, wherein R is a bond, C$_1$-C$_6$ alkylene, where the alkylene can comprise one or more double or triple bonds; and R' is a substituted nitrogen atom.

[00129]   In some embodiments, the copolymer comprises at least one monomer having the formula –CH(CO$_2$H)-R-CH(C(O)R')CH$_2$C(Me$_2$)- or –CH(C(O)R')-R-CH(CO$_2$H)-

CH$_2$C(Me$_2$)-, wherein R is a bond, C$_1$-C$_6$ alkylene, where the alkylene can comprise one or more double or triple bonds; and R' is a substituted nitrogen atom. Preferably, R is a bond.

[00130]   In some embodiments, the copolymer comprises between 50% to 100%, inclusive of monomers having the formula –CH(CO$_2$H)-R-CH(C(O)R')CH$_2$C(Me$_2$)- or –CH(C(O)R')-R-CH(CO$_2$H)-CH$_2$C(Me$_2$)-, wherein R is a bond, C$_1$-C$_6$ alkylene, where the alkylene can comprise one or more double or triple bonds; and R' is a substituted nitrogen atom.

[00131]   In some embodiments, the copolymer comprises at least 90% of monomers having the formula –CH(CO$_2$H)-R-CH(C(O)R')CH$_2$C(Me$_2$)- or –CH(C(O)R')-R-CH(CO$_2$H)-CH$_2$C(Me$_2$)-, wherein R is a bond, C$_1$-C$_6$ alkylene, where the alkylene can comprise one or more double or triple bonds; and R' is a substituted nitrogen atom.

[00132]   In some embodiments, R' is or – NH(CH$_2$CH$_2$O)$_m$CH$_3$, wherein m is 1-150.

[00133]   These polymers can be used for formulating nanoparticles and gels which can be used for drug delivery. Thus, the invention also provides nanoparticles comprising a polymer described herein and one or more bioactive active agent ("bioactive agent").

[00134]   Compositions described herein can be used in methods for sustained release of bioactive active agents. In one embodiment, the method comprising: (a) providing or administering to a subject a composition described herein, wherein the composition contains the bioactive agent. As used herein, "bioactive agents" refer to naturally occurring biological materials, for example, extracellular matrix materials such as fibronectin, vitronection, and laminin; cytokins; and growth factors and differentiation factors. "Bioactive agents" also refer to artificially synthesized materials, molecules or compounds that have a biological effect on a biological cell, tissue or organ.

[00135]   Suitable growth factors and cytokines include, but are not limited, to stem cell factor (SCF), granulocyte-colony stimulating factor (G-CSF), granulocyte-macrophage stimulating factor (GM-CSF), stromal cell-derived factor-1, steel factor, VEGF, TGFβ, platelet derived growth factor (PDGF), angiopoeitins (Ang), epidermal growth factor (EGF), bFGF, HNF, NGF, bone morphogenic protein (BMP), fibroblast growth factor (FGF), hepatocye growth factor, insulin-like growth factor (IGF-1), interleukin (IL)-3, IL-1α, IL-1β, IL-6, IL-7, IL-8, IL-11, and IL-13, colony-stimulating factors, thrombopoietin,

erythropoietin, fit3-ligand, and tumor necrosis factor α (TNFα). Other examples are described in Dijke et al., "Growth Factors for Wound Healing", Bio/Technology, 7:793-798 (1989); Mulder GD, Haberer PA, Jeter KF, eds. Clinicians' Pocket Guide to Chronic Wound Repair. 4th ed. Springhouse, PA: Springhouse Corporation; 1998:85; Ziegler T.R., Pierce, G.F., and Herndon, D.N., 1997, International Symposium on Growth Factors and Wound Healing: Basic Science & Potential Clinical Applications (Boston, 1995, Serono Symposia USA), Publisher: Springer Verlag.

[00136]   In some embodiments, suitable bioactive agents include but not limited to therapeutic agents. As used herein, the term "therapeutic agent" refers to a substance used in the diagnosis, treatment, or prevention of a disease. Any therapeutic agent known to those of ordinary skill in the art to be of benefit in the diagnosis, treatment or prevention of a disease is contemplated as a therapeutic agent in the context of the present invention. Therapeutic agents include pharmaceutically active compounds, hormones, growth factors, enzymes, DNA, plasmid DNA, RNA, siRNA, viruses, proteins, lipids, pro-inflammatory molecules, antibodies, antibiotics, anti-inflammatory agents, anti-sense nucleotides and transforming nucleic acids or combinations thereof. Any of the therapeutic agents may be combined to the extent such combination is biologically compatible.

[00137]   Exemplary therapeutic agents include, but are not limited to, those found in *Harrison's Principles of Internal Medicine*, 13th Edition, Eds. T.R. Harrison *et al.* McGraw-Hill N.Y., NY; Physicians Desk Reference, 50th Edition, 1997, Oradell New Jersey, Medical Economics Co.; Pharmacological Basis of Therapeutics, 8th Edition, Goodman and Gilman, 1990; United States Pharmacopeia, The National Formulary, USP XII NF XVII, 1990; current edition of Goodman and Oilman's *The Pharmacological Basis of Therapeutics*; and current edition of *The Merck Index*, the complete contents of all of which are incorporated herein by reference.

[00138]   Examples of therapeutic agents which may be incorporated in the composition, include but are not limited to, narcotic analgesic drugs; salts of gold; corticosteroids; hormones; antimalarial drugs; indole derivatives; pharmaceuticals for arthritis treatment; antibiotics, including Tetracyclines, Penicillin, Streptomycin and Aureomycin; antihelmintic and canine distemper drugs, applied to domestic animals and large cattle, such, as, for example, phenothiazine; drugs based on sulfur, such, as sulfioxazole; antitumor drugs; pharmaceuticals supervising addictions, such as agents controlling alcohol addiction and

agents controlling tobacco addiction; antagonists of drug addiction, such, as methadone; weightcontrolling drugs; thyroid gland controlling drugs; analgesics; drugs controlling fertilization or contraception hormones; amphetamines; antihypertensive drugs; antiinflammatories agents; antitussives; sedatives; neuromuscular relaxants; antiepileptic drugs; antidepressants; antidisrhythmic drugs; vasodilating drugs; antihypertensive diuretics; antidiabetic agents; anticoagulants; antituberculous agents; antipsyhotic agents; hormones and peptides. It is understood that above list is not full and simply represents the wide diversification of therapeutic agents that may be included in the compositions. In some embodiments, therapeutic agent is Mitoxantrone, protein (e.g. VEGF) or plasmid DNA.

[00139]   The amount of therapeutic agent distributed in a composition depends on various factors including, for example, specific agent; function which it should carry out; required period of time for release of a the agent; quantity to be administered. Generally, dosage of a therapeutic agent i.e. amount of therapeutic agent in composition, is selected from the range about from 0.001% (w/w) up to 95% (w/w), preferably, from about 5% (w/w) to about 75% (w/w), and, most preferably, from about 10% (w/w) to about 60% (w/w).

[00140]   Cisplatin [cis-dichlorodiammineplatinum(II)] (CDDP) has emerged as an important class of antitumor agents, and is widely used for the treatment of many malignancies including testicular , ovarian , cervical, head and neck, and non-small cell lung cancer (Jamieson, et al, Chem. Rev. (1999), 99(9): 2467-2498). It was also shown to be active in triple negative breast cancer (Leong, et al., J. Clin. Invest. (2007), 117(5): 1370-80). Its use is however dose-limited mainly because of nephrotoxicity or toxicity to the kidney (Madias, NE and Harrington, JT, Am. J. (1978), 65(2): 307-14). To address this limitation, two directions of research has evolved, the first focused on the synthesis of platinum analogues, the second is to engineer novel nanodelivery systems as a mean to target the drug directly to the tumor site. It is now well established that nanoparticles in the size range 80-120 nm home preferentially into tumors resulting from the enhanced permeability and retention (EPR) effect (Moghimi, et al., Pharmacol. Rev. (2001), 53(2): 283-318). This can reduce systemic side effects and exhibit increased intratumoral delivery. A nanoliposomal formulation of cisplatin was found to deliver 50-200 times more drug to the tumor as compared to administration of free cisplatin (Harrington, et al. Ann. Oncol. (2001) 12: 493-496). Although there was minimal toxicity with the nanoliposomal formulation, it had only modest antitumor activity as compared to cisplatin; reflecting the challenges of not only delivering platinum in a relatively inactive form, but the subsequent need to achieve

significant release and activation within the tumor. A second strategy of encapsulating cisplatin into polymeric systems has been a challenge as a result of its insolubility in organic solvents and partial solubility in water, which resulted in poor loading or inability to maintain sustained release. This has required the development of platinum (IV) prodrugs that can be modified to increase hydrophobicity, and increase loading in polylactide-polyglycolide copolymer nanoparticles (Dhar et al., 2009). Alternatively, cisplatin was conjugated to N-(2-hydroxypropyl) methacrylamide (HPMA) through peptidyl side-chains, and were shown to be biologically active(Lin X, Zhang Q, Rice JR, Stewart DR, Nowotnik DP, Howell SB. Improved targeting of platinum chemotherapeutics. The antitumour activity of the HPMA copolymer platinum agent AP5280 in murine tumour models. Eur J Cancer. 2004 Jan;40(2):291-7). However, such approaches require processing through enzymatic cleavage or intracellular reduction for activation of the drug.   Similarly, a PAMAM dendrimers-platinum complex, which increased drug loading, was found to be 200-550-fold less toxic than cisplatin as a result of strong bonds that are formed between the polymer and Pt (Haxton KJ, Burt HM. Polymeric drug delivery of platinum-based anticancer agents. J Pharm Sci. 2009 Jul;98(7):2299-316).

[00141]   To engineer a nanoformulation of cisplatin that is facile but overcomes the challenges associated with current approaches, the inventors integrated the existing information on the biotransformation of cisplatin and understanding of the structure activity relationship that has emerged through the development of cisplatin analogues. Cisplatin gets activated through intracellular aquation of one of the two chloride leaving groups to form $[Pt(NH_3)_2Cl(OH_2)]^+$ and $[Pt(NH_3)_2(OH_2)]^{2+}$, following which the Pt forms covalent bonds to the N_7 position of purine bases to form intrastrand and interstrand crosslinks (Huifang Huang, Leiming Zhu, Brian R. Reid, Gary P. Drobny, Paul B. Hopkins. Solution Structure of a Cisplatin-Induced DNA Interstrand Cross-Link. *Science* 1995: 270. 1842 – 1845). In comparison, carboplatin and oxaloplatin, have a cyclobutane-1,1-decarboxylate and an oxalate respectively as the leaving groups, which chelate the platinum more strongly thus confering greater stability to the leaving group-PT complex and as a result exhibit fewer side effects than cisplatin but also lower efficacy than cisplatin (Richard J. Knox, Frank Friedlos, David A. Lydall and John J. Roberts Mechanism of Cytotoxicity of Anticancer Platinum Drugs: Evidence That *cis*-Diamminedichloroplatinum(II) and *cis*-Diammine-(1,1-cyclobutanedicarboxylato) platinum(II) Differ Only in the Kinetics of Their Interaction with DNA. *Cancer Research* 46, 1972-1979, April 1, 1986; and Ronald S. Go, Alex A. Adjei. Review of the Comparative Pharmacology and Clinical Activity of Cisplatin and Carboplatin.

Journal of Clinical Oncology, Vol 17, Issue 1 (January), 1999: 409). The inventors selected a 40-mer Poly(isobutylene-alt-maleic acid) (PIMA or PMA) as the polymer because each monomer exhibits dicarboxylato groups that can be complexed with cisplatin(OH)$_2$. allowed the loading of a cisplatin molecule. Furthermore, hydrogenation of maleic acid generates succinic acid, which is a component of the Krebs cycle. Poly(isobutylene-alt-maleic acid) **2** was synthesized from Poly(isobutylene-alt-maleic anhydride) **1** by reaction with water in DMF in one step as shown in Figure 1. Further conjugation of cisplatin to Poly(isobutylene-alt-maleic acid) (PIMA) **2** was achieved by stirring hydrated cisplatin for 48 hours gave PMA-Cisplatin **6**. The non-conjugated cisplatin was removed by dialysis and amount of loading was determined by NMR and spectrophotometry. Interestingly, the complexation process led to the generation of nanoparticles through a self-assembly process, with the size defined by the number of cisplatin molecules loaded per polymer. Measurement using dynamic laser light scatter revealed that saturating all the complexation sites with cisplatin resulted in a gel formation while loading 15 molecules of cisplatin per polymer resulted in a nanoparticle in the size range of 100 nm. This was validated by transmission electron microscopy (data not shown).

[00142]   Cisplatin is a first line therapy for lung cancer, and as a result the inventors studied the effect of PMA-Cisplatin on the viability of Lewis lung cancer cells. Treatment with both cisplatin and PMA-cisplatin induced identical cell kill (Fig. 1C). However, PMA also induced tumor cell death. The inventors discovered that this can be overcome through derivatization of PMA. The inventors derivatized the polymer with ethylene diamine under basic conditions (Fig. 2). Interestingly, although the derivatization failed to remove the cytotoxicity of PMA, it increased the cytotoxicity of the PMA-cisplatin complex. This could potentially arise from the fact that the leaving group is less tightly bound as compared to underivatized PMA. Indeed, such an effect has been seen in the case of carboplatin, which has a lower rate constant for aquation than cisplatin, and as a result is also less cytotoxic. The native PMA-cisplatin may be tightly held as compared with PMA-EDA because of strong chelation formed by two carboxy groups. To further make the polymer more biocompatible the inventors modified the polymer with glucosamine (GA). PMA-GA-cisplatin was synthesized starting with PMA (**1**) by reacting with Glucosamine and then with aqueous cisplatin (Figs. 3 and 11B). All the carrier polymers synthesized were platinated in aqueous phase at room temperature 25°C for 2 days, with aquated cisplatin as platination agent, giving conjugates. At different time points, the inventors aliquoted out a small fraction and quantified the total loading of cisplatin on the polymer. The inventors observed a loading

efficiency of ~60% by 5 hours of complexation, ~80% by 30 hours and 100% by 48 hours of platination. The total drug loaded was 6mg/15 mg of polymer. Aquation of cisplatin was achieved using equimolar cisplatin and $AgNO_3$ under dark for 48h. All carriers were routinely fractionated by dialysis and isolated by freeze-drying for spectroscopic characterization. Using DBU resulted in the synthesis of the glucosamine-PMA conjugate as seen in the distinct polymer and sugar peaks in the NMR results that matches with the predicted NMR values. However, treatments with bases, triethylamine or DIPEA, failed to give the predicted product, but the NMR traces provided valuable clue to defining the final functional product.

[00143]   Complexation of cisplatin with PMA-GA resulted in the self assembly of the complex into nanoparticles. In certain cases, passing the nanoparticles through a 0.22 micron filter resulted in the generation of nanoparticles that were in the sub 100nm range, which is critical for the particles to home in specifically to the tumor using the EPR effect. Interestingly, cell viability studies revealed that the PMA-GA derivative was devoid of any inherent toxicity to the cells. In contrast, it retained the efficacy of the aquated Cisplatin (Fig. 4B). Furthermore, derivatization of PMA with polyethylene glycol also removed the inherent toxicity associated with PMA. Additionally, the same goal can be achieved by conjugating maleic acid to a polymeric backbone that is biocompatible.

[00144]   The increased efficacy with the derivatized chelated polymers as compared with the native polymer indicates that the monocarboxylato-chelated release drug much easily and showed superior activity over dicarboxylato-chelated (6). The inventors discovered that the polymeric monocarboxylato-chelated platinum compounds represent a sizeable advantage over the conjugates in which the metal is bound via dicarboxylic acid. Smooth hydrolytic drug liberation from the carrier in the monocarboxylato-chelated derivatized PMA conjugates, as compared to the more retarded hydrolytic fission of the dicarboxylato-chelated in PMA, may explain this enormous difference in cell killing performance. To study this further, the inventors incubated the drug-polymer conjugate with Lewis Lung Cancer cell lysate in a dialysis chamber, and quantified the release of free drug using a calorimetric assay. The inventors obtained a rapid and sustained release of the active agent (Fig. 4A). It should be noted that the same formulation had been dialyzed in water for 48 hours to remove any free cisplatin and the inventors had obtained 100% loading efficiency, suggesting that the active agent is not released in neutral conditions but is rapidly released in the presence of tumor cell lysate.

[00145] The compositions described herein can be formulated into gels and used for sustained released delivery of bioactive agents at specific locations in a subject. For example, the composition can be used for sustained release delivery of platinum compounds at site of tumors. In some embodiments, the composition is used for sustain delivery of a platinum compound after a tumor has been removed.

Pharmaceutical Compositions

[00146] For administration to a subject, the polymer linked platinum compound can be provided in pharmaceutically acceptable compositions. These pharmaceutically acceptable compositions comprise a therapeutically-effective amount of one or more of the platinum compounds described herein, formulated together with one or more pharmaceutically acceptable carriers (additives) and/or diluents. As described in detail below, the pharmaceutical compositions of the present invention can be specially formulated for administration in solid or liquid form, including those adapted for the following: (1) oral administration, for example, drenches (aqueous or non-aqueous solutions or suspensions), lozenges, dragees, capsules, pills, tablets (e.g., those targeted for buccal, sublingual, and systemic absorption), boluses, powders, granules, pastes for application to the tongue; (2) parenteral administration, for example, by subcutaneous, intramuscular, intravenous or epidural injection as, for example, a sterile solution or suspension, or sustained-release formulation; (3) topical application, for example, as a cream, ointment, or a controlled-release patch or spray applied to the skin; (4) intravaginally or intrarectally, for example, as a pessary, cream or foam; (5) sublingually; (6) ocularly; (7) transdermally; (8) transmucosally; or (9) nasally. Additionally, compounds can be implanted into a patient or injected using a drug delivery system. See, for example, Urquhart, et al., Ann. Rev. Pharmacol. Toxicol. 24: 199-236 (1984); Lewis, ed. "Controlled Release of Pesticides and Pharmaceuticals" (Plenum Press, New York, 1981); U.S. Pat. No. 3,773,919; and U.S. Pat. No. 35 3,270,960.

[00147] As used here, the term "pharmaceutically acceptable" refers to those compounds, materials, compositions, and/or dosage forms which are, within the scope of sound medical judgment, suitable for use in contact with the tissues of human beings and animals without excessive toxicity, irritation, allergic response, or other problem or complication, commensurate with a reasonable benefit/risk ratio.

[00148] As used here, the term "pharmaceutically-acceptable carrier" means a pharmaceutically-acceptable material, composition or vehicle, such as a liquid or solid filler, diluent, excipient, manufacturing aid (e.g., lubricant, talc magnesium, calcium or zinc

stearate, or steric acid), or solvent encapsulating material, involved in carrying or transporting the subject compound from one organ, or portion of the body, to another organ, or portion of the body. Each carrier must be "acceptable" in the sense of being compatible with the other ingredients of the formulation and not injurious to the patient. Some examples of materials which can serve as pharmaceutically-acceptable carriers include: (1) sugars, such as lactose, glucose and sucrose; (2) starches, such as corn starch and potato starch; (3) cellulose, and its derivatives, such as sodium carboxymethyl cellulose, methylcellulose, ethyl cellulose, microcrystalline cellulose and cellulose acetate; (4) powdered tragacanth; (5) malt; (6) gelatin; (7) lubricating agents, such as magnesium stearate, sodium lauryl sulfate and talc; (8) excipients, such as cocoa butter and suppository waxes; (9) oils, such as peanut oil, cottonseed oil, safflower oil, sesame oil, olive oil, corn oil and soybean oil; (10) glycols, such as propylene glycol; (11) polyols, such as glycerin, sorbitol, mannitol and polyethylene glycol (PEG); (12) esters, such as ethyl oleate and ethyl laurate; (13) agar; (14) buffering agents, such as magnesium hydroxide and aluminum hydroxide; (15) alginic acid; (16) pyrogen-free water; (17) isotonic saline; (18) Ringer's solution; (19) ethyl alcohol; (20) pH buffered solutions; (21) polyesters, polycarbonates and/or polyanhydrides; (22) bulking agents, such as polypeptides and amino acids (23) serum component, such as serum albumin, HDL and LDL; (22) C_2-C_{12} alchols, such as ethanol; and (23) other non-toxic compatible substances employed in pharmaceutical formulations. Wetting agents, coloring agents, release agents, coating agents, sweetening agents, flavoring agents, perfuming agents, preservative and antioxidants can also be present in the formulation. The terms such as "excipient", "carrier", "pharmaceutically acceptable carrier" or the like are used interchangeably herein.

[00149]   The phrase "therapeutically-effective amount" as used herein means that amount of a compound, material, or composition comprising a compound of the present invention which is effective for producing some desired therapeutic effect in at least a sub-population of cells in an animal at a reasonable benefit/risk ratio applicable to any medical treatment. For example, an amount of a compound administered to a subject that is sufficient to produce a statistically significant, measurable change in at least one symptom of cancer or metastasis.

[00150]   Determination of a therapeutically effective amount is well within the capability of those skilled in the art. Generally, a therapeutically effective amount can vary with the subject's history, age, condition, sex, as well as the severity and type of the medical condition in the subject, and administration of other pharmaceutically active agents.

[00151]   As used herein, the term "administer" refers to the placement of a composition into a subject by a method or route which results in at least partial localization of the composition at a desired site such that desired effect is produced. A compound or composition described herein can be administered by any appropriate route known in the art including, but not limited to, oral or parenteral routes, including intravenous, intramuscular, subcutaneous, transdermal, airway (aerosol), pulmonary, nasal, rectal, and topical (including buccal and sublingual) administration.

[00152]   Exemplary modes of administration include, but are not limited to, injection, infusion, instillation, inhalation, or ingestion. "Injection" includes, without limitation, intravenous, intramuscular, intraarterial, intrathecal, intraventricular, intracapsular, intraorbital, intracardiac, intradermal, intraperitoneal, transtracheal, subcutaneous, subcuticular, intraarticular, sub capsular, subarachnoid, intraspinal, intracerebro spinal, and intrasternal injection and infusion. In preferred embodiments, the compositions are administered by intravenous infusion or injection.

[00153]   By "treatment", "prevention" or "amelioration" of a disease or disorder is meant delaying or preventing the onset of such a disease or disorder, reversing, alleviating, ameliorating, inhibiting, slowing down or stopping the progression, aggravation or deterioration the progression or severity of a condition associated with such a disease or disorder. In one embodiment, at least one symptom of a disease or disorder is alleviated by at least 5%, at least 10%, at least 20%, at least 30%, at least 40%, or at least 50%.

[00154]   As used herein, a "subject" means a human or animal. Usually the animal is a vertebrate such as a primate, rodent, domestic animal or game animal. Primates include chimpanzees, cynomologous monkeys, spider monkeys, and macaques, e.g., Rhesus. Rodents include mice, rats, woodchucks, ferrets, rabbits and hamsters. Domestic and game animals include cows, horses, pigs, deer, bison, buffalo, feline species, e.g., domestic cat, canine species, e.g., dog, fox, wolf, avian species, e.g., chicken, emu, ostrich, and fish, e.g., trout, catfish and salmon. Patient or subject includes any subset of the foregoing, e.g., all of the above, but excluding one or more groups or species such as humans, primates or rodents. In certain embodiments, the subject is a mammal, e.g., a primate, e.g., a human. The terms, "patient" and "subject" are used interchangeably herein. The terms, "patient" and "subject" are used interchangeably herein.

[00155]   Preferably, the subject is a mammal. The mammal can be a human, non-human primate, mouse, rat, dog, cat, horse, or cow, but are not limited to these examples.

Mammals other than humans can be advantageously used as subjects that represent animal models of disorders associated with inflammation.

[00156]   In addition, the methods described herein can be used to treat domesticated animals and/or pets. A subject can be male or female. A subject can be one who has been previously diagnosed with or identified as suffering from or having a disorder a cancer or metastasis, but need not have already undergone treatment.

[00157]   As used herein, the term "cancer" includes, but is not limited to, solid tumors and blood born tumors. The term cancer refers to disease of skin, tissues, organs, bone, cartilage, blood and vessels. The term "cancer" further encompasses primary and metastatic cancers. Examples of cancers that can be treated with the compounds of the invention include, but are not limited to, carcinoma, including that of the bladder, breast, colon, kidney, lung, ovary, pancreas, stomach, cervix, thyroid, and skin, including squamous cell carcinoma; hematopoietic tumors of lymphoid lineage, including, but not limited to, leukemia, acute lymphocytic leukemia, acute lymphoblastic leukemia, B-cell lymphoma, T-cell lymphoma, Hodgkins lymphoma, non-Hodgkins lymphoma, hairy cell lymphoma, and Burketts lymphoma; hematopoietic tumors of myeloid lineage including, but not limited to, acute and chronic myelogenous leukemias and promyelocytic leukemia; tumors of mesenchymal origin including, but not limited to, fibrosarcoma, rhabdomyosarcoma, and osteosarcoma; other tumors including melanoma, seminoma, tetratocarcinoma, neuroblastoma, and glioma; tumors of the central and peripheral nervous system including, but not limited to, astrocytoma, neuroblastoma, glioma, and schwannomas; and other tumors including, but not limited to, xenoderma, pigmentosum, keratoactanthoma, thyroid follicular cancer, and teratocarcinoma. The compounds of the invention are useful for treating patients who have been previously treated for cancer, as well as those who have not previously been treated for cancer. Indeed, the methods and compositions of this invention can be used in first-line and second-line cancer treatments.

[00158]   The compounds of the invention are also useful in combination with known anti-cancer treatments, including radiation. The methods of the invention are especially useful in combination with anti-cancer treatments that involve administering a second drug that acts in a different phase of the cell cycle, e.g., S phase, than the epothilones of Formula (la) or (Ib), which exert their effects at the G2-M phase.

Definitions

[00159]   Unless stated otherwise, or implicit from context, the following terms and phrases include the meanings provided below. Unless explicitly stated otherwise, or apparent from context, the terms and phrases below do not exclude the meaning that the term or phrase has acquired in the art to which it pertains. The definitions are provided to aid in describing particular embodiments, and are not intended to limit the claimed invention, because the scope of the invention is limited only by the claims. Further, unless otherwise required by context, singular terms shall include pluralities and plural terms shall include the singular.

[00160]   As used herein the term "comprising" or "comprises" is used in reference to compositions, methods, and respective component(s) thereof, that are essential to the invention, yet open to the inclusion of unspecified elements, whether essential or not.

[00161]   Other than in the operating examples, or where otherwise indicated, all numbers expressing quantities of ingredients or reaction conditions used herein should be understood as modified in all instances by the term "about." The term "about" when used in connection with percentages may mean ±1%.

[00162]   The singular terms "a," "an," and "the" include plural referents unless context clearly indicates otherwise. Similarly, the word "or" is intended to include "and" unless the context clearly indicates otherwise.

[00163]   Although methods and materials similar or equivalent to those described herein can be used in the practice or testing of this disclosure, suitable methods and materials are described below. The term "comprises" means "includes." The abbreviation, "e.g." is derived from the Latin exempli gratia, and is used herein to indicate a non-limiting example. Thus, the abbreviation "e.g." is synonymous with the term "for example."

[00164]   The term "alkyl" refers to saturated non-aromatic hydrocarbon chains that may be a straight chain or branched chain, containing the indicated number of carbon atoms (these include without limitation methyl, ethyl, propyl, iso-propyl, butyl, 2-methyl-ethyl, t-butyl, allyl, or propargyl), which may be optionally inserted with N, O, or S. For example, C_1-C_6 indicates that the group may have from 1 to 6 (inclusive) carbon atoms in it.

[00165]   The term "alkenyl" refers to an alkyl that comprises at least one double bond. Exemplary alkenyl groups include, but are not limited to, for example, ethenyl, propenyl, butenyl, 1-methyl-2-buten-1-yl and the like.

[00166]   The term "alkynyl" refers to an alkyl that comprises at least one triple bond.

[00167]   The term "aryl" refers to monocyclic, bicyclic, or tricyclic aromatic ring system wherein 0, 1, 2, 3, or 4 atoms of each ring may be substituted by a substituent.

Examplary aryl groups include, but are not limited to, benzyl, phenyl, naphthyl, anthracenyl, azulenyl, fluorenyl, indanyl, indenyl, naphthyl, phenyl, tetrahydronaphthyl, and the like.

[00168]   The term "cyclyl" or "cycloalkyl" refers to saturated and partially unsaturated cyclic hydrocarbon groups having 3 to 12 carbons, for example, 3 to 8 carbons, and, for example, 3 to 6 carbons, wherein the cycloalkyl group additionally may be optionally substituted. Exemplary cycloalkyl groups include, but are not limited to, cyclopropyl, cyclobutyl, cyclopentyl, cyclopentenyl, cyclohexyl, cyclohexenyl, cycloheptyl, cyclooctyl, and the like.

[00169]   The term "heteroaryl" refers to an aromatic 5-8 membered monocyclic, 8-12 membered bicyclic, or 11-14 membered tricyclic ring system having 1-3 heteroatoms if monocyclic, 1-6 heteroatoms if bicyclic, or 1-9 heteroatoms if tricyclic, said heteroatoms selected from O, N, or S (*e.g.*, carbon atoms and 1-3, 1-6, or 1-9 heteroatoms of N, O, or S if monocyclic, bicyclic, or tricyclic, respectively), wherein 0, 1, 2, 3, or 4 atoms of each ring may be substituted by a substituent. Examplary heteroaryl groups include, but are not limited to, pyridyl, furyl or furanyl, imidazolyl, benzimidazolyl, pyrimidinyl, thiophenyl or thienyl, pyridazinyl, pyrazinyl, quinolinyl, indolyl, thiazolyl, naphthyridinyl, and the like.

[00170]   The term "heterocyclyl" refers to a nonaromatic 5-8 membered monocyclic, 8-12 membered bicyclic, or 11-14 membered tricyclic ring system having 1-3 heteroatoms if monocyclic, 1-6 heteroatoms if bicyclic, or 1-9 heteroatoms if tricyclic, said heteroatoms selected from O, N, or S (*e.g.*, carbon atoms and 1-3, 1-6, or 1-9 heteroatoms of N, O, or S if monocyclic, bicyclic, or tricyclic, respectively), wherein 0, 1, 2 or 3 atoms of each ring may be substituted by a substituent. Examplary heterocyclyl groups include, but are not limited to piperazinyl, pyrrolidinyl, dioxanyl, morpholinyl, tetrahydrofuranyl, and the like.

[00171]   The term "optionally substituted" means that the specified group or moiety, such as an alkyl group, alkenyl group, and the like, is unsubstituted or is substituted with one or more (typically 1-4 substituents) independently selected from the group of substituents listed below in the definition for "substituents" or otherwise specified.

[00172]   The term "substituents" refers to a group "substituted" on an alkyl, alkenyl, alkynyl, cycloalkyl, aryl, heterocyclyl, or heteroaryl group at any atom of that group. Suitable substituents include, without limitation, halogen, hydroxy, oxo, nitro, haloalkyl, alkyl, alkenyl, alkynyl, alkaryl, aryl, aralkyl, alkoxy, aryloxy, amino, acylamino, alkylcarbanoyl, arylcarbanoyl, aminoalkyl, alkoxycarbonyl, carboxy, hydroxyalkyl, alkanesulfonyl, arenesulfonyl, alkanesulfonamido, arenesulfonamido, aralkylsulfonamido,

alkylcarbonyl, acyloxy, cyano or ureido. In some cases, two substituents, together with the carbons to which they are attached to can form a ring.

[00173]   As used herein, the term "polymer" refers to the product of a polymerization reaction, and is inclusive of homopolymers, copolymers, terpolymers, tetrapolymers, etc. The term "polymer" is also inclusive of random polymers, block polymers, graft polymers, copolymers, block copolymers, and graft copolymers. As used herein, the term "copolymer" refers to polymers formed by the polymerization reaction of at least two different monomers.

[00174]   The term "copolymer backbone" as used herein refers to that portion of the polymer which is a continuous chain comprising the bonds formed between monomers upon polymerization. The composition of the copolymner backbone can be described in terms of the identity of the monomers from which it is formed without regard to the composition of branches, or sidechains, of the polymer backbone. The term "sidechain" refers to portions of the monomer which, following polymerization, forms an extension of the copolymer backbone.

[00175]   As used herein, the term "biocompatible" refers to a material that is capable of interacting with a biological system without causing cytotoxicity, undesired protein or nucleic acid modification or activation of an undesired immune response. "Biocompatibility" also includes essentially no interactions with recognition proteins, e.g., naturally occurring antibodies, cell proteins, cells and other components of biological systems.

[00176]   As used herein an ester sidechains means a sidechains of the formula -R'''C(O)-OR^E, where RE is independently C1-C6alkyl, C1-C6alkenyl, C1-C6alkynyl, cyclyl, heterocycly, aryl, or heteroaryl, each of which can be optionally substituted; and R''' is a bond or C1-C6 alkylene, were the alkylene can comprise one or more double or triple bonds and/or the backbone of the alkylene can be interrupted by O, S, S(O), NH, or C(O). Preferably R''' is a bond.

[00177]   As used herein an amide sidechains means a sidechains of the formula -R''C(O)-N(R^A)$_2$, where RA is independently H, C1-C6alkyl, C1-C6alkenyl, C1-C6alkynyl, cyclyl, heterocycly, aryl, heteroaryl, saccharide, disaccharide, or trisaccharide, each of which can be optionally substituted; and R'' is a bond or C1-C6 alkylene, were the alkylene can comprise one or more double or triple bonds and/or the backbone of the alkylene can be interrupted by O, S, S(O), NH, or C(O). Preferably R'' is a bond.

[00178]   As used herein a carboxylic acid chain means a sidechains of the formula -R''''C(O)OH where R'''' is a bond or C1-C6 alkylene, were the alkylene can comprise one or

more double or triple bonds and/or the backbone of the alkylene can be interrupted by O, S, S(O), NH, or C(O). Preferably R'''' is a bond.

[00179]   Some non-exhaustive examples of biocompatible polymers include polyamides, polycarbonates, polyalkylenes, polyalkylene glycols, polyalkylene oxides, polyalkylene terepthalates, polyvinyl alcohols, polyvinyl ethers, polyvinyl esters, polyvinyl halides, polyvinylpyrrolidone, polyglycolides, polysiloxanes, polyurethanes and copolymers thereof, alkyl cellulose, hydroxyalkyl celluloses, cellulose ethers, cellulose esters, nitro celluloses, polymers of acrylic and methacrylic esters, methyl cellulose, ethyl cellulose, hydroxypropyl cellulose, hydroxy-propyl methyl cellulose, hydroxybutyl methyl cellulose, cellulose acetate, cellulose propionate, cellulose acetate butyrate, cellulose acetate phthalate, carboxylethyl cellulose, cellulose triacetate, cellulose sulphate sodium salt, poly(methylmethacryl ate), poly (ethylmethacrylate), poly(butylmethacrylate), poly (isobutylmethacrylate), poly(hexlmethacrylate), poly (isodecylmethacrylate), poly(laurylmethacrylate), poly (phenylmethacrylate), poly(methacrylate), poly (isopropacrylate), poly(isobutacrylate), poly (octadecacrylate), polyethylene, polypropylene poly (ethylene glycol), poly(ethylene oxide), poly(ethylene terephthalate), poly(vinyl alcohols), poly(vinyl acetate), poly vinyl chloride, polystyrene, polyhyaluronic acids, casein, gelatin, gluten, polyanhydrides, polyacrylic acid, alginate, chitosan, any copolymers thereof, and any combination of any of these. Additionally, biocompatible polymers and copolymers that have been modified for desirable enzymatic degradation, or change upon application of light, ultrasonic energy, radiation, a change in temperature, pH, osmolarity, solute or solvent concentration are also amenable to the present invention.

[00180]   The present invention may be defined in any of the following numbered paragraphs:

1.   A biocompatible conjugated polymer nanoparticle comprising:

a copolymer backbone;

a plurality of sidechains covalently linked to said backbone; and

a plurality of platinum compounds dissociably linked to said sidechains.

2.   The nanoparticle of paragraph 1, wherein said plurality of platinum compounds is selected from Pt(II) compounds, Pt(IV) compounds, and any combinations thereof.

3.   The nanoparticle of paragraph 1 or 2, wherein at least one of said plurality of platinum compounds is linked to said sidechain through at least one coordination bond.

4.   The nanoparticle of paragraph 3, wherein said coordination bond is between an oxygen of the sidechains and the platinum atom of the platinum compound.

5.   The nanoparticle of paragraph 4, wherein said oxygen is a carbonyl oxygen.

6.   The nanoparticle of paragraph 4, wherein said oxygen is an amide oxygen.

7.   The nanoparticle of any of paragraphs 1-6, wherein said copolymer comprises maleic acid monomers.

8.   The nanoparticle of paragraph 7, wherein at least one carboxylic acid of the maleic acid is derivatized to an amide.

9.   The nanoparticle of any of paragraphs 1-8, wherein said copolymer is poly(isobutylene-*alt*-maleic acid) (PIMA).

10.   The nanoparticle of any of paragraphs 1-9, wherein said copolymer comprises from 2 to 100 monomer units.

11.   The nanoparticle of any of paragraphs 1-10, wherein said copolymer comprises from 25 to 50 monomer units.

12.   The nanoparticle of any of paragraphs 1-11, wherein said sidechains are selected from the group consisting of polymers, monosaccharides, dicarboxylic acids, and combinations thereof.

13.   The nanoparticle of any of paragraphs 1-12, wherein said sidechains are polyethylene glycol (PEG).

14.   The nanoparticle of paragraph 13, wherein said PEG sidechains have a molecular weight of from 100 to 5000 Dalton.

15.   The nanoparticle of paragraph 13, wherein said PEG sidechains have a molecular weight of from 1000 to 3000 Dalton.

16.   The nanoparticle of paragraph 13, wherein said PEG sidechains have a molecular weight of about 2000 Dalton.

17.   The nanoparticle of any of paragraphs 1-12, wherein said sidechains are monosaccharides.

18.   The nanoparticle of paragraph 17, wherein said monosaccharides are glucosamine.

19.   The nanoparticle of any of paragraphs 1-18, wherein said platinum compound is a Pt(II) compound selected from the group consisting of cisplatin, oxaliplatin, carboplatin, paraplatin, sartraplatin, and combinations thereof.

20.   The nanoparticle of paragraph 19, wherein said platinum (II) compound is cisplatin.

21.   The nanoparticle of paragraph 19, wherein said platinum compound is oxaliplatin.

22.   The nanoparticle of any of paragraphs 1-21, wherein the number of sidechains corresponds between 50% and 100% of the number of monomeric units of said polymer backbone.

23.   The nanoparticle of any of paragraphs 1-22, wherein the number of said sidechains corresponds to a number greater than 90% of the number of monomeric units of said polymer backbone.

24.   The nanoparticle of any of paragraphs 1-23, wherein the number of said platinum compounds corresponds between 10% and 100% of the number of monomeric units of said polymer backbone.

25.   The nanoparticle of any of paragraphs 1-24, wherein the number of said platinum compounds corresponds between 25% and 75% of the number of monomeric units of said polymer backbone.

26.   The nanoparticle of any of paragraphs 1-25, wherein said sidechains comprise dicarboxylic acids.

27.   The nanoparticle of paragraph 26, wherein said dicarboxylic acids are of the formula HOOC-R-COOH, wherein R is a C_1-C_6alkyl, C_2-C_6alkenyl, or C_2-C_6alkynyl.

28.   The nanoparticle of paragraph 27, wherein said dicarboxylic acid is maleic acid.

29.   A biocompatible conjugated polymer nanoparticle comprising:

a poly(isobutylene-*alt*-maleic acid) backbone, wherein said backbone contains 25 to 50 monomer units;

a plurality of PEG sidechains covalently linked to said backbone, wherein said PEG sidechains have a molecular weight of from 1000 to 3000 Dalton and wherein the number of said PEG sidechains corresponds to between 50% and 100% of the number of monomeric units of said polymer backbone; and

a plurality of cisplatin sidegroups dissociably linked to said backbone wherein the number of said cisplatin sidegroups is between 25% and 75% of the number of monomeric units of said polymer backbone.

30.   A biocompatible conjugated polymer nanoparticle comprising:

a poly(isobutylene-*alt*-maleic acid) backbone, wherein said backbone consist of 40 monomers;

a plurality of PEG sidechains covalently linked to said backbone, wherein said PEG sidechains have a molecular weight of 2000 Dalton and wherein the number of said PEG sidechains is greater than 90% of monomeric units of said polymer backbone; and

a plurality of cisplatin sidegroups dissociably linked to said backbone, wherein the number of said cisplatin sidegroups is between 25% and 75% of the number of monomeric units of said polymer backbone.

31.   A biocompatible conjugated polymer nanoparticle comprising:

a poly(isobutylene-*alt*-maleic acid) backbone, wherein said backbone comprises from 25 to 50 monomers;

a plurality of glucosamine sidechains covalently linked to said backbone and wherein the number of said glucosamine sidechains is between 50% and 100% of monomeric units of said polymer backbone; and

a plurality of cisplatin sidegroups dissociably linked to said backbone, wherein the number of said cisplatin sidegroups is between 25% and 75% of the number of monomeric units of said polymer backbone.

32.   A biocompatible conjugated polymer nanoparticle comprising:

a poly(isobutylene-*alt*-maleic acid) backbone, wherein said backbone comprises from 25 to 50 monomers;

a plurality of glucosamine sidechains covalently linked to said backbone and wherein the number of said glucosamine sidechains is greater than 90% of monomeric units of said polymer backbone; and

a plurality of cisplatin sidegroups dissociably linked to said backbone, wherein the number of said cisplatin sidegroups is between 25% and 75%, inclusive, of the number of monomeric units of said polymer backbone.

33.   A carboxylic acid-platinum compound complex conjugated nanoparticle comprising:

a carboxylic acid-platinum compound complex; and

a plurality of lipid-polymer chains, wherein the carboxylic acid portion of said carboxylic acid-platinum compound complex is covalently bound to said lipid-polymer chains.

34.   The nanoparticle of paragraph 33, wherein the carboxylic acid is maleic acid.

35.   The nanoparticle of any of paragraphs 33-34, wherein the polymer is PEG.

36.   The nanoparticle of any of paragraphs 33-35, wherein the platinum compound is a Pt(II) compound selected from the group consisting of cisplatin, oxaliplatin, carboplatin, paraplatin, sartraplatin, and combinations thereof.

37.   The nanoparticle of paragraph 36, wherein the Pt(II) compound is cisplatin.

38.   The nanoparticle of any of paragraphs 33-37, wherein the platinum compound loading is from 1%-30%.

39. The nanoparticle of any of paragraphs 33-38, wherein the platinum compound loading is from 1%-6%.

40. A vesicle, micelle, or liposome compound comprising a plurality of nanoparticles of any of paragraphs 33-39.

41. A dicarbonyl-lipid compound having the structure
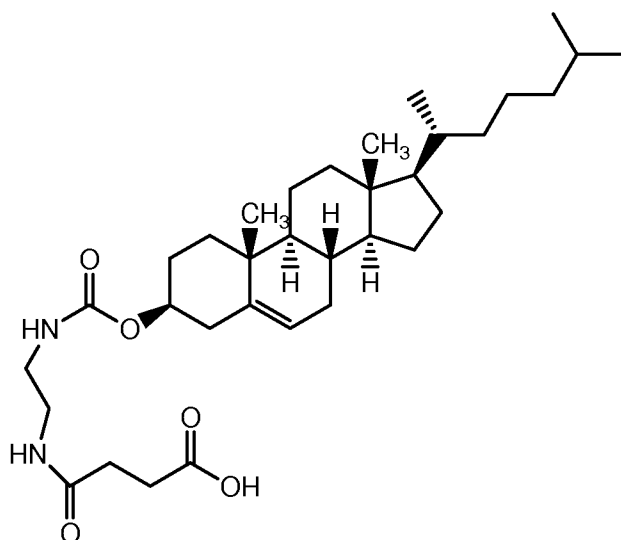
.

42. A vesicle, micelle, liposome or nanoparticle compound comprising a dicarbonyl-lipid compound of paragraph 41 and a platinum compound, wherein the platinum compound is dissociably linked to the compound of paragraph 41.

43. The nanoparticle of paragraph 42, wherein the platinum compound is selected from Pt(II) compounds, Pt(IV) compounds, and any combinations thereof.

44. The nanoparticle of paragraph 43, wherein said platinum compound is a Pt(II) compound selected from the group consisting of cisplatin, oxaliplatin, carboplatin, paraplatin, sartraplatin, and combinations thereof.

45. The nanoparticle of paragraph 43, wherein said platinum (II) compound is cisplatin.

46. The nanoparticle of paragraph 43, wherein said platinum compound is oxaliplatin.

47. A nanoparticle compound comprising a biocompatible polymer, wherein the polymer comprises at least one monomer having the formula $-CH(CO_2H)-R-CH(C(O)R')-$, wherein R is a bond, C_1-C_6 alkylene, where the alkylene can comprise one or more double or triple bonds; and R' is a substituted nitrogen atom. Preferably, R is a bond.

48. The nanoparticle of paragraph 47, wherein the polymer comprises from 2 to 100 monomeric units having the formula $-CH(CO_2H)-R-CH(C(O)R')-$.

49. The nanoparticle of any of paragraphs 47-48, wherein the polymer comprises from 25 to 50 monomeric units having the formula $-CH(CO_2H)-R-CH(C(O)R')-$.

50.   The nanoparticle of any of paragraphs 47-49, wherein R'

is or –NH(CH$_2$CH$_2$O)$_m$CH$_3$, wherein m is 1-150.
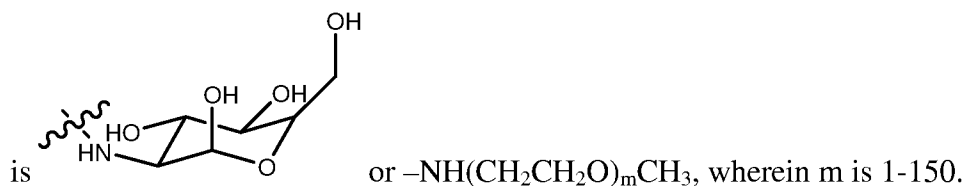
51.   The nanoparticle of any of paragraphs 47-50, further comprising a bioactive agent.

52.   A pharmaceutical composition comprising:

the nanoparticle or compound of paragraphs 1-51; and

a pharmaceutically acceptable carrier.

53.   A method of treating cancer or metastasis comprising:

administering to a subject in need thereof an effective amount of the composition of any of paragraphs 1-52.

54.   The method of paragraph 53, wherein said cancer or metastasis is selected from the group consisting of platinum susceptible or resistant tumors.

55.   The method of paragraph 54, wherein said cancer or metastasis is selected from the group consisting of breast, head and neck, ovarian, testicular, pancreatic, oral-esophageal, gastrointestinal, liver, gall bladder, lung, melanoma, skin cancer, sarcomas, blood cancers, brain tumors, glioblastomas, tumors of neuroectodermal origin and any combinations thereof.

56.   A method of sustain release of a platinum compound at a specific location in a subject comprising: providing at the location a composition of paragraph the composition of any of paragraphs 1-52.

57.   The method of paragraph 56, wherein composition is in the form of a gel.

58.   The method of any of paragraphs 56-57, wherein the location is a tumor.

59.   The method of paragraph 58, wherein the tumor was removed before providing the composition.

[00181]   To the extent not already indicated, it will be understood by those of ordinary skill in the art that any one of the various embodiments herein described and illustrated may be further modified to incorporate features shown in any of the other embodiments disclosed herein.

[00182]   The following examples illustrate some embodiments and aspects of the invention. It will be apparent to those skilled in the relevant art that various modifications, additions, substitutions, and the like can be performed without altering the spirit or scope of

the invention, and such modifications and variations are encompassed within the scope of the invention as defined in the claims which follow. The following examples do not in any way limit the invention.

EXAMPLES

Materials and methods

[00183]   CellTiter 96 AQueous One Solution Cell Proliferation Assay [3-(4,5-dimethylthiazol-2-yl)-5-(3-carboxymethoxyphenyl)-2-(4-sulfophenyl)-2H-tetrazolium, inner salt (MTS) assay] reagent was from Promega (Madison, WI). All Polymer solutions were dialyzed in cellulose membrane tubing, types Spectra/Por 4 and Spectra/Por 6 (wet tubing), with mass-average molecular mass cut-off limits of 1000 and 3500 respectively. Operations were performed against several batches of stirred deionized H2O. Commercially supplied (Sigma, Fluka AG, Aldrich Chemie GmbH) chemicals, reagent grade, were used as received. These included N,N-Dimethylformamide (DMF), Poly(isobutylene-alt-maleic anhydride), Glucosamine.HCl, mPEG2000NH$_2$, Diaza(1,3)bicycle[5.4.0]udecane (DBU), Triethyl amine. ^{1}H NMR and ^{13}C NMR were measured at 300 and 400 MHz, respectively, with a Varion-300 or a Brucker-400 spectrometer. 1H NMR chemical shifts are reported as δ values in parts per million (ppm) relative to either tetramethylsilane (0.0 ppm) or deuterium oxide (4.80 ppm). Data is reported as follows: chemical shift, multiplicity (s = singlet, d = doublet, t = triplet, q = quartet, m = mutliplet, b = broad), coupling constants (hertz), and integration. Carbon-13 chemical shifts are reported in ppm relative to CDCl3 (76.9 ppm) or relative to DMSOd$_6$ (39.5 ppm). ^{195}Pt NMR chemical shifts are reported as δ in ppm relative to Na$_2$PtCl$_6$ (0.0 ppm). In some experiments, ^{1}H NMR and ^{13}C NMR were measured at 500 and 125 MHz, respectively, with a Varion 500 or a Brucker-400 spectrometer.

[00184]   Starting materials were azeotropically dried prior to reaction as required, and all air- and/or moisture-sensitive reactions were conducted in flame- and/or oven-dried glassware under an anhydrous nitrogen atmosphere with standard precautions taken to exclude moisture.

Cell Culture and Cell Viability Assay

[00185]   The Lewis Lung Carcinoma cell lines (LLC) and Breast Cancer cell line (4T1) were purchased from American Type Culture Collection (ATCC, Rockville, MD, USA). Lewis Lung Carcinoma cells were cultured in Dulbecco's Modified Eagle's Medium

supplemented with 10% FBS, 50 unit/ml penicillin and 50 unit/ml streptomycin. The 4T1 cells were cultured in RPMI medium supplemented with 10% FBS, 50 unit/ml penicillin and 50 unit/ml streptomycin. Trypsinized cultured LLC and 4T1 cells were washed twice with PBS and seeded into 96-well flat bottomed plates at a density of 2×10^3 cells in 100 μl of medium. Different concentrations of conjugates were tested in triplicate in the same 96-well plate for each experiment. Medium alone was kept as negative control and CDDP as positive control. The plates were then incubated for 48 h in a 5% CO_2 atmosphere at 37 °C. The cells were washed and incubated with 100 μl phenol- red free medium (without FBS) containing 20 μl of the CellTiter 96 Aqueous One Solution reagent (Promega, WI, USA). This assay [3-(4,5-dimethylthiazol- 2-yl)-5-(3-carboxymethoxyphenyl)-2-(4-sulfophenyl)-2H-tetrazolium, inner salt] (MTS) is a colorimetric method for determining the number of viable cells in proliferation or cytotoxicity assays. After 2-h incubation in a 5% CO_2 atmosphere at 37 °C, the absorbance in each well was recorded at 490 nm using a VERSA max plate reader (Molecular Devices, Sunnyvale, CA, USA).

[00186]   The absorbance reflects the number of surviving cells. Blanks were subtracted from all data and results analyzed using Origin software (OriginLab Corporation, Northampton, USA). The mean of triplicated absorbance data for each tested dose was divided by the mean of untreated control cells. The log of the quotient was used to plot a graph as a function of given dose, i.e. Y = (Tested Absorbance Mean-Background)/(Untreated Absorbance Mean-Background) vs. X = tested dose.

Particle Size Measurement

[00187]   High resolution TEM images were obtained on a JEOL 2011 high contrast digital TEM. Samples were prepared on carbon 300 mesh copper grids (Electron Microscopy Sciences) by adding drops of aqueous nanoparticles at different concentrations, and allowed to air-dry. The size distribution of nanoparticles was studied by dynamic light scattering (DLS), which was performed at 25°C on a DLS-system (Malvern NanoZetasizer) equipped with a He Ne laser.

Physicochemical Release Kinetics Studies

[00188]   PIMA-GA-CDDP was suspended in 1 mL of hypoxic-cell lysate from LLC cell line and sealed in a dialysis bag (MWCO ~ 1000 Da). The dialysis bag was incubated in 1 mL of PBS buffer at room temperature with gentle shaking. 10 μL of aliquot was extracted

from the incubation medium at predetermined time intervals, treated with 90 µL of 1,2-phenylene diamine solution (1.2 mg in 1 mL DMF) and incubated for 3h at 100°C. The released Pt(IV) was quantified by UV-VIS spectroscopy at characteristic wavelength $\lambda = 704$ nm of Pt(IV)-1,2-phenylene diamine complex. After withdrawing each aliquot the incubation medium was replenished by 10 µL of fresh PBS.

[00189]   Alternatively, concentrated PIMA-GA-cisplatin conjugate was resuspended into 100 µL of double distilled water with pH adjusted to 8.5 or 5.5 using 1N sodium hydroxide or 1N nitric acid and transferred to a dialysis tube (MWCO: 1000 KD, Spectrapor). The dialysis tube was put into a tube containing magnetic pallet and 2 mL solutions of different pH phosphate-buffered saline. Cisplatin release was studied by gently stirring the dialysis bag at 300 rpm using IKA stirrer at 25oC. 10 µL aliquots were taken from the outside solution of dialysis membrane bag at predetermined time intervals and subjected to next UV-Vis active complex formation reaction by adding 100 µL of ortho-phenyldiamine (1.2 mg/ml in DMF) and heating the resulting solution for 3h. 10 µL of fresh solution was added back to outside solution of dialysis membrane bag to maintain same volume. The amount of the drug that was released was evaluated by UV-spectrophotometer (Shimadzu UV 2450) at 706 nm.

FACS analysis for apoptosis

[00190]   Cells were grown in 6-well plates incubated in the presence of cisplatin nanoparticle or free cisplatin at 37°C for 24 h. After 24 h, the cells were washed with PBS and collected at 0°C. The cells were then treated with annexin V-Alexa Fluor 488 conjugate (Molecular Probes, Invitrogen) and incubated in the dark, at room temperature, for 15 min. The cells were then washed with PBS and incubated with propidium iodide (PI) solution (50 g/mL; Sigma) containing RNase (1 mg/mL; Sigma). The cell suspensions were then transferred to FACS tubes and analyzed for AnnexinV/PI staining on a BD FACS Calibur instrument. Data were analyzed using a CellQuestPro software (BD Biosciences).

Cellular Uptake Studies

[00191]   LLC and 4T1 cells were seeded on glass coverslips in 24-well plates, 50000 cells per well. When cells reached 70% confluency, they were treated with fluorescein isothiocyanate (FITC)-conjudated cisplatin nanoparticles for different durations of 30 min, 2 h, 6 h, 12 h, and 24 h, respectively. For colocalization studies, at indicated time points, the cells were washed with PBS and incubated with Lysotracker Red (Molecular Probes) at 37°C for 30 min to allow internalization. The cells were then fixed with 4% paraformaldehyde for

20 min at room temperature, then washed twice with PBS and mounted on glass slides using Prolong Gold Antifade Reagent (Molecular Probes). Images were obtained using a Nikon Eclipse TE2000 fluorescence microscope equipped with green and red filters for FITC and Lysotracker Red, respectively.

In Vivo Murine LLC Lung Cancer and 4T1 Breast Cancer Tumor Model

[00192]   The LLC Lung Cancer cells and 4T1 Breast Cancer cells (3x105) were implanted subcutaneously in the flanks of 4-week-old C57/ BL6 and BALB/c mice (weighing 20 g, Charles River Laboratories, MA) respectively. The drug therapy was started after the tumors attained volume of 50 mm^3. The tumor therapy consisted of administration of cisplatin nanoparticle and free cisplatin or oxaliplatin and free oxaliplatin. The formulations were prepared and validated such that 100 μL of cisplatin nanoparticle and free cisplatin contained 1.25 and 3 mg/kg of cisplatin or 100 μL of oxaliplatin nanoparticle and free oxaliplatin contained 5 and 15 mg/kg of oxaliplatin Administration was by tail vein injection. PBS (100 μL) administered by tail-vein injection was used as a control for drug treatment. The tumor volumes and body weights were monitored on a daily basis. The animals were sacrificed when the average tumor size of the control exceeded 2000 mm^3 in the control group. The tumors were harvested immediately following sacrifice and stored in 10% formalin for further analysis. All animal procedures were approved by Harvard institutional IUCAC.

In Vivo Murine Ovarian Cancer Tumor Model

[00193]   Ovarian adenocarcinomas were induced in genetically-engineered K-ras$^{LSL/+}$/Pten$^{fl/fl}$ mice via intrabursal delivery of adenovirus carrying Cre recombinase, as described previously. Tumor cells were engineered to express luciferase once activated by Adeno-Cre, in order to make tumor imaging feasible before and after drug treatment. Once mice developed medium to large tumors they were placed into one of four treatment groups (controls, cisplatin NP1.25 mg/kg, cisplatin NP-3 mg/kg, and free cisplatin), with all drugs administered intravenously (i.v.).

Tumor Imaging and Efficacy Assessment of Drug Treatment

[00194]   Tumor imaging in vivo was performed with the IVIS Lumina II Imaging System. Quantification of bioluminescence was achieved by using the Living Image Software 3.1 (Caliper Life Sciences). Mice received 150 mg/kg of D-luciferin firefly potassium salt via

intraperitoneal (i.p.) injection prior to imaging. Five minutes post-luciferin injection, animals were anesthetized in a 2.5% isoflurane induction chamber. Once anesthesized, mice were placed into the imaging chamber where they were kept under anesthesia by a manifold supplying isoflurane and their body temperature was maintained by a 37°C temperature stage. Bioluminescent signal was collected fifteen minutes after luciferin administration for an exposure time of thirty seconds. Images were taken a day prior to treatment (day 0, baseline), in the middle of the treatment cycle, and one day following the final treatment. Treatment efficacy was quantified by examining the fold increase in bioluminescence of the post-treatment signal as compared to baseline. Statistical analysis of the toxicity data was analyzed using a one-way ANOVA test with the Prism 5™ software.

Biodistribution of Cisplatin

[00195]   Cisplatin-nanoparticles and free cisplatin were injected i.v. (dose equivalent to 8 mg/Kg of cisplatin) in mice to study its distribution. After 24 hours of injections, the animals were sacrificed and necropsy was performed to harvest the tumor and kidney. In another study, the animals were dosed repeatedly following the efficacy study protocols, and the animals were sacrificed at the end of the multiple dosing study. The organs were then weighed and dissolved in Conc. HNO_3 (approx. 10 mL) by shaking for 24 hours at room temperature and then heating at 100°C for 12 hours. To these mixtures were then added 30% H_2O_2, the resulting solutions were stirred for 24 hours at room temperature and then heated for another 12 hours to evaporate the liquids. All solid residues were re-dissolved in 1 mL water and then amount of platinum was measured by inductively coupled plasma-spectrometry (ICP).

Histopathology and TUNEL assay (Apoptotic assay)

[00196]   The tissues were fixed in 10% formalin, paraffin embedded, sectioned and stained with H&E at the Harvard Medical School Core Facility. Tumor and Kidney paraffin sections were deparaffinized and stained with standard TMR-red fluorescent terminal deoxynucleotidyl transferase-mediated dUTP nick end labeling (TUNEL) kit following the manufacturer's protocol (In Situ Cell Death Detection Kit, TMR Red, Roche). Images were obtained using a Nikon Eclipse TE2000 fluorescence microscope equipped with red filter.

Toxicity Assessment of Drug Treatment

[00197]   Body weights were recorded daily to assess toxicity. In addition, livers and spleens were removed at the end of treatment to record weights and perform extensive pathological examination to assess toxicity of vital organs. Cell apoptosis in vital organs was measured using TUNNEL assay. Statistical analysis of the toxicity data was performed using a two-way ANOVA test with the Prism 5™ software.

Statistical Analysis

[00198]   Data were expressed as means ± S.D from at least n=3. Statistical analysis was conducted using the GraphPad Prism software (GraphPad, San Diego, CA). The statistical differences were determined by ANOVA followed by Newman Keuls Post Hoc test or Student's t test. $p < 0.05$ was consideredtoindicate significant differences.

Example 1 – Synthesis of Polymeric Carriers

Poly(isobutylene-alt-maleic acid) PIMA (2)

[00199]   Poly(isobutylene-alt-maleic anhydride) 1 (1g) was dissolved in 5 ml of dry DMF in 10 mL round bottom flask to which was added double distilled water (1mL) and then resulting reaction mixture was stirred at 80°C for 48h. Solvent was removed under vacuum and low molecular weight impurities were removed using dialysis. Aqueous polymer solution was dialyzed for 3 days in cellulose membrane tubing, types Spectra/Por 4 and with mass-average molecular mass cut-off limits of 1000. The colorless solution was then lyophilized to get 732 mg of white colored polymer Poly(isobutylene-alt-maleic acid) PIMA (2). ^{1}H NMR (300 MHz, D_2O) δ 3.3-3.5 (m), 2.8 (s), 2.6-2.7 (m), 2.5 (s), 2.2-2.3 (m), 0.8-0.9 (m).

PIMA-EDA (3)

[00200]   The 10 mL RB flask equipped with magnetic stirrer and dry nitrogen balloon was charged with Poly(isobutylene-alt-maleic anhydride) PIMA 1 (1g), dry DMF (5mL), Triethyl amine (0.1mL) and excess Ethylendiamine dihydrochloride (1g). The resulting mixture was stirred at 25°C for 48h. Solvent was removed under vacuum and polymer was purified by removing low molecular weight impurities such as excess Ethylendiamine using dialysis bag of molecular cut off of 3.5KD for 3 days. The polymer solution was then lyophilized to get 0.89 g of PIMA-EDA (3). ^{1}H-NMR (300 MHz, D_2O) δ 3.1-3.2 (m), 2.9-3.0 (m), 2.6-2.8 (m), 2.5 (m), 0.8-1.0 (m).

PIMA-GA Polymer (4)

[00201]   Poly(isobutylene-alt-maleic anhydride) PIMA **1** (0.0064 g, 0.001 mmol) was

dissolved in DMF (5 mL) and then was added DBU (0.032 mL, dissolved in 1 mL dry DMF,

0.21 mmol) and the mixture was stirred at 25 °C for 1h. To this solution was added

Glucosamine (0.046 g 0.21 mmol) directly. The resulting reaction mixture was allowed to stir

at room temperature for 48 h and then quenched by adding double distilled water (1mL). The

organic solvent was evaporated under vacuum for 12 hours. The resulting pale yellow solid

was purified by dialysis for 3 days using dialysis bag supplied by Pierce (Thermoscientific)

of molecular cut off of 3.5KD to colorless solution. Lyophilization gave 104 mg of white

colored PIMA-GA (4) polymer. ^{1}H-NMR (300 MHz, CDC[13]) δ 7.54-7.65 (m, 2 H), 7.33-7.45

(m, 2 H), 7.02-7.19 (m, 14 H), 6.93-6.97 (m, 2 H), 6.83-6.89 (m, 2 H), 6.55 (s, 2 H), 6.15-

6.19 (m, 2 H), 3.90 (s, 2 H), 3.58 (s, 6 H). ^{1}H-NMR (300 MHz, D_2O) δ 8.2-8.3 (m), 7.0-7.1

(m), 5.0-5.1 (m), 3.0-3.9 (m), 2.1-2.3 (m), 1.1-1.9 (m), 0.7-1.0 (m).

[00202]   In another experiment, PIMA (0.045 g) was dissolved in DMF (5 mL) and

then was added solution of DBU (0.23 mL) and glucosamine (0.323 g dissolved in 5 mL dry

DMF). The resulting reaction mixture was allowed to stir at room temperature for 48 h and

then quenched by adding dd water (1mL). The organic solvent was evaporated under

vacuum. The resulting pale yellow solid was purified by dialysis for 3 days using dialysis bag

of molecular cut off of 3.5KD. Lyophilization gave 104 mg of slightly yellow colored PIMA-

GA polymer. ^{1}H-NMR (300 MHz, D_2O) δ 8.2-8.3 (m), 7.07.1 (m), 5.0-5.1 (m), 3.0-3.9 (m),

2.1-2.3 (m), 1.1-1.9 (m), 0.7-1.0 (m).

PIMA-PEG Polymer (5)

[00203]   The Poly(isobutylene-alt-maleic anhydride) PIMA **1** (3 mg, 0.0005 mmol) and

DBU (0.0023 mL, 0.015 mmol) was dissolved in Dry DMF (10 mL) in 25 mL RB flask under

N_2 for 1 h and then was added PEG-NH_2 (20 mg, 0.01 mmol), the resulting reaction solution

was then heated at 80 °C with continuous stirring for 3days. The reaction was allowed to cool

to room temperature and then water (1 mL) was added and continue stirring for 1 h. Solvents

are removed under vacuum and unreacted PEG-NH_2 of MW 2KD was removed from

required polymer by dialysis. Dialysis was carried out for 5 days using membrane of

molecular cut off of 3.5KD supplied by Pierce (Thermoscientific) to give colorless solution

which was then lyophilized to give 19 mg white colored PIMA-PEG (**5**). ^{1}H-NMR (300

MHz, D_2O) δ 3.5-3.7 (m), 3.0-3.1 (m), 2.5-2.8 (m), 0.7-1.0 (m).

Example 2 - Synthesis of conjugates

Aquation of CDDP

[00204]   CDDP (30mg) and AgNO$_3$ (17mg) was added to 10ml double distilled water. The resulting solution was stirred in dark at room temperature for 24h. AgCl precipitates were found after reaction. AgCl precipitates are removed from reaction by centrifugation at 10000 rpm for 10 min. The supernatant was further purified by passing through 0.2μm filter.

PIMA-CDDP (6)

[00205]   Poly(isobutylene-alt-maleic acid) PIMA 2 (0.006 g, 0.001 mmol) was dissolved in 1ml double distilled water containing CDDP (0.00084 g, 0.0028 mmol) in 10 mL round bottom flask to and then resulting reaction mixture was stirred at room temperature (25°C) for 48h. The PIMA-CDDP (6) conjugate was further purified by dialyzing it in cellulose membrane tubing, types Spectra/Por 4 and with mass-average molecular mass cut-off limits of 1000. The resulting turbid solution was then lyophilized to get white colored PIMA-CDDP (6) conjugate. The conjugate was re-suspended for cell culture experiments.

PIMA-EDA-CDDP (7)

[00206]   In 10 mL RB flask was weighed PIMA-EDA 3 (0.007 g, 0.001 mmol) polymer to which was added CDDP (0.0084 g, 0.0028 mmol) dissolved in double distilled water (1 mL). The solution was then stirred at room temperature (25°C) for 48h. Dialysis using cellulose membrane with molecular mass cut-off limits of 1000 and lyophilization gave yellowish colored PIMA-EDA-CDDP (7) conjugate.

PIMA-GA-CDDP (8)

[00207]   To PIMA-GA 4 (0.0036 g, 0.0003 mmol) weighed in 10 mL RB flask equipped with magnetic stirrer was added 1ml double distilled water containing CDDP (0.001 g, 0.0033 mmol) and then the solution was stirred at room temperature (25°C) for 48h. The PIMA-GA-CDDP (8) conjugate formed in solution was further purified by dialysis to remove unattached CDDP with mass-average molecular mass cut-off limits of 1000 for 2-3 hours. Lyophilization of the dialyzed solution resulted in slightly yellow colored PIMA-GA-CDDP (8) conjugate.

PIMA-PEG-CDDP (9)

[00208]   The brush polymer PIMA-PEG **5** (0.019 g, 0.00007 mmol) was taken in 10

mL RB flask mixed with CDDP (0.0002 g, 0.0007 mmol) dissolved in 0.3 mL double

distilled water. After stirring for 3 days at room temperature (25°C) the resulting turbid

reaction mixture was dialyzed. The solution containing PIMA-PEG-CDDP (**2**) conjugate was

further purified by dialyzing it in cellulose membrane tubing, types Spectra/Por 4 and with

mass-average molecular mass cut-off limits of 1000 for 2-3 hours to remove free CDDP.

PIMA-PEG-CDDP (**9**) conjugate was then lyophilized to get white colored solid. The

conjugate was re-suspended in double distilled water for cell culture experiments.

FITC-labeled PIMA-GA-CDDP

[00209]   Poly(isobutylene-alt-maleic anhydride) PIMA (0.006 g) was dissolved in

DMF (5 mL) and then was added a solution of DBU (0.0053 mL in DMF) and Glucosamine

(0.0075 g dissolved in 5 mL dry DMF) the mixture was stirred at 25°C for 1h. The resulting

reaction mixture was allowed to stir at 25°C for 48 h and then to which was added 0.0022 g

FITC-EDA (FITC-EDA was synthesized by stirring Fluorescein isothiocyanate in excess

ethylene diamine at 25°C for 12 h in DMSO) and continue stirring for another 12 h, reaction

mixture was quenched by adding double distlled water (1mL). The organic solvent was

evaporated under vacuum. The resulting orange solid was purified by dialysis for 3 days

using dialysis bag of molecular cut off of 3.5KD. Lyophilization gave fluorescent orange

PIMA-GA-FITC polymer. To this FITC labeled polymer (PIMA-GA-FITC, 0.004 g) was

added 1ml double distilled water containing cisplatin (0.001 g) and then the solution was

stirred at room temperature (25°C) for 48h. The PIMA-GA-FITC-cisplatin conjugate formed

in solution was further purified by dialysis to remove unattached cisplatin with mass-average

molecular mass cut-off limits of 1000. Lyophilization of the dialyzed solution resulted in

orange colored FITC labeled PIMA-GAFITC-cisplatin conjugate nanoparticles.

PIMA-Oxaliplatin

[00210]   Poly(isobutylene-alt-maleic acid) (PIMA) (6mg) was dissolved in 1ml double

distilled water containing oxaliplatin-OH (1mg) in a round bottom flask to and then resulting

reaction mixture was stirred at room temperature (25oC) for 48h. The PIMA-oxaliplatin

conjugate was further purified by dialyzing it in cellulose membrane tubing, types

Spectra/Por 4 and with mass-average molecular mass cut-off limits of 1000. The resulting

turbid solution was then lyophilized to get PIMA-oxaliplatin conjugate. The conjugate was re-suspended for cell culture experiments.

PIMA-GA-Oxaliplatin

[00211]   To PIMA-GA (12mg) weighed in 10 mL RB flask equipped with magnetic stirrer was added 1ml double distilled water containing oxaliplatinOH (1mg) and then the solution was stirred at room temperature (25°C) for 48h. The PIMA-GA-oxaliplatin conjugate formed in solution was further purified by dialysis to remove unattached oxaliplatin with mass-average molecular mass cut-off limits of 1000. Lyophilization of the dialyed solution resulted in yellow colored PIMA-GA-oxaliplatin conjugate.

Example 3 – NMR analysis of PIMA-GA polymer synthesis using different bases

Synthesis of PIMA-GA using DBU as the base

[00212]   Glucosamine hydrochloride (360 mg, 1.66 mmol, 200 equiv) was suspended in 5 mL DMF and treated with DBU (250 µL, 1.66 mmol, 200 equiv) at room temperature for 1h. After 1h glucosamine/DBU (in DMF) solution was added drop wise into poly (isobutylene-alt-maleic anhydride) (50 mg, 0.008 mmol, 1 equiv) solution in 5 mL DMF and the reaction mixture was stirred for 72h at room temperature. The reaction mixture was quenched with 3 mL of dd-water. The PIMA-GA conjugate was purified by dialysis using 2000 MWCO dialysis bag for 72h. The product was lyophilized for 48h to obtain 100 mg cream yellow powder. The product was characterized by ^{1}H NMR spectroscopy (300 MHz). Solubility: product was soluble in water but not soluble in organic solvent e.g. acetone, methanol or acetonitrile. ^{1}H NMR (300 MHz): δ (ppm) = 5.2-5.3 (m, 0.14 H, sugar proton), 5.0-5.1 (m, 0.4 H, sugar proton), 3.6-4.0 (m, 13.07 H, sugar proton), 3.25-3.5 (m, 15.48 H, sugar proton), 3.0-3.2 (m, 6.98 H, sugar proton), 2.5-2.6 (m, 6.97 H, PIMA proton), 1.4-1.7 (m, 19.86 H, PIMA proton), 0.7-1.2 (m, 23.77 H, PIMA proton). Total sugar protons: total PIMA protons =36.07: 50.6= 0.71. This fits well with the predicted structure if all the residues are derivatized sugar protons and PIMA protons in PIMA-GA conjugate monomer.

Synthesis of PIMA-GA using diisoproylethylamine (DIPEA) as base

[00213]   Glucosamine hydrochloride (179 mg, 0.83 mmol, 100 equiv) was suspended in 2 mL DMF and treated with DIPEA (145 µL, 0.83 mmol, 100 equiv) at room temperature for 1h. After 1h poly (isobutylene-alt-maleic anhydride) (50 mg, 0.008 mmol, 1 equiv) (dissolved in 3 mL DMF) was added into the reaction mixture and stirred for 24h at room

temperature. The reaction mixture was quenched with 3 mL of dd-water. The PIMA-GA conjugate was purified by dialysis using 1000 MWCO dialysis bag for 24h. The product was lyophilized for 48h to obtain 106 mg white powder. The product was characterized by ^{1}H NMR spectroscopy (300 MHz). Solubility: product was soluble in water but not soluble in organic solvent e.g. acetone, methanol or acetonitrile. ^{1}H NMR (300 MHz): δ (ppm) = 5.2-5.3 (m, 0.4 H, sugar proton), 4.9-5.1 (m, 2.0 H, sugar proton), 3.4-3.6 (m, 21.86 H, sugar proton), 3.2-3.3 (m, 6.16 H, sugar proton), 2.9-3.1 (m, 3.81 H, sugar proton), 2.4-2.7 (broad, 4.39 H, PIMA proton), 2.1-2.4 (broad, 4.54 H, PIMA proton), 1.7-2.0 (broad, 3.13 H, PIMA proton), 1.3-1.5 (braod, 1.58 H, PIMA proton), 1.1-1.2 (m, 24.12 H, PIMA proton), 0.6-0.9 (m, 27.94 H, PIMA proton). Total sugar protons: total PIMA protons = 39.21: 61.11 = 0.64.

Synthesis of PIMA-GA using trietylamine as base

[00214]   Glucosamine hydrochloride (143 mg, 0.66 mmol, 80 equiv) was suspended in 2 mL DMF and treated with triethylamine (100 μL, 0.66 mmol, 80 equiv) at room temperature for 1h. After 1h poly (isobutylene-alt-maleic anhydride) (50 mg, 0.008 mmol, 1 equiv) was added into the reaction mixture and stirred for 24h at room temperature. The reaction mixture was quenched with 3 mL of dd-water. The PIMA-GA conjugate was purified by dialysis using 1000 MWCO dialysis bag for 24h. The product was lyophilized for 48h to obtain 100 mg white powder. The product was characterized by ^{1}H NMR spectroscopy (300 MHz). Solubility: product was soluble in water but not soluble in organic solvent e.g. acetone, methanol or acetonitrile. ^{1}H NMR (300 MHz): δ (ppm) = 5.2-5.3 (m, 0.44 H, sugar proton), 4.9-5.1 (m, 1.51H, sugar proton), 3.7-3.8 (m, 19.01 H, sugar proton), 3.3-3.4 (m, 6.43 H, sugar proton), 3.1-3.2 (m, 11.82, sugar proton), 2.93-2.94 (m, 2.23 H, PIMA proton), 2.6-2.7 (m, 5.84 H, PIMA proton), 2.2-2.5 (broad, 4.91 H, PIMA proton), 1.8-2.1 (broad, 3.83 H, PIMA proton), 1.4-1.6 (broad, 2.52 H, PIMA proton), 1.8-1.2 (m, 18.04 H, PIMA proton), 0.9-1.0 (m, 23.77 H, PIMA proton). Total sugar protons: total PIMA protons = 34.31: 65.7 = 0.52.

Example 4 - Time dependent loading efficiency of PIMA-GA-CDDP.

[00215]   Method: PIMA-GA conjugate (50 mg, 0.004 mmol) was dissolved in 1 mL dd-water followed by the addition of $(NH_2)_2Pt(OH)_2$ (3mL, 0.057 mmol). The reaction was stirred at room temperature for 48h. 200 μL of aliquots were taken out from the reaction mixture after each pre-determined time points (5h, 31h and 48h). The aliquots were filtered through Microcon centrifugal filter device having regenerated cellulose membrane of 3000

MWCO to separate the PIMA-GA-CDDP conjugate. The polymer was washed thoroughly (200 μL x 2) with dd-water to remove any platinum reagent. The platinum content in polymer was determined by the method described before.

[00216] Result: The change in Pt-loading efficiency in PIMA-GA conjugate was determined by the ability of conjugating 1,2-phenylenediamine with Pt giving rise to UV-VIS spectra at wavelength λ = 706 nm. Neither the polymer nor 1,2-phenyldiamine has any characteristic peak at this wavelength. How the Pt-content changes with time in the reaction between PIMA-GA and hydroxy-platin was monitored by UV-VIS spectra. At different pre-determined time points (5h, 31h and 48h) 200 μL of aliquots were taken out from the reaction mixture and the Pt-loading in the polymer conjugate was determined. The figure shows that loading of platinum in the polymer conjugate increases with time from 190μg/mg (5h) to 210 μg/mg (31h) and reaches maximum 347μg/mg at 48h. This indicates almost 100% of the Pt is complexed with the polymer at this time point as the maximal predicted loading is 37.5% per polymer unit, and we attain 34.7% Pt per polymer.

Example 5 - Rational optimization of the polymer based on structure-activity relationship.

[00217] In order to improve efficacy of the nanoparticles, the inventors derivatized one arm of each monomer of the polymer with biocompatible glucosamine to generate PIMA-glucosamine conjugate (PIMA-GA) (Fig.11B). This converted the dicarboxylato bonds with Pt to a monocarboxylato bond and a coordinate bond, which can release Pt more easily given that a coordinate bond is less stable than a monocarboxylato linkage (Fig. 11 B).

[00218] Nuclear magnetic resonance (NMR) characterization of the Pt environment revealed that complexation of PIMA-GA and cisplatin in an acidic pH (pH 6.5) generated an isomeric state [PIMA-GA-Cisplatin (O->Pt)] (**8**) characterized by the monocarboxylato and a O->Pt coordination complex as characterized by a single Pt NMR peak at -1611.54 (Fig. 11B). Interestingly, complexing the cisplatin with PIMA-GA at an alkaline pH (pH 8.5) favored the formation of an isomeric PIMA-GA-Cisplatin (N->Pt) complex (**10**), where the Pt is complexed through a monocarboxylato and a more stable N->Pt coordinate bond characterized by a unique peak at -2210 (Fig. 11B). Excitingly, the existing of these two pH-dependent states allowed the inventors to further dissect the impact of Pt environment, specifically the leaving groups, on the biological efficacy.

[00219] The complexation of cisplatin to PIMA-glucosamine (PIMA-GA) polymer at a ratio of 15:1 resulted in self assembly into nanoparticles in the desired narrow size bandwidth

of 80-150 nm as confirmed by high-resolution transmission electron microscopy (data not shown) and DLS (Fig.12A). Furthermore, the inventors achieved a loading of 175 ± 5 μg/mg of polymer (Fig.12B), which is significantly higher than can be achieved using traditional nanoparticle formulations (Avgoustakis K, Beletsi A, Panagi Z, Klepetsanis P, Karydas AG, Ithakissios DS. PLGA-mPEG nanoparticles of cisplatin: in vitro nanoparticle degradation, in vitro drug release and in vivo drug residence in blood properties. J Control Release. 2002 Feb 19;79(1-3):123-35).

Example 6 - Characterizing the uptake and efficacy of nanoparticles in vitro

[00220]   Tagging the polymer with fluorescein (Fig. 15) enabled the temporal tracking of uptake of the nanoparticles into the cells, which were co-labeled with a lysotracker-red dye to label the endolysosomal compartments. A rapid uptake of the nanoparticles was observed in the LLC cells within 15 min of treatment with internalization into the endolysosomal compartment as evident by colocalization of the FITC-nanoparticles and the Lysotracker-Red dye (data not shown). In contrast, the uptake into 4T1 cells was delayed, with internalization into the endolysosomal compartment evident only after 2 hours post-incubation. Over a 12 hour period, the fluorescent signals from the lysosomal compartment and the FITC-conjugated dissociate, suggesting a cytosolic distribution of the polymer after processing within the lysosome (data not shown).

[00221]   To test the efficacy of the PIMA-GA-cisplatin nanoparticles in vitro, the inventors performed cell viability assays using Lewis lung carcinoma (LLC) and 4T1 breast cancer cell lines. Cell viability was quantified using a MTS assay at 48 hours post-incubation. Interestingly, the LLC cells (Fig.13A) were more susceptible to cisplatin-nanoparticles than the 4T1 breast cancer cells (Fig.13B). Excitingly, PIMA-GA-cisplatin (O->Pt) nanoparticles (8) demonstrated significant LLC cell kill with IC50 values (4.25 ± 0.16μM) similar (P>0.05) to cisplatin (IC50 = 3.87 ± 0.37μM), and superior to carboplatin (IC50 = 14.75 ± 0.38μM), which supports the hypothesis that the rate of aquation is critical for efficacy (Fig.13). A similar efficacy was observed when the inventors replaced glucosamine with ethylene diamine, which creates a similar Pt complexation environment as glucosamine (Fig.13A). This was additionally supported by the observation that PIMA-GA-cisplatin (N->Pt) nanoparticles (IC50= 6.36 ± 0.19μM) were significantly less active than cisplatin, suggesting that the platinum environment is critical in defining the rate of aquation. To further validate the role of complexation environment, the inventors generated PIMA-GA(20), where only 20 of the 40 monomers comprising a PIMA polymer were derivatized with glucosamine, thereby

introducing dicarboxylato bonds and reducing the monocarboxylato plus coordinate bonds that complex Pt to PIMA-GA. As shown in Fig.16F, the concentration-efficacy curve shifts to the right with PIMA-GA(20)-cisplatin (EC50= 5.85 ± 0.13μM) as compared with PIMA-GA-cisplatin (O->Pt) nanoparticles, where all the 40 monomers are derivatized with glucosamine. Empty PIMA-GA polymer had no effect on the cell viability. Table summarizes the EC50 values.

[00222]   As shown in Fig. 13A, while the polymer alone induced cell death at the highest concentrations, complexation of cisplatin significantly shifted the concentration-effect curve to the left, indicating that the PIMA-cisplatin nanoparticle induces cell kill. However, even at a concentration of 50 uM, the PIMA cisplatin failed to induce complete cell kill. In contrast, cisplatin exerts complete cell kill at a concentration greater than 20 uM. This reduction in the efficacy of palatinate when complexed with PIMA can be explained by the dicaroboxylateo linkage between the platinum and the maleci acid monomers, which tightly binds the Pt similar to the linkage that exists in carboplatin, which similarly is less efficacious than cisplatin.

[00223]   Labeling the cells for expression of phosphatidylserine on the cell surface, revealed that the cisplatin treatments could induce apoptotic cell death, with LLCs being more susceptible than 4T1 cells (Fig. 14).

Table 1: EC50 values for various complexes

	EC50 (μM)
PIMA30: PIMA-GA-Cisplatin [acidic]	5.29 ± 0.11
PIMA30: PIMA-GA-Cisplatin [basic]	6.84 ± 0.14
Cisplatin	3.87 ± 0.37
Carboplatin	14.75 ± 0.38
PIMA40-200: PIMA-GA-Cisplatin [acidic]	4.25 ± 0.16
PIMA40-200: PIMA-GA-Cisplatin [basic]	6.36 ± 0.19
PIMA-GA20-Cisplatin [acidic]	5.85 ± 0.13

Example 7 - The release of active cisplatin from nanoparticle is pH-dependent

[00224]   Given that the nanoparticles localized to the lysosomal compartment, the inventors tested the release of Pt from the nanoparticles at pH 5.5, mimicking the acidic pH of the endolysosomal compartment of the tumor (Lin, et al., Eur. J. Cancer, 2004 40(2):291-297). The inventors also selected pH8.5 as a reference pH in the alkaline range. As shown

in Fig. 16, at pH5.5 PIMA-GA-cisplatin (O->Pt) nanoparticles resulted in a sustained but significant release of cisplatin monitored over a 70 hour period. In contrast the release at pH8.5 was significantly lower, indicating a pH-dependent release of Pt. Interestingly, PIMA-GA-cisplatin (N->Pt) released significantly lower amounts of Pt even at pH5.5, consistent with the fact that the N->Pt coordinate bond is stronger than the O->Pt linkage. As expected, the inventors observed that PIMA-cisplatin nanoparticles exhibited significantly lower rates of Pt release as compared with both PIMA-GA-cisplatin (N->Pt) and PIMA-GA-cisplatin (O->Pt) as the Pt is held by more stable dicarboxylato bonds instead of a monocarboxylato and a coordinate bond.

Example 8 - Nanoparticle induces tumor growth delay and regression with reduced nephrotoxicity

[00225] As PIMA-GA-cisplatin (O->Pt) nanoparticles exhibited the desired release rates for platinum and also exhibited in vitro efficacy comparable to cisplatin, the inventors validated the therapeutic efficacy of the nanoparticles in vivo. They randomly sorted mice bearing established Lewis lung carcinoma or 4T1 breast cancer into five groups respectively and treated each group with three doses of (i) PBS (control); (ii) Cisplatin (1.25 mg/kg); (iii) Cisplatin(3mg/kg); (iv) PIMA-GA-Cisplatin (O->Pt) nanoparticles (1.25 mg/kg); (v) PIMA-GA-Cisplatin (O->Pt) nanoparticles (3 mg/kg). The mice injected with PBS formed large tumors by day 16 (day after the last injection), and consequently, were euthanized. The animals in the other groups were also sacrificed at the same time point to evaluate the effect of the treatments on tumor pathology. As shown in Fig. 5, cisplatin induced dose-dependent tumor inhibition, and at a dose equivalent to 1.25 mg/kg of cisplatin, administration of the nanoparticle formulation resulted in greater inhibition of lung carcinoma progression as compared with the free drug. However, at a dose equivalent to 3mg/kg, free cisplatin resulted in a significant reduction in body weight indicating systemic toxicity. In contrast, animals treated with nanoparticles equivalent to 3mg/kg of cisplatin exhibited weight gain, although tumor inhibition was similar in both treatment groups (data not shown). Furthermore, necropsy revealed that treatment with free cisplatin resulted in a significant reduction in the weights of kidney and spleen (Figs. 5D and 5E), indicating nephrotoxicity and hematotoxicity consistent with previous reports. Excitingly, cisplatin nanoparticles had no effect on the weights of the kidneys, and reduced spleen size only at the highest dose (Fig. 5D and 5E). This was further validated by pathological analysis of kidney H&E stained cross-sections, which revealed significant tubular necrosis in the animals treated with free cisplatin as

compared with cisplatin nanoparticle. To elucidate the mechanism underlying tumor inhibition, the inventors labeled the tumor cross sections for TUNEL, which revealed a significant induction of apoptosis following treatment with both free cisplatin and PIMA-GAcisplatin(O->Pt) nanoparticles (data not shown). Interestingly, labeling the kidney sections for TUNEL demonstrated significant apoptosis in the animals treated with free cisplatin as opposed to minimal nephrotoxicity in the nanoparticle-treated group (data not shown). Indeed, biodistribution studies using inductively coupled plasma-spectrometry (ICP) revealed that the concentration of Pt in the kidney following administration of the cisplatin nanoparticle is 50% of that attained following administration of free drug (Fig. 5E), which can explain the reduction in nephrotoxicity.

[00226]   Treatment with cisplatin (1.25mg/kg) exhibited only a minor tumor growth inhibition as compared with control; in contrast, treatment with nanoparticle-cisplatin at the same dose exerted a dramatic increase in the antitumor efficacy (Fig. 5A). This is consistent with the fact that nanoparticles enable a significantly higher concentration of the active agent to be attained within the tumor as compared to free drug[20]. At the higher dose, both the free drug and the nanoparticle achieved similar antitumor efficacy (Fig. 5A), which is potentially the theoretical limit of the drug. However, the free drug at this dose resulted in a greater than 20% loss of body weight (Fig. 5B), which is an indicator of non-specific toxicity. Indeed, it induced significant nephrotoxicity as seen by the loss of weight of the kidney (Fig. 5D). Furthermore, although the blood counts were not different between the various treatment groups (Fig. 5C), there was significant loss of weight of the spleen at the highest dose of the free cisplatin (Fig. 5E). In contrast, nanoparticle-cisplatin exhibited no such toxicity even at the highest dose, open up the possibility of dosing at higher levels or for longer time periods, both of which can dramatically impact antitumor outcomes. Furthermore, the ease of manufacturing, the low costs of materials and the increase in therapeutic efficacy and reduction of toxicity can become an example of nanotechnology impacting global health. Without wishing to be bound by theory, the increased therapeutic index can arise from a preferential accumulation of the nanoparticles in the tumors arising from the well-studied EPR effect, and circumventing the kidney as it exceeds the size limit for clearance, which in a previous study was shown to be less than 5 nm (Choi HS, Liu W, Misra P, Tanaka E, Zimmer JP, Itty Ipe B, Bawendi MG, Frangioni JV. Renal clearance of quantum dots. Nat Biotechnol. 2007;25:1165-70).

[00227]   Both free cisplatin and PIMA-GA-cisplatin(O->Pt) nanoparticles resulted in similar levels of tumor growth inhibition in the 4T1 breast cancer model (Fig. 17).

Interestingly, both 1.25mg/kg and 3mg/kg free cisplatin induced a significant loss of body weight as compared with the cisplatin-nanoparticle treated groups. Consistent with the observations in the lung cancer model, while free cisplatin induced significant apoptosis in the kidney, the nanoparticle-cisplatin treated groups exhibited minimal apoptosis in the kidney but significant levels of apoptosis in the tumor.

[00228]   In addition to lung and breast cancer models, the inventors further evaluated the PIMA-GA-cisplatin(O->Pt) nanoparticle in an ovarian cancer model. Epithelial ovarian cancer is the deadliest malignancies of the female reproductive cycle. The discovery of frequent somatic PTEN mutations and loss of heterozygosity at the 10q23 PTEN locus in endometrioid ovarian cancer implicates a key role for PTEN in the etiology of this epithelial ovarian cancer subtype (Obata, K. *et al.* Frequent PTEN/MMAC1 mutations in endometrioid but not serous or mucinous epithelial ovarian tumors. *Cancer Res.* 58, 2095–2097 (1998) and Sato, et al., Cancer Res. 2000, 60: 7052-7056 and Sato, et al., Cancer Res. 2000, 60: 7052-7056). Similarly, K-RAS oncogene is also mutated in endometrioid ovarian cancer, albeit at a lesser frequency (Cuatrecasas, et al., Cancer (1998) 82:1088-1095). In a recent study, the combination of these two mutations in the ovarian surface epithelium was found to induce invasive and widely metastatic endometrioid ovarian adenocarcinomas with complete penetrance, making it a good model for mimicking human tumor progression. In this transgenic model vehicle-treated animals exhibited rapid tumor progression as quantified by luciferase expression. Treatment with the cisplatin nanoparticles resulted in a dose-dependent inhibition of tumor progression, with the lower dose equivalent to 1.25 mg/kg exerting a similar inhibition as a 3mg/kg dose of free cisplatin (Fig. 18). Treatment with the higher dose of cisplatin-nanoparticle (equivalent to 3mg/kg of cisplatin) resulted in greater tumor inhibition without any significant loss of body weight as observed with an equidose of free cisplatin, which is approved for clinical use in ovarian cancer (Fig. 18). Furthermore, TUNEL staining revealed significant apoptosis in the kidney at 3 mg/kg of free cisplatin while the cisplatinnanoparticles at equivalent Pt concentration did not induce apoptosis of the nephrons.

Example 9 - Biodistribution of cisplatin-nanoparticles following multiple dosing

[00229]   To study the biodistribution of the cisplatin nanoparticles, the inventors harvested the tumors at the end of the multiple-dosing experiments, where each animal received three doses of free drug or the cisplatin nanoparticle. As shown in Fig. 19, there was a preferential accumulation Pt in both breast and ovarian tumors when administered as a nanoparticle as opposed to when delivered as free cisplatin.

Example 10 - Toxicity Assessment of Treatment with PIMA-GA-oxaliplatin

[00230]   As seen in Fig. 23B, at a dose of 15mg/kg of free oxaliplatin, all the animals died due to systemic toxicity.   In contrast no toxicity was evident even at this dose in the case of oxaliplatin nanoparticle.

Example 11 - Synthetic scheme of lipid-cisplatin conjugate

[00231]   In addition to the PMA-GA-cisplatin conjugate, the inventors have also engineered an analog, where maleic acid is conjugated to PEG end of a pegylated lipid (PEG2000-DSPE). The inventors complexed Pt to the maleic acid, resulting in the formation of a platinated lipid derivative where the Pt is at the hydrophilic end and the lipid forms the hydrophobic end. These form micelles in water, and the loading efficiency is 45 μg/mg of lipid derivative. This can be increased by using a lower molecular weight PEG or lipid. See Fig. 10.

Example 12 - Cisplatin-liponanoparticles

Materials and Method

[00232]   All reactions were performed under inert conditions unless otherwise indicated. All commercially obtained compounds were used without further purification. DCM, dry DCM, Methanol, Cholesteryl Chloroformate, Cholesterol, Ethylenediamine, Succinic Anhydride, Silver Nitrate, Sodium Sulphate, Pyridine, Cisplatin, L-a-Phosphatidylcholine, Sephadex G-25 and 1,2-Phenylenediamine were bought from Sigma-Aldrich. 1,2-Distearoyl-sn-Glycero-3-Phosphoethanolamine-N-[Amino(Polythylene Glycol)2000] and the mini handheld Extruder kit (including 0.2 μm Whatman Nucleopore Track-Etch Membrane, Whatman filter supports and 1.0 mL Hamiltonian syringes) were bought from Avanti Polar Lipids Inc. Anhydrous solvent DMF was supplied by Acros Organics. Phosphotungstic Acid was from Ted Pella, Inc. Analytical thin-layer chromatography (TLC) was performed using precoated silica gel Aluminium sheets 60 F254 bought from EMD Laboratories. Spots on the TLC plates were visualized using alkanine permanganate or 6% Ninhydrin solution in Acetone. 1H NMR (300 MHz) spectra were obtained on a Varian Mercury 300 spectrophotometer. The chemical shifts are expressed in parts per million (ppm) using suitable deuterated NMR solvents with reference to TMS at 0 ppm. MTS reagent was supplied by Promega. The cell viability assay and release kinetic data were plotted using GraphPad Prism software. Each sample was done in triplicate.

Synthesis of (11):

[00233]   1044 µL (15 eq) of ethylene diamine (12) was dissolved in 5.0 mL anhydrous DCM followed by cooling down to 0-5 °C with ice. 500.0 mg (1.0 eq) of Cholesteryl Chloroformate was dissolved in 5.0 mL anhydrous DCM and was added to the reaction mixture drop-wise over a period 15 minutes with vigorous stirring and was continued overnight until it comes to rt. The reaction was worked up using water (50 mLX3) and DCM (50 mL), followed by saturated Brine water wash. The organic layer was dried over anhydrous Sodium Sulphate, and evaporated with the help of a rotary evaporator. Light yellow colored clear oily product (13) was separated with 99.1% yield. 1H-NMR (300 MHz) d(ppm) = 5.37 (s, 1H), 5.06 (S, 1H), 4.49 (bs, 1H), 3.22-3.20 (m, 2H), 2.82-2.81 (m, 2H), 2.34-2.26 (m, 2H), 2.02-1.83 (m, 6H), 1.54-0.84 (m, 37H)

Synthesis of 15:

[00234]   350 mg (0.74 mmol, 1 eq) of starting material (13) was dissolved in 5.0 mL anhydrous DCM. To it 370.0 mg (3.7 mmols, 5 eq) of Succinic Anhydride (14) and catalytic amount of Pyridine was added. The stirring was continued for 1d followed by work up in 0.1(N) HCl and DCM for several times. The organic layer was dried over Sodium Sulphate and evaporated to get white amorphous solid compound (15). Yield: 95% 1H-NMR (300 MHz) d(ppm) = 7.72-7.70 (m, 1H), 7.54-7.53 (m, 1H), 5.37 (s, 1H), 5.07 (s, 1H), 4.49 (bs, 1H), 4.22-4.19 (m, 2H), 3.36-3.30 (m, 4H), 2.68-2.33 (m, 4H), 2.02-1.83 (m, 6H), 1.54-0.84 (m, 37H).

Synthesis of 16:

[00235]   50 mg (0.166 mmol, 1 eq) of Cisplatin (16) was partially dissolved in 10.0 mL of H2O. To it 28.0 mg (0.166 mmol, 1 eq) Silver Nitrate was added and the resulting reaction mixture was stirred at rt for 1d. It looked milky white and Silver Chloride was removed by centrifuging at 25000 Xg for 1h. Synthesis of 7: 200 mg (0.35 mmol, 1.0 eq) of 5 was dissolved in 5.0 mL DMF. To it 20.0 mL of product 6 (conc 5.0mg/mL, 1.0 eq) was added and stirred for 1d. The reaction mixture was dried with the help of a lyophilizer. The dried product (17) was used for lipo-nanoparticle synthesis without any further purification.

General Procedure of Synthesizing Lipo-nanoparticles:

[00236]   10.0 mg of L-a-Phosphatidylcholine, 5.0 mg of Cholesterol (or Pt(II)-cholesterol conjugate) and 1.0 mg of 1,2-Distearoyl-sn-Glycero-3-Phosphoethanolamine-N-[Amino(Polythylene Glycol)2000] were dissolved in 10.0 mL DCM. It was evaporated into a thin and uniform film with the help of a rotary evaporator. After thorough drying with pump it was hydrated with 1.0 mL H2O for 2 h at 60 °C. The hydrated lipo-nanoparticles looked light yellow to white with little viscous texture. It was passed though Sephadex G-25 column and extruded at 65 °C.

General Method of Pt(II) Quantification in Lipo-nanoparticles

[00237]   A measured amount of the extruded lipo-nanoparticle was heated at 100 °C in 1.2 mg/mL concentration of 1,2-Phenylenediamine in DMF for 2h. Pt(II) amount was calculated by UV Spectrophotometry (Shimadzu 2450).

Release Kinetics

[00238]   Concentrated drug loaded lipo-nanoparticles were suspended with buffer (or cell lysate) and sealed in a dialysis membrane (MW cutoff 1000, Spectrum Lab). The dialysis bags were incubated in 1.0 mL PBS buffer at room temperature with gentle shaking. A 10 μL portion of the aliquot was collected from the incubation medium at predetermined time intervals, and the released drug was quantified by UV Spectrophotometer (Shimadzu 2450). The results are plotted as percentage release.

Sample Preparation for TEM

[00239]   High resolution TEM images were obtained on a Jeol 2011 high contrast digital TEM. For sample preparation, lacy carbon 300 mesh copper grids (Electron microscopy Science) were dipped in the aqueous solution of the lipo-nanoparticle. It was allowed to air dry followed by staining it with 2% aqueous solution of Phosphotungstic acid. The size distribution of lipo-nanoparticles was studied by dynamic light scattering (DLS), which was performed at 26°C on a Malvern Zetasizer DLS-system equipped with a He-Ne laser.

Cell Viability Assay

[00240]   In a 96 well plate, 2×10^3 cells were plated. After 4h, cells were treated with different concentrations of free drug or lipo-nanoparticles. Cells without any treatment were

kept as control. After 48 h, cell viability was assessed using standard MTS assay according to manufacturer's instructions.

In vivo Efficacy and Toxicity Studies

[00241]   BALB/c mice were inoculated s.c. with 1×10^5 of 4T1 breast tumor cells in 100 μL PBS on right flank of mice. Treatment with different anticancer agents either free or entrapped in nanoparticles was started on day when tumor volume reached 200 mm^3. Typically the animals received free drug alone or in nanoparticles through i.v route every alternate day for total of three dosages. Once the tumor volume reached 2000 mm3 in control group, mice were sacrificed. Tumor, kidney, spleen, lung, liver were harvested and processed for paraffin embedding and sectioning.

[00242]   All patents and publications cited herein are hereby incorporated by reference.

WHAT IS CLAIMED:

1. A biocompatible conjugated polymer nanoparticle comprising:

    a copolymer backbone;

    a plurality of sidechains covalently linked to said backbone; and

    a plurality of platinum compounds dissociably linked to said sidechains.

2. The nanoparticle of claim 1, wherein said plurality of platinum compounds is selected from Pt(II) compounds, Pt(IV) compounds, and any combinations thereof.

3. The nanoparticle of claim 1 or 2, wherein at least one of said plurality of platinum compounds is linked to said sidechain through at least one coordination bond.

4. The nanoparticle of claim 3, wherein said coordination bond is between an oxygen of the sidechains and the platinum atom of the platinum compound.

5. The nanoparticle of claim 4, wherein said oxygen is a carbonyl oxygen.

6. The nanoparticle of claim 4, wherein said oxygen is an amide oxygen.

7. The nanoparticle of any of claims 1-6, wherein said copolymer comprises maleic acid monomers.

8. The nanoparticle of claim 7, wherein at least one carboxylic acid of the maleic acid is derivatized to an amide.

9. The nanoparticle of any of claims 1-8, wherein said copolymer is poly(isobutylene-*alt*-maleic acid) (PIMA).

10. The nanoparticle of any of claims 1-9, wherein said copolymer comprises from 2 to 100 monomer units.

11. The nanoparticle of any of claims 1-10, wherein said copolymer comprises from 25 to 50 monomer units.

12. The nanoparticle of any of claims 1-11, wherein said sidechains are selected from the group consisting of polymers, monosaccharides, dicarboxylic acids, and combinations thereof.

13. The nanoparticle of any of claims 1-12, wherein said sidechains are polyethylene glycol (PEG).

14. The nanoparticle of claim 13, wherein said PEG sidechains have a molecular weight of from 100 to 5000 Dalton.

15. The nanoparticle of claim 13, wherein said PEG sidechains have a molecular weight of from 1000 to 3000 Dalton.

16.   The nanoparticle of claim 13, wherein said PEG sidechains have a molecular weight of about 2000 Dalton.

17.   The nanoparticle of any of claims 1-12, wherein said sidechains are monosaccharides.

18.   The nanoparticle of claim 17, wherein said monosaccharides are glucosamine.

19.   The nanoparticle of any of claims 1-18, wherein said platinum compound is a Pt(II) compound selected from the group consisting of cisplatin, oxaliplatin, carboplatin, paraplatin, sartraplatin, and combinations thereof.

20.   The nanoparticle of claim 19, wherein said platinum (II) compound is cisplatin.

21.   The nanoparticle of claim 19, wherein said platinum compound is oxaliplatin.

22.   The nanoparticle of any of claims 1-21, wherein the number of sidechains corresponds between 50% and 100% of the number of monomeric units of said polymer backbone.

23.   The nanoparticle of any of claims 1-22, wherein the number of said sidechains corresponds to a number greater than 90% of the number of monomeric units of said polymer backbone.

24.   The nanoparticle of any of claims 1-23, wherein the number of said platinum compounds corresponds between 10% and 100% of the number of monomeric units of said polymer backbone.

25.   The nanoparticle of any of claims 1-24, wherein the number of said platinum compounds corresponds between 25% and 75% of the number of monomeric units of said polymer backbone.

26.   The nanoparticle of any of claims 1-25, wherein said sidechains comprise dicarboxylic acids.

27.   The nanoparticle of claim 26, wherein said dicarboxylic acids are of the formula HOOC-R-COOH, wherein R is a C_1-C_6alkyl, C_2-C_6alkenyl, or C_2-C_6alkynyl.

28.   The nanoparticle of claim 27, wherein said dicarboxylic acid is maleic acid.

29.   A biocompatible conjugated polymer nanoparticle comprising:
        a poly(isobutylene-*alt*-maleic acid) backbone, wherein said backbone contains 25 to 50 monomer units;
        a plurality of PEG sidechains covalently linked to said backbone, wherein said PEG sidechains have a molecular weight of from 1000 to 3000 Dalton and wherein the number of said PEG sidechains corresponds to between 50% and 100% of the number of monomeric units of said polymer backbone; and

a plurality of cisplatin sidegroups dissociably linked to said backbone wherein the number of said cisplatin sidegroups is between 25% and 75% of the number of monomeric units of said polymer backbone.

30.   A biocompatible conjugated polymer nanoparticle comprising:

a poly(isobutylene-*alt*-maleic acid) backbone, wherein said backbone consist of 40 monomers;

a plurality of PEG sidechains covalently linked to said backbone, wherein said PEG sidechains have a molecular weight of 2000 Dalton and wherein the number of said PEG sidechains is greater than 90% of monomeric units of said polymer backbone; and

a plurality of cisplatin sidegroups dissociably linked to said backbone, wherein the number of said cisplatin sidegroups is between 25% and 75% of the number of monomeric units of said polymer backbone.

31.   A biocompatible conjugated polymer nanoparticle comprising:

a poly(isobutylene-*alt*-maleic acid) backbone, wherein said backbone comprises from 25 to 50 monomers;

a plurality of glucosamine sidechains covalently linked to said backbone and wherein the number of said glucosamine sidechains is between 50% and 100% of monomeric units of said polymer backbone; and

a plurality of cisplatin sidegroups dissociably linked to said backbone, wherein the number of said cisplatin sidegroups is between 25% and 75% of the number of monomeric units of said polymer backbone.

32.   A biocompatible conjugated polymer nanoparticle comprising:

a poly(isobutylene-*alt*-maleic acid) backbone, wherein said backbone comprises from 25 to 50 monomers;

a plurality of glucosamine sidechains covalently linked to said backbone and wherein the number of said glucosamine sidechains is greater than 90% of monomeric units of said polymer backbone; and

a plurality of cisplatin sidegroups dissociably linked to said backbone, wherein the number of said cisplatin sidegroups is between 25% and 75%, inclusive, of the number of monomeric units of said polymer backbone.

33.   A carboxylic acid-platinum compound complex conjugated nanoparticle comprising:
a carboxylic acid-platinum compound complex; and

a plurality of lipid-polymer chains, wherein the carboxylic acid portion of said carboxylic acid-platinum compound complex is covalently bound to said lipid-polymer chains.

34.   The nanoparticle of claim 33, wherein the carboxylic acid is maleic acid.

35.   The nanoparticle of any of claims 33-34, wherein the polymer is PEG.

36.   The nanoparticle of any of claims 33-35, wherein the platinum compound is a Pt(II) compound selected from the group consisting of cisplatin, oxaliplatin, carboplatin, paraplatin, sartraplatin, and combinations thereof.

37.   The nanoparticle of claim 36, wherein the Pt(II) compound is cisplatin.

38.   The nanoparticle of any of claims 33-37, wherein the platinum compound loading is from 1%-30%.

39.   The nanoparticle of any of claims 33-38, wherein the platinum compound loading is from 1%-6%.

40.   A vesicle, micelle, or liposome compound comprising a plurality of nanoparticles of any of claims 33-39.

41.   A dicarbonyl-lipid compound having the structure
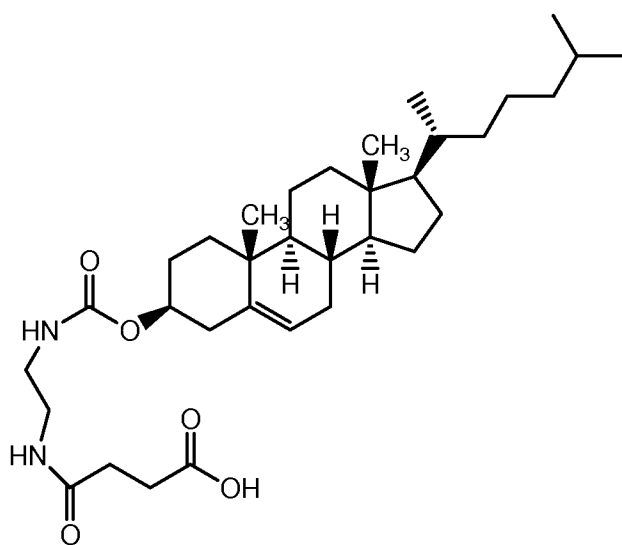
42.   A vesicle, micelle, liposome or nanoparticle compound comprising a dicarbonyl-lipid compound of claim 41 and a platinum compound, wherein the platinum compound is dissociably linked to the compound of claim 41.

43.   The nanoparticle of claim 42, wherein the platinum compound is selected from Pt(II) compounds, Pt(IV) compounds, and any combinations thereof.

44.   The nanoparticle of claim 43, wherein said platinum compound is a Pt(II) compound selected from the group consisting of cisplatin, oxaliplatin, carboplatin, paraplatin, sartraplatin, and combinations thereof.

45.   The nanoparticle of claim 43, wherein said platinum (II) compound is cisplatin.

46.   The nanoparticle of claim 43, wherein said platinum compound is oxaliplatin.

47.   A nanoparticle compound comprising a biocompatible polymer, wherein the polymer comprises at least one monomer having the formula $-CH(CO_2H)-R-CH(C(O)R')-$, wherein R is a bond, C_1-C_6 alkylene, where the alkylene can comprise one or more double or triple bonds; and R' is a substituted nitrogen atom. Preferably, R is a bond.

48.   The nanoparticle of claim 47, wherein the polymer comprises from 2 to 100 monomeric units having the formula $-CH(CO_2H)-R-CH(C(O)R')-$.

49.   The nanoparticle of any of claims 47-48, wherein the polymer comprises from 25 to 50 monomeric units having the formula $-CH(CO_2H)-R-CH(C(O)R')-$.
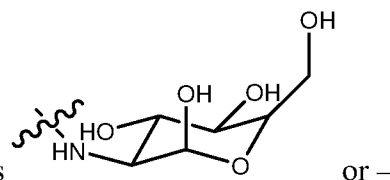
50.   The nanoparticle of any of claims 47-49, wherein R' is or $-NH(CH_2CH_2O)_mCH_3$, wherein m is 1-150.

51.   The nanoparticle of any of claims 47-50, further comprising a bioactive agent.

52.   A pharmaceutical composition comprising:
        the nanoparticle or compound of claims 1-51; and
        a pharmaceutically acceptable carrier.

53.   A method of treating cancer or metastasis comprising:
        administering to a subject in need thereof an effective amount of the composition of any of claims 1-52.

54.   The method of claim 53, wherein said cancer or metastasis is selected from the group consisting of platinum susceptible or resistant tumors.

55.   The method of claim 54, wherein said cancer or metastasis is selected from the group consisting of breast, head and neck, ovarian, testicular, pancreatic, oral-esophageal, gastrointestinal, liver, gall bladder, lung, melanoma, skin cancer, sarcomas, blood cancers, brain tumors, glioblastomas, tumors of neuroectodermal origin and any combinations thereof.

56.   A method of sustain release of a platinum compound at a specific location in a subject comprising: providing at the location a composition of claim the composition of any of claims 1-52.

57.   The method of claim 56, wherein composition is in the form of a gel.

58. The method of any of claims 56-57, wherein the location is a tumor.

59. The method of claim 58, wherein the tumor had been removed before providing the composition.

1/40

FIG. 1A

FIG. 1B

3/40

FIG. 1C

4/40

FIG. 2

FIG. 3

SB2_129_Pt_RK_LLC

◇ LLC

Pt CONTENT (ug)

180
160
140
120
100
80
60
40
20
0

0h 1h 2h 3h 4h 5h 6h 7h 8h 21h 24h

TIME (HOUR)

FIG. 4A

○ PMA-GA-CISPLATIN
△ CISPLATIN
▽ PMA-GA

CELL VIABILITY

160
140
120
100
80
60
40
20
0

0   10^{-7} 10^{-6} 10^{-5} 2×10^{-7} 5×10^{-7}

CISPLATIN [M]

FIG. 4B

• Nano-CISPLATIN [1.25 mg/kg]
▲ Nano-CISPLATIN [3 mg/kg]
□ CISPLATIN [1.25 mg/kg]
○ CISPLATIN [3 mg/kg]
◇ VEHICLE CONTROL

FIG. 5A

• Nano-CISPLATIN [1.25 mg/kg]
▲ Nano-CISPLATIN [3 mg/kg]
□ CISPLATIN [1.25 mg/kg]
○ CISPLATIN [3 mg/kg]
◇ VEHICLE CONTROL

FIG. 5B

FIG. 5C

FIG. 5F

FIG. 5D

FIG. 5E

FIG. 6

FIG. 7

▽ PMA-PEG-Cis [1.25 mg]
▲ PMA-PEG-Cis [4 mg]
▫ Cis [1.25 mg]
○ Cis [4 mg/kg]
◇ VEHICLE CONTROL

FIG. 8A

▽ PMA-PEG-Cis [1.25 mg]
▲ PMA-PEG-Cis [4 mg]
▫ Cis [1.25 mg]
○ Cis [4 mg]
◇ VEHICLE

FIG. 8B

SB2_137_LOADING

FIG. 9

13/40

FIG. 10

14/40

FIG. 11A

15/40

FIG. 11B

FIG. 12B

FIG. 12A

— □ — PIMA

— ◆ — PIMA-GA

---△--- PIMA-Cisplatin

— ● — PIMA-EDA

---▽--- Cisplatin

— ◇ — PIMA-EDA-Cisplatin

— ○ — PIMA-GA-Cisplatin [ACIDIC]

— ■ — Cisplatin

---▲--- Carboplatin

---▼--- PIMA

— ○ — PIMA-GA-Cisplatin [ACIDIC]

— ◇ — PIMA-GA-Cisplatin [BASIC]

FIG. 13A

FIG. 13B

PIMA-GA 30

- ■— PIMA-30GA-Cisplatin [a]
- ▲— PIMA-30GA-Cisplatin [b]
- ▼--- Cisplatin
- ○— Carboplatin

FIG. 13C

PIMA-GA 40

- ■— PIMA-30GA-Cisplatin [a]
- ▲— PIMA-30GA-Cisplatin [b]
- ▼--- Cisplatin
- ○— Carboplatin

FIG. 13D

PIMA-GA 200

- ■ — PIMA-30GA-Cisplatin [a]
- ▲ — PIMA-30GA-Cisplatin [b]
- ▼ ---- Cisplatin
- ○ — Carboplatin

FIG. 13E

- ■ — PIMA-GA 40 (ACIDIC)
- ▲ — PIMA-GA 20 (ACIDIC)
- ▼ ---- Cisplatin
- ○ — Carboplatin

FIG. 13F

CARBOPLATIN 1μM

FIG. 14A

CISPLATIN 1μM

FIG. 14B

CISPLATIN-PIMA-GA 1μM

FIG. 14C

CONTROL

FIG. 14D

CARBOPLATIN 1μM

FIG. 14E

CISPLATIN 1μM

FIG. 14F

CISPLATIN-PIMA-GA 1μM

FIG. 14G

CONTROL

FIG. 14H

FIG. 14J

FIG. 14I

FIG. 15

FIG. 16

■ CISPLATIN (1.25mg/kg)
▲ CISPLATIN (3mg/kg)
◇ VEHICLE CONTROL
○ PIMA-GA-Cis (1.25mg/kg)
□ PIMA-GA-Cis (3mg/kg)

■ CISPLATIN (1.25mg/kg)
▲ CISPLATIN (3mg/kg)
○ Cis-PIMA-GA (1.25mg/kg)
□ Cis-PIMA-GA (3mg/kg)
◇ VEHICLE CONTROL

FIG. 17A

FIG. 17B

FIG. 17C

FIG. 17D

FIG. 18B

FIG. 18A

FIG. 19A

Pt DISTRIBUTION (OVARIAN CANCER)

- ■ PBS
- ▨ FREE CisPt 3
- ▨ PIMA-GA-CisPt (1.25mg/kg)
- ▨ PIMA-GA-CisPt (3mg/kg)

μg/g

12.5
10.0
7.5
5.0
2.5
0.0

TUMOR   KIDNEY   SPLEEN   LIVER

FIG. 19B

OXALIPLATIN

FIG. 20A

OXALIPLATIN-CI

OXALIPLATIN-OH

OXALIPLATIN-PIMA

OXALIPLATIN-PIMA-GA (O-Pt)

OXALIPLATIN-PIMA-GA (N-Pt)

pH<7

pH>7

H_2O, 48h

FIG. 20B

30/40

FIG. 21A

FIG. 21B

■ CONTROL
▲ OXALIPLATIN 5mg/kg
▼ OXALIPLATIN 15mg/kg
◇ Ox-NP 5mg/kg
○ Ox-NP 15mg/kg

OXALIPLATIN TUMOR VOLUME

FIG. 22A

■ CONTROL
▲ OXALIPLATIN 5mg/kg
▼ OXALIPLATIN 15mg/kg
◇ OXALIPLATIN-NP 5mg/kg
○ OXALIPLATIN-NP 15mg/kg

OXALIPLATIN BODY WEIGHT

FIG. 22B

■ PBS
□ FREE Ox 5
▨ FREE Ox 15
▦ PIMA-GA-Ox 5
■ PIMA-GA-Ox 15

TUMOR WEIGHTS

WEIGHT (mg)

FIG. 22C

■ PBS
□ FREE Ox 5
▨ FREE Ox 15
▦ PIMA-GA-Ox 5
■ PIMA-GA-Ox 15

KIDNEY WEIGHTS

WEIGHT (mg)

FIG. 22D

■ PBS
□ FREE Ox 5
▨ FREE Ox 15
▦ PIMA-GA-Ox 5
■ PIMA-GA-Ox 15

SPLEEN WEIGHT
COMPARISON

WEIGHT (mg)

FIG. 22E

FIG. 23

FIG. 24

FIG. 25A

FIG. 25B

FIG. 26

FIG. 27A

FIG. 27B

□ CISPLATIN
△ CARBOPLATIN
MTS ASSAY 48h 4T1 CELLS   ○ CDDP LIPOSOME

FIG. 27C

38/40

FIG. 28A

FIG. 28B

39/40

■ VEHICLE
▲ FREE CDDP (1mg/kg)
▽ FREE CDDP (3mg/kg)
◇ CDDP-LIPO (1mg/kg)
○ CDDP-LIPO (3mg/kg)
↑ DAYS OF INJECTION   □ CARBOPLATIN (3mg/kg)

■ VEHICLE
▲ FREE CDDP (1mg/kg)
▽ FREE CDDP (3mg/kg)
◇ LIPOSOME-CDDP (1mg/kg)
○ LIPOSOME-CDDP (3mg/kg)
□ CARBOPLATIN (3mg/kg)

FIG. 29A

FIG. 29B

FIG. 29C

VEHICLE
CDDP (1mg/kg)
CDDP (3mg/kg)
CDDP-Lipo (1mg/kg)
CDDP-Lipo (3mg/kg)
CARBOPLATIN (3mg/kg)

KIDNEY WEIGHT COMPARISON

FIG. 29D

VEHICLE
CDDP (1mg/kg)
CDDP (3mg/kg)
CDDP-Lipo (1mg/kg)
CDDP-Lipo (3mg/kg)
CARBOPLATIN (3mg/kg)

SPLEEN WEIGHT COMPARISON

FIG. 29E